

University of Montana

ScholarWorks at University of Montana

Graduate Student Theses, Dissertations, &
Professional Papers

Graduate School

1999

Kinetics of formation of di-D-fructose dianhydrides from thermal treatments of inulin

Ted Joseph Christian
The University of Montana

Follow this and additional works at: <https://scholarworks.umt.edu/etd>

Let us know how access to this document benefits you.

Recommended Citation

Christian, Ted Joseph, "Kinetics of formation of di-D-fructose dianhydrides from thermal treatments of inulin" (1999). *Graduate Student Theses, Dissertations, & Professional Papers*. 10581.
<https://scholarworks.umt.edu/etd/10581>

This Dissertation is brought to you for free and open access by the Graduate School at ScholarWorks at University of Montana. It has been accepted for inclusion in Graduate Student Theses, Dissertations, & Professional Papers by an authorized administrator of ScholarWorks at University of Montana. For more information, please contact scholarworks@mso.umt.edu.

INFORMATION TO USERS

This manuscript has been reproduced from the microfilm master. UMI films the text directly from the original or copy submitted. Thus, some thesis and dissertation copies are in typewriter face, while others may be from any type of computer printer.

The quality of this reproduction is dependent upon the quality of the copy submitted. Broken or indistinct print, colored or poor quality illustrations and photographs, print bleedthrough, substandard margins, and improper alignment can adversely affect reproduction.

In the unlikely event that the author did not send UMI a complete manuscript and there are missing pages, these will be noted. Also, if unauthorized copyright material had to be removed, a note will indicate the deletion.

Oversize materials (e.g., maps, drawings, charts) are reproduced by sectioning the original, beginning at the upper left-hand corner and continuing from left to right in equal sections with small overlaps. Each original is also photographed in one exposure and is included in reduced form at the back of the book.

Photographs included in the original manuscript have been reproduced xerographically in this copy. Higher quality 6" x 9" black and white photographic prints are available for any photographs or illustrations appearing in this copy for an additional charge. Contact UMI directly to order.

UMI[®]

**Bell & Howell Information and Learning
300 North Zeeb Road, Ann Arbor, MI 48106-1346 USA
800-521-0600**

Kinetics of Formation of Di-D-fructose Dianhydrides
from Thermal Treatments of Inulin

by

Ted Joseph Christian
The University of Montana
Missoula, MT, USA

and

The University of Waikato
School of Science & Technology
Hamilton, New Zealand

presented in partial fulfillment of the requirements

for the degree of

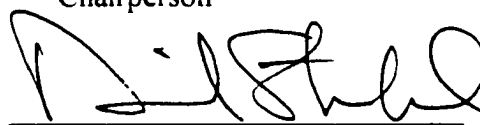
Doctor of Philosophy, Chemistry

The University of Montana

1999

Approved by:


Chairperson


Dean, Graduate School

8-17-99

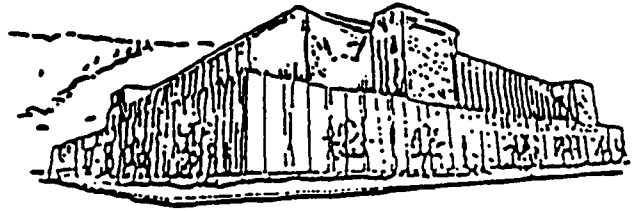
Date

UMI Number: 9940582

UMI Microform 9940582
Copyright 1999, by UMI Company. All rights reserved.

**This microform edition is protected against unauthorized
copying under Title 17, United States Code.**

UMI
300 North Zeeb Road
Ann Arbor, MI 48103



Maureen and Mike
MANSFIELD LIBRARY

The University of **MONTANA**

Permission is granted by the author to reproduce this material in its entirety, provided that this material is used for scholarly purposes and is properly cited in published works and reports.

*** Please check "Yes" or "No" and provide signature ***

Yes, I grant permission
No, I do not grant permission

Author's Signature Ted J. Christensen

Date 8-4-99

Any copying for commercial purposes or financial gain may be undertaken only with the author's explicit consent.

Abstract

Ted J. Christian

M.S. August, 1996

Chemistry

Kinetics of Formation of Di-D-fructose Dianhydrides from Thermal Treatments of Inulin

Committee Chair: Richard J. Field *RJF*

Mixtures of inulin and citric acid react at elevated temperatures to form 14 separate di-D-fructose dianhydrides (DFDAs). At temperatures from 160 to 180°C and citric acid concentrations from 1.0 to 2.9% by weight, DFDAs form rapidly and comprise up to ~35% by weight of the products after 20-40 minutes, after which the DFDA content of the mixture decreases for 40 hours. The remaining mass of starting material is composed of glycosylated DFDA trimers and tetramers, the monomers glucose and fructose, and non-specific degradation products. The pH of thermolysis samples remains constant; acid catalysis that is pseudo order with respect to hydrogen ion is assumed.

Three individual DFDAs - α -D-fructofuranose β -D-fructofuranose 1,2':2,1'-dianhydride, α -D-fructofuranose β -D-fructopyranose 1,2':2,1'-dianhydride, and α -D-fructopyranose β -D-fructopyranose 1,2':2,1'-dianhydride - were isolated and thermolyzed under conditions similar to those used for inulin. The difuranose degraded rapidly and was accompanied by isomerization to other DFDAs. Neither of the other two degraded to any extent. The presence of one or two pyranose rings increased thermal stability significantly under these conditions. At 160°C and 1.5% citric acid, inulin was shown qualitatively to disappear almost completely within 15 minutes; the maximum DFDA concentration for this system occurred at 25 minutes. D-fructose was present from the outset and increased slightly in abundance for ~15 minutes.

A kinetic mechanism is proposed to account for the formation and decay of all 14 DFDAs. This mechanism is subdivided into four partial mechanisms that address unique formation pathways. The five difuranoses that contain at least one β -D-fructose moiety form directly from inulin oligomers. Four more DFDAs form from inulin oligomers whose terminal β -D-fructofuranose residue has isomerized *via* a 2,6-anhydro intermediate to the fructopyranose isomer. The remaining five DFDAs arise, not from inulin, but from other source material that includes fructose and DFDAs that have isomerized. The fructosyl carbocation is central to all of these reaction pathways.

Nonlinear least squares curve-fitting of a simple 1st order parallel-consecutive mechanism provided initial estimates for growth and decay rate constants. These were employed in numerical simulations using LSODE (Livermore Solver for Ordinary Differential Equations). Simulations using the four partial mechanisms were successful in replicating the data.

Dedication

To my mother Phyllis Elaine, my late father Dean Earle,
and Peggy, Jesse, Dean, and Norma.

I will always love you.

Acknowledgments

This research was funded by the Cooperative State Research, Education and Extension Service, U.S. Department of Agriculture, under Agreement No. 95-37500-2098.

There are many people to thank. First and foremost is Merilyn. Her professional commitment to me is unsurpassed, her continuing friendship a blessing. Very few students receive both of these gifts from the same research advisor. I also thank my committee members in Montana for their continued support. To Dick Field, thank you for your friendship, but also for your intuition and patient sculpting of my sometimes insufficient understanding of the principles of chemical kinetics. To Geoff Richards, Ed Rosenberg, and Don Kiely, thank you for keeping me honest. There is nothing quite like a formidable and reputable group of scientists to inspire someone to do their best.

There are two great ladies in my life who live in Montana and from whom I received unquestioning faith. Thank you Christine and Bevs.

The students, faculty, and staff of the University of Waikato restored my belief in humankind. They welcomed me, provided assistance and friendship, and sent me home with a very warm heart indeed. Thanks especially to Lyndsay Main for your generosity, within the chemistry department and without, and to Jannine Sims for your kind acceptance. I made many other friends in the Waikato. Many thanks to you kiwis, especially the original "Smoko Club", Randall, Wouter and Lusha.

To Dirk, Robyn Renae, and Long Sean Silver, you're on my mind. You shaped me years ago and I done got educated. Meet me at Whistler's Bench.

And to Peg, J.C. and Dean, what love you show! What a wreck I'd be without you.

TABLE OF CONTENTS

Abstract	ii
Dedication	iii
Acknowledgments	iv
List of Tables	ix
List of Illustrations	xi
List of Abbreviations	xv

INTRODUCTION

Inulin Structure	1
Inulin in Nutrition	2
Industrial Uses of Inulin	3
Effect of Heat upon Inulin	4
DFDA Nomenclature	6
General Mechanisms of Formation of DFDAs	9
Thermal Treatments of Fructose-containing Substrates	11
<i>Sucrose Degradation in DMSO</i>	11
<i>Hydrolysis</i>	15
DFDA Formation from Fructose-containing Substrates	16
<i>Anhydrous HF</i>	16
<i>Pyrolysis of Inulin</i>	18
<i>DFDA Formation from D-Fructose</i>	20
Acid Stability of DFDAs	27
Statement of Purpose for the Current Study	28

THERMOLYSIS RESULTS AND DISCUSSION

Chapter Introduction	29
Quality Assurance and Preliminary Experiments	31
<i>Purity of Reagents</i>	31

<i>Precision of Weight and Volume Measurements</i>	31
<i>Consistency of Detector Response</i>	32
<i>Melting Points of Inulin Citric Acid Mixtures</i>	35
<i>Temperature Equilibration in Reaction Vials</i>	36
<i>Response Factors</i>	37
<i>Confirmation of DFDA Identities</i>	38
<i>Mass Balance and ESMS</i>	41
General Features of GCFID Chromatograms	53
Isolation of Individual DFDA's	58
<i>DFDA 10 from Inulin citric acid</i>	59
<i>DFDA's 6, 9, and 13 from Fructose HCl</i>	61
Thermolysis of Individual DFDA's	64
<i>Degradation of DFDA 6</i>	64
<i>Degradation of DFDA 9</i>	65
<i>Degradation of DFDA 10</i>	67
Thermolysis of Inulin/1.5% Citric Acid at 160°C	71
<i>Total DFDA's from Inulin 1.5% Citric Acid 160 °C</i>	71
<i>Individual DFDA's from Inulin 1.5% Citric Acid 160 °C</i>	75
<i>General Trends in Individual DFDA Conversion Data</i>	76
<i>Structural Properties as Partial Explanation for Relative Abundance</i> ..	77
<i>Disappearance of Inulin by HPLC</i>	83

KINETICS RESULTS AND DISCUSSION

Chapter Introduction	89
Estimating Individual DFDA Rate Constants	91
<i>Derivation of 1st Order Parallel-Consecutive Rate Equation</i>	91
<i>Curve-fitting Treatments of DFDA Decay</i>	99
1 st Order Decay of DFDA 10 ($v=k[A]$)	100
2 nd Order Decay of DFDA 10 ($v=k[A]^2$)	102

2 nd Order Decay of DFDA 10 ($v=k[A][B]$)	104
<i>The Role of Citric Acid in DFDA decay</i>	106
pH During Thermolysis	109
Effect of Citric Acid Concentration on Wt% Conversion	110
<i>Thermolysis at Higher Temperature</i>	114
Reaction Mechanisms	116
<i>Assembling a Mechanism</i>	118
<i>Use of LSODE on a Single DFDA</i>	119
Simple 1 st Order Growth and Decay	120
Inclusion of Isomerization	122
A 2 nd Order Decay Pathway	123
<i>Extension of Numerical Simulation to Four Difuranoses</i>	124
<i>DFDAs from Inulin via the Anhydro Intermediate</i>	128
<i>Indirect Formation of DFDAs</i>	133
A Unique Mechanism for DFDA 8	133
An Additional Anhydro Species	136
<i>Modeling of Combined Reaction Mechanisms</i>	140
Five Difuranoses from Inulin	141
A Mechanism for all 14 DFDAs	143
CONCLUSION	147
FURTHER WORK	149

EXPERIMENTAL

Instrumentation	150
<i>Gas Chromatography</i>	150
<i>Liquid Chromatography</i>	150
<i>NMR Spectroscopy</i>	152
<i>Electrospray Mass Spectroscopy</i>	152
Thermolysis of Inulin, Nystose, and Individual DFDAs	152

<i>Preparation of starting material</i>	152
<i>Thermolysis</i>	153
<i>Derivatization</i>	153
<i>Sample cleanup</i>	153
<i>Analysis</i>	154
<i>Preparation of 1-Kestose and Nystose</i>	154
<i>Individual DFDA's</i>	155
Preparation of Individual DFDA's	155
<i>Inulin citric acid</i>	155
<i>Fructose HCl</i>	155
Miscellaneous Procedures	156
<i>Mass Balance</i>	156
<i>Response Factors</i>	156
<i>Mass, freeze drying, thermolysis temperature, melting point</i>	157
Data Analysis and Kinetic Modeling	158
<i>Quantitation</i>	158
<i>Preliminary Curve-Fitting</i>	158
<i>Kinetic Plots of DFDA Degradation</i>	159
<i>Kinetic Modeling</i>	159
REFERENCES	161

LIST OF TABLES

Table 1 - Some registered trade names and manufacturers of inulin and fructo-oligosaccharides.	3
Table 2 - Applications, properties, and uses of inulin and fructo-oligosaccharides.	4
Table 3 - Comparison of selected peak area ratios for repeated injections using split/splitless injector.	33
Table 4 - Comparison of selected peak area ratios for repeated injections using on-column injector.	34
Table 5 - Approximate melting points (°C) for inulin/citric acid mixtures.	35
Table 6 - Response factors of per- <i>O</i> -trimethylsilylated derivatives of 6 , 9 , 10 , 13 , fructose, glucose, and sucrose relative to internal standard xylitol.	37
Table 7 - ¹³ C chemical shifts for 6 , 9 , 10 , and 13 . Published values ^{54,61} in parentheses.	40
Table 8 - Recovery of product mass from 20 minute thermolysis of inulin/1.5% citric acid at 160°C.	42
Table 9 - Percentage composition of preparative LC fractions A-F from fructose/HCl digestion.	63
Table 10 - Relative abundance of DFDAs - highest to lowest from left to right - at 2, 6, 30, 80, and 300 minutes. (Inulin/1.5% citric acid/160°C).	76
Table 11 - Anomeric configuration, dianhydride linkage, and central ring conformation of individual DFDAs.	78
Table 12 - First estimates of rate constants from nonlinear least squares curve fitting to 1 st order parallel-consecutive mechanism.	96
Table 13 - pH of citric acid and inulin/citric acid mixtures after thermolysis at 160°C.	109
Table 14 - Average ratio and % decrease of difuranoses to pyranose-containing DFDAs at 40 and 210 minutes.	113
Table 15 - Simulated rate constants for DFDAs 1 , 3 , 5 , 10 , and 12	127
Table 16 - Simulated rate constants for DFDAs 2 , 4 , 7 , and 13	132

Table 17 - Simulated rate constants for DFDA 8, 9, 11, and 14.	139
Table 18 - Elution gradient and electrode potentials for Dionex LC system.	151

LIST OF ILLUSTRATIONS

Reaction Schemes

Scheme 1 - Di-L-sorbose dianhydrides from L-sorbose	9
Scheme 2 - Hexa- <i>O</i> -acetyl di-D-Fruf-1,2':2,1'-dianhydride from acetylated inulin	11
Scheme 3 - Acid catalyzed thermolysis of sucrose in DMSO	13
Scheme 4 - General mechanism for specific acid catalysis of sucrose hydrolysis	15
Scheme 5 - DFDA formation in anhydrous hydrogen fluoride	17
Scheme 6 - Formation of 3 di-D-fructofuranose dianhydrides from pyrolyzed inulin	19
Scheme 7 - 2 nd order kinetic mechanism for diheterolevulosans I-IV from sucrose	22
Scheme 8 - Formation of 9 di-D-fructose dianhydrides from inulin/1.5% citric acid	81
Scheme 9 - DFDA from inulin <i>via</i> 1 st order parallel-consecutive mechanism	92
Scheme 10 - Rate controlling steps in ketal protonation	106
Scheme 11 - Acid catalyzed degradation of difuranose dianhydrides	107
Scheme 12 - Formation of D-fructose from DFDA	143

Figures

Figure 1 - Structure of inulin.	1
Figure 2 - Example of DFDA naming conventions.	7
Figure 3 - DFDA structures and shorthand and trivial names.	8
Figure 4 - The four DFDA products of Chu and Berglund.	20
Figure 5 - Formation and decay of the four DFDA products of Chu and Berglund.	21
Figure 6 - Effect of pH on the rate of disappearance of fructose. ⁶²	23
Figure 7 - Precision of 200 μ L Gilson pipetter.	32
Figure 8 - Reaction vial equilibration time at 160°C.	36
Figure 9 - Plot of response factor versus concentration for 6, 9, 10, 13 ; fructose and glucose; and sucrose.	38
Figure 10 - DFDA peak areas and retention times relative to (a) xylitol, current study; and (b) glucitol. ⁶¹	39
Figure 11 - SEC chromatogram of six fractions (1-6) collected for mass balance experiments.	41

Figure 12 - ESMS spectrum of mass balance SEC fraction 1.	43
Figure 13 - ESMS spectrum of mass balance SEC fraction 2.	45
Figure 14 - ESMS spectrum of mass balance SEC fraction 3.	45
Figure 15 - ESMS spectrum of mass balance SEC fraction 4.	46
Figure 16 - ESMS spectrum of mass balance SEC fraction 5.	46
Figure 17 - ESMS spectrum of mass balance SEC fraction 6.	47
Figure 18 - ESMS spectra of sucrose (a), and a mixture of 1-kestose and nystose at cone voltages of 80V (b) and 180V (c).	49
Figure 19 - ESMS spectra of (a) α -D-Fruf-1,2':2,1'- β -D-Frup (9) and of α -D-Fruf-1,2':2,1'- β -D-Fruf (10) at cone voltages of 180V (b) and 80V (c).	50
Figure 20 - ESMS spectra of (a) citric acid, (b) SEC fraction 1, and (c) the typical background at the time of the analysis.	52
Figure 21 - GCFID chromatogram of 8 minute thermolysis of inulin/1.5% citric acid.	53
Figure 22 - Monomer region of 8 minute thermolysis of inulin/1.5% citric acid.	54
Figure 23 - Dimer region, showing 14 DFDA's, of 8 minute thermolysis of inulin/1.5% citric acid.	55
Figure 24 - Typical preparative LC chromatogram from 20 minute thermolysis of inulin/1.5% citric acid at 160°C.	59
Figure 25 - Typical preparative LC chromatogram from fructose/HCl digestion.	62
Figure 26 - Thermolysis of α -D-Frup-1,2':2,1'- β -D-Frup (6) at 160°C in the presence of 1.5% citric acid.	65
Figure 27 - Thermolysis of α -D-Fruf-1,2':2,1'- β -D-Frup (9) at 160°C in the presence of 1.5% citric acid.	66
Figure 28 - Thermolysis of α -D-Fruf-1,2':2,1'- β -D-Fruf (10) at 160°C in the presence of 1.5% citric acid.	67
Figure 29 - Mono-, di-, and trisaccharides accompanying degradation of α -D-Fruf-1,2':2,1'- β -D-Fruf (10).	68
Figure 30 - Conversion (0-40 hr) of inulin/1.5% citric acid to DFDA's at 160°C.	72

Figure 31 - Conversion (0-60 min) of inulin/1.5% citric acid to DFDA's at 160°C. . . .	73
Figure 32 - Wt% individual DFDA's from thermolysis of inulin/1.5% citric acid at 160°C.	75
Figure 33 - Comparison of HPAE-PED chromatograms of inulin/1.5% citric acid after 0, 1, and 3 minutes at 160°C.	83
Figure 34 - Comparison of HPAE-PED chromatograms of inulin/1.5% citric acid after 5, 10, and 15 minutes at 160°C.	84
Figure 35 - Comparison of HPAE-PED chromatograms of a 3 minute thermolysis sample with glucose, fructose, sucrose, 1-kestose, nystose, and DFDA standards.	85
Figure 36 - Glucose, fructose, and sucrose in inulin/1.5% citric acid thermolysis samples.	87
Figure 37 - Nonlinear least squares curve-fitting to DFDA's 1, 10, 5, 8, 9, and 12.	94
Figure 38 - Nonlinear least squares curve-fitting to DFDA's 3, (6)7, 11, 13, 2, and 4. .	95
Figure 39 - Nonlinear least squares curve-fitting to DFDA 14.	96
Figure 40 - Effect of varying the inulin disappearance rate constant on nonlinear least squares curve for α -D-Fruf-1,2':2,1'- β -D-Fruf (10).	98
Figure 41 - 1 st order nonlinear least squares curve-fitting to decay of α -D-Fruf-1,2':2,1'- β -D- Fru f (10).	101
Figure 42 - 1 st order nonlinear least squares curve-fitting to decay of α -D-Fruf-1,2':2,1'- β -D- Fru f (10) with $[A]_0 = 10.2$ wt%.	102
Figure 43 - 2 nd order nonlinear least squares curve-fitting to decay of α -D-Fruf-1,2':2,1'- β -D- Fru f (10) with $[A]_0 = 10.2$ wt%.	104
Figure 44 - Mean wt% conversion (0-60 min) to total DFDA's from inulin with citric acid concentrations of 1.0, 1.5, 2.0, and 2.9 wt%.	111
Figure 45 - Mean wt% conversion (0-300 min) of inulin to total DFDA's from inulin with citric acid concentrations of 1.0, 1.5, 2.0, and 2.9 wt%.	112
Figure 46 - Inulin/1.5% thermolysis at 160, 170, and 180°C.	115
Figure 47 - Comparison of mechanism 1 simulated curve to wt% conversion data for DFDA 10. (Inulin/1.5% citric acid/160°C)	121

Figure 48 - Comparison of mechanism 2 simulated curve to wt% conversion data for DFDA 10. (Inulin/1.5% citric acid/160°C)	123
Figure 49 - Comparison of mechanism 3 simulated curve to wt% conversion data for DFDA 10. (Inulin/1.5% citric acid/160°C)	124
Figure 50 - Simulated curves for DFDA 1, 3, 5, 10, and 12.	125
Figure 51 - Simulated curves for DFDA 2, 4, 7, and 13.	131
Figure 52 - HPAE-PED chromatogram showing D-fructose content of inulin/1.5% citric acid.	134
Figure 53 - Simulation of DFDA 8 according to mechanism 5	136
Figure 54 - Simulated curves for DFDA 9, 11, and 14.	138
Figure 55 - Combined simulation of difuranoses that form directly from inulin.	142
Figure 56 - Overall reaction mechanism applied to 1, 3, 5, 10, and 12.	145
Figure 57 - Overall reaction mechanism applied to remaining 9 DFDA.	146

LIST OF ABBREVIATIONS

μL	microliter	HPAE-PED	High Performance Anion Exchange chromatography with Pulsed Electrochemical Detection
^{13}C	carbon isotope of 13 atomic mass units	HPLC	High Performance Liquid Chromatography
$^2\text{C}_5$	six-membered fructose ring in chair conformation with C-2 extending above the plane of the ring and C-5 extending below	hr	hour
2°	secondary	L	OH group of the highest numbered chiral center points to the left in the Fischer projection
3°	tertiary	LC	liquid chromatography
$^1\text{C}_2$	six-membered fructose ring in chair conformation with C-5 extending above the plane of the ring and C-2 extending below	LS	least squares
C	Celsius (centigrade)	LSODE	Livermore Solver for Ordinary Differential Equations
D	OH group of the highest numbered chiral center points to the right in the Fischer projection	M	context specific - mole/liter or molecular ion
Da/e	mass to charge ratio	M_w	molecular weight
DFA	difructose anhydride	m.p.	melting point
DFDA	di-D-fructose dianhydride	MeOH	methanol
DHL	diheterolevulosan	mg	milligram
DMSO	dimethylsulfoxide	min	minute
dp	degree of polymerization	mL	milliliter
<i>e.g.</i>	for example	mm	millimeter
ESMS	Electrospray Mass Spectrometry	mM	millimole/liter
EtOH	ethanol	mol	mole
FID	flame ionization detector	N	Normality
FOS	fructo-oligosaccharides	NMR	Nuclear Magnetic Resonance
Fru $'$	fructofuranose	OH	hydroxyl functional group
Frup	fructopyranose	ppm	parts per million
fur	fura	pyr	pyranose
g	gram	ref	reference
GC	gas chromatography	RF	response factor
GCFID	Gas Chromatograph with Flame Ionization Detector	RSD	relative standard deviation
GCMS	Gas Chromatograph with quadrupole Mass Spectral detector	SEC	Size Exclusion Chromatography
HMF	5-(hydroxymethyl)-2-furaldehyde	SH $^+$	protonated sucrose
		V	volt
		wt%	weight (as determined in grams, etc.) of analyte relative to total weight, more accurately mass%

Inulin in Nutrition

The β -(2 \rightarrow 1) fructofuranoside linkage of inulin resists the action of mammalian digestive enzymes.² Undigested oligomers of inulin passing into the colon stimulate the growth of colonic microflora, most notably *Bifidobacterium spp.*³⁻⁶ Bifidobacteria are part of the normal colonic microflora in most vertebrates including humans and many domestic animals.⁷ The benefits attributed to the presence of a healthy population of bifidobacteria in the gut include inhibition of carcinogenesis,⁸⁻¹⁰ suppression of putrefactive substances,¹¹ lowering of blood pressure and blood cholesterol in hypercholesteremic subjects,^{12,13} synthesis of B-complex vitamins,¹³ and inhibition of unfavorable bacteria such as *C. perfringens* and *E. coli*.^{14,15} These factors point to inulin as a valuable prebiotic.[‡] In fact, human consumption of inulin and its oligomers has increased steadily since the commercial production in Japan in the early 1980's of Neosugar[®], a synthetic FOS obtained by the action of a fungal fructosyltransferase.¹ This increase is largely attributable to the health benefits that ensue from ingestion of inulin and FOS. **Table 1** lists some registered trade names for products that contain inulin or its oligomers.

Di-D-fructose dianhydrides (DFDAs) are thought to have similar health benefits in animals. In two recent studies^{16,17} broiler chickens were fed caramel obtained from the thermolysis of sucrose, a process which is known to produce DFDAs.¹⁸ The results point in both cases to potential health and weight gain improvements as a consequence of feeding sucrose caramel. Several representative articles offer the reader a more complete treatment

[‡] A prebiotic is a non-digestible food substance that selectively stimulates the growth and/or activity of one or a number of bacteria in the colon, and thus improves the health of the host.

of the role of fructo-oligosaccharides as prebiotics.^{2,18-24}

Trade Name	Manufacturer	Source
Neosugar [®]	Meiji Seika Co., Japan	produced from sucrose by <i>Aspergillus niger</i> fructosyltransferase
Raftiline [®] , Raftilose [®]	Raffinerie Tirlemontoise S.A. (Orafti), Belgium	dried chicory root extract, varying degrees of hydrolysis
Fibruline [®] , Fibrulose [®] , Fructuline [®]	Cosucra S.A., Belgium	dried chicory root extract, varying degrees of hydrolysis
Inubio [®]	Hankintatukku Oy, Finland	dried chicory root extract
Inutest [®]	Lacvosan-GmbH, Linz, Austria	"sinistrin" branched inulin-like fructan from <i>Scilla maritima</i>

Table 1 - Some registered trade names and manufacturers of inulin and fructo-oligosaccharides.

Industrial Uses of Inulin

The major users of inulin are pharmaceutical and food companies, many of which house nutraceutical departments specifically to research products with real or perceived health benefits.²⁵ **Table 2** lists some of the marketable health attributes, applications, and uses of inulin, inulin-containing plant parts, and FOS. One estimate states that in Europe some individuals may consume as much as 12g inulin per day.¹ The world market for these functional food products in 1995 was estimated at \$US 10 billion.²⁵

Application Type	Properties	Occurrence/Use
Health	emulsifier, non-digestible, bifidofactor	fiber supplement, prebiotic
Food	emulsifier, flavor enhancer, gelling agent, bulking agent, mouth feel enhancer, fermentation (agave juice, Mexico)	coffee, tea, yogurt, frozen desserts, biscuits, soups, salad dressings, whipped cream, baked goods, low-fat cheeses, no-fat icings and glazes, chocolate, breakfast cereals, confectionery, low-fat margarine, chicken breast, sausages, processed meats, tequila
Medical	nontoxic, not metabolized, freely filtered through kidney glomeruli, not secreted or reabsorbed by renal tubules, rapidly and evenly distributed in the vascular and extracellular spaces, inulin conjugates are rapidly and completely excreted by kidney into urinary tract	assessment of renal function, assessment of glomerular filtration rate (GFR), conjugation and carrier of drugs, measurement of extracellular space, measurement of cardiac output, detection and measurement of pulmonary edema, indicator of gastric mucosal damage, probe for liposome deposition (radio labeled), potential anti-cancer activity
Industrial	cyclize, derivatize, alkaline/acid degradation, hydrolyze	cycloinulin for molecular encapsulation, phosphate substitute in detergents (after oxidation), feedstock in production of glycerol, substrate for microbial fermentations (ethanol, acetone, butanediol, succinate), precursor of HMF, levulinic acid, mannitol

Table 2 - Applications, properties, and uses of inulin and fructo-oligosaccharides.

Effect of Heat upon Inulin

This study focuses primarily on the reactions of inulin in the presence of citric acid to form di-D-fructose dianhydrides (DFDAs). The experiments all take place at elevated temperatures in anhydrous environments. But even much milder conditions can generate DFDAs from fructose and its polymers. The detrimental economic impact of DFDA formation has already been felt by the sugar processing industry, where DFDAs may form during processing,²⁶ thus interfering with process monitoring²⁷ and inhibiting crystallization.²⁸ In these contexts, DFDAs are nuisance compounds with adverse economic impacts. A number of patents exist, however, for the production of DFDAs, most claiming them as non-

calorific or non-cariogenic sweeteners. (See for example refs²⁹⁻³²). In general, DFDA's may be expected to be present to some degree in any preparation or treatment that involves fructo-oligosaccharides that have been heated, especially in the presence of catalytic amounts of organic acids. Roasted chicory, for example, enjoys a significant presence worldwide as a coffee additive. One study³³ identified four di-D-fructofuranose dianhydrides in a commercially available water soluble extract of chicory. Total DFDA content was ~10%. Baked goods containing inulin as bulking agent or FOS as low calorie sweetener might also be expected to incorporate DFDA's as a result of heating.

DFDA Nomenclature

The 14 DFDA products described in this work differ from one another in subtle, but distinct ways. It can be frustrating at first trying to recognize, let alone ascribe any importance to, the various isomers. Furthermore, historical naming conventions commonly appear in the literature and it is often left to the reader to become familiar with the structures. The most unambiguous naming convention is set forth by the International Union of Pure and Applied Chemistry (IUPAC). A 1997 review of carbohydrate nomenclature³⁴ explains the precedents for naming dihexulose dianhydrides, of which DFDA are a sub-category containing only fructose. The IUPAC name specifies the following for both residues:

1. parent monosaccharide - fructose, sorbose, glucose, etc.
2. ring size - 5-membered furanose, 6-membered pyranose, etc.
3. configuration of the highest numbered chiral carbon - D or L
4. anomeric configuration - α or β
5. anhydride linkage - 1,2':2,1', etc.

A recent review by Manley-Harris and Richards³⁵ proposes a convenient shorthand notation for DFDA. It is this notation that will be most useful to the reader, and that will be used throughout this work. In general, structure illustrations adhere to the Haworth convention, in which the first-mentioned monosaccharide is depicted on the left in the "normal" orientation. The other monosaccharide is drawn to most conveniently show the dianhydride linkages. The linkages appear in the name as pairs of locants, the first (unprimed) locant referring to the carbon of that number in the left-hand residue. The primed locant always refers to the right-hand residue. **Figure 2** highlights the assignment of the first part of the shorthand name α -D-Fruf-1,2':2,1'- β -D-Fruf, which is common to the inulin/citric acid

systems in this work. The reader may work out the remainder of the assignment by analogy.

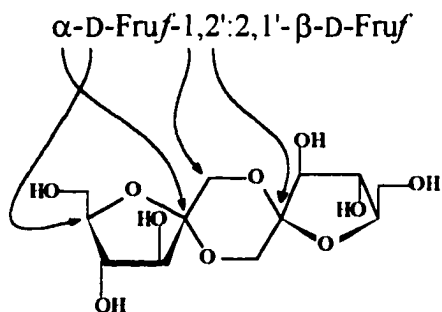


Figure 2 - Example of DFDA naming conventions.

Figure 3 on the following page lists the structures, shorthand names, and trivial names for each of the 14 DFDA's that occur in inulin/citric acid thermolyses. They are presented, for convenience only, in order of elution on capillary GC from earliest to latest. DFA is an abbreviation for difructose anhydride, the historical reference to DFDA's containing only fructofuranose. Similarly, DHL refers to the historical name diheterolevulosan, which applies to DFDA's containing at least one fructopyranose.

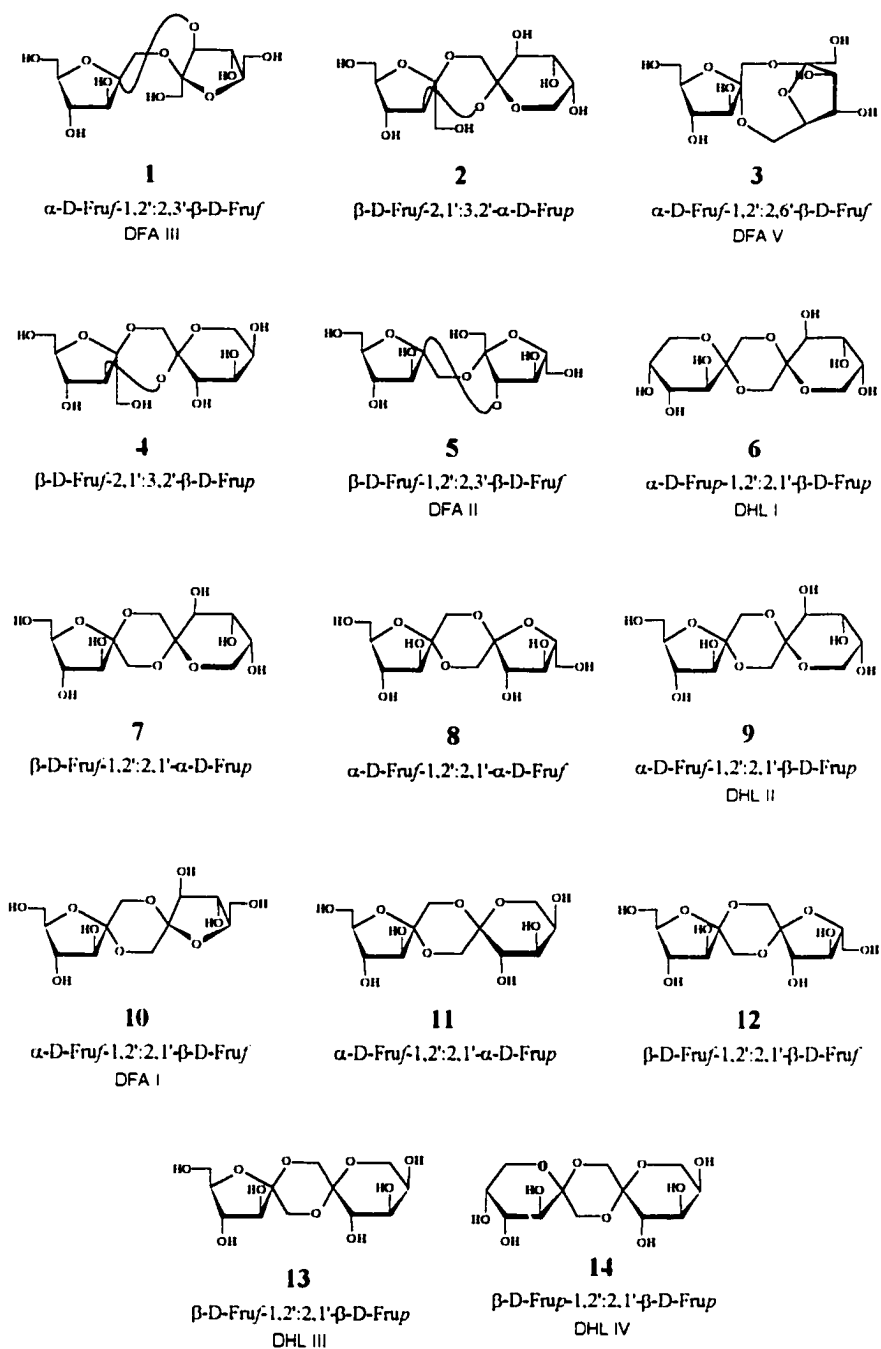
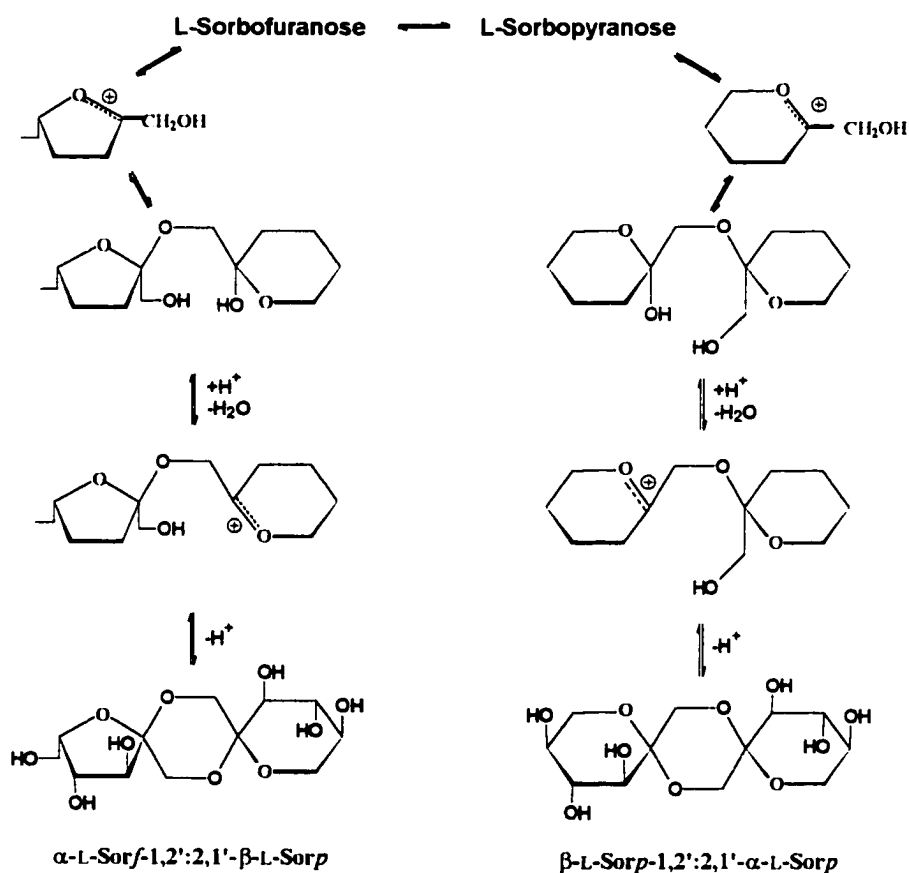


Figure 3 - DFDA structures and shorthand and trivial names.

General Mechanisms of Formation of DFDAs

Although the discovery of di-D-fructose dianhydrides (DFDAs) dates back to the mid 1920's,³⁶ the specific mechanisms by which they form and the kinetic and thermodynamic factors that control their formation under various reaction conditions are little understood. In 1952 Wolfram and Hilton³⁷ proposed a mechanism (**Scheme 1**) that follows the general scheme of Lowry³⁸ for acid catalysis. (A substrate accepts a proton, undergoes some form of bond rearrangement, and releases a proton.) In concentrated HCl, the C-2 hydroxyl (O-2) of L-sorbose is protonated and lost as water to give a sorbofuranosyl or sorbopyranosyl cation



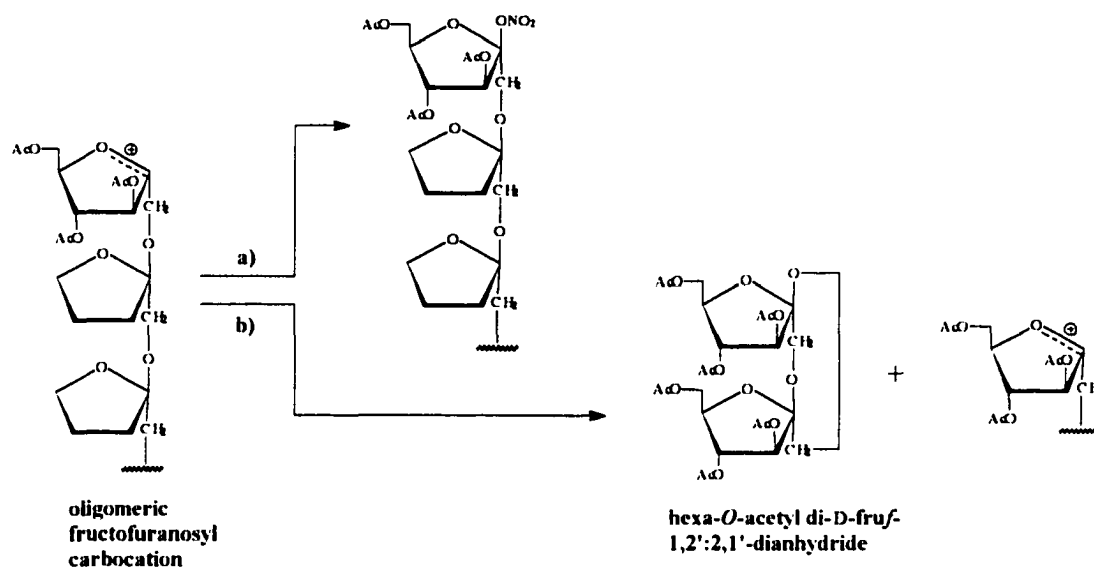
Scheme 1

that is sp^2 hybridized at C2. This cation is subject to nucleophilic attack by OH groups from other sorbose molecules, the products of which are disaccharides containing five and/or six membered rings. One residue of these disaccharides then accepts a proton in similar fashion, loses an OH as water, and forms a carbocation, which reacts intramolecularly with the other residue to form a dianhydride. A number of linkages and anomeric configurations may result from this series of reactions. **Scheme 1** shows two dianhydrides that were isolated by Wolfram and Hilton.[‡] One was identified as di-L-sorbopyranose 1,2':2,1'-dianhydride. The identity of the other product was assumed to be L-sorbofuranose L-sorbopyranose 1,2':2,1'-dianhydride. This general scheme recurs throughout the literature, with minor modifications, right through to the present discussion of DFDA formation.

Boggs and Smith³⁹ proposed a modification of this general mechanism to explain the formation of hexa-*O*-acetyl di-D-fructofuranose-1,2':2,1'-dianhydride from inulin triacetate in fuming nitric acid (**Scheme 2**). In this case, a glycosidic oxygen accepts a proton and the inulin is hydrolyzed. The resultant oligomeric carbocation reacts with either a) nitrate ion, or b) the glycosidic oxygen of the next residue in the chain to form the dianhydride. The acetylated O-3, O-4, and O-6 of each fructose residue in the chain preclude the formation of other linkages *e.g.* 2,3':1,2'; the acetyl group does not easily carry a positive charge in a manner analogous to the loss of a proton, and is therefore not easily displaced. This also means that at least three fructose residues must be present in the chain in order for DFDA to form, the third residue carrying the positive charge - as a carbocation - once the

[‡] Wolfram and Hilton were not able to assign anomeric configurations. The anomers shown in Scheme 1 were arbitrarily chosen to illustrate the general mechanism.

dianhydride is formed.



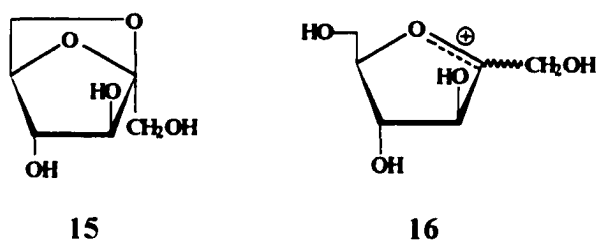
Scheme 2

Discussion of the mechanisms of DFDA formation did not reappear in the literature until the 1980's. In the meantime, the advent of NMR spectroscopy and its application to DFDA's allowed researchers to assign anomeric configurations and ring conformations to DFDA's that until that time were largely speculative. (See for example refs⁴⁰⁻⁴³)

Thermal Treatments of Fructose-containing Substrates

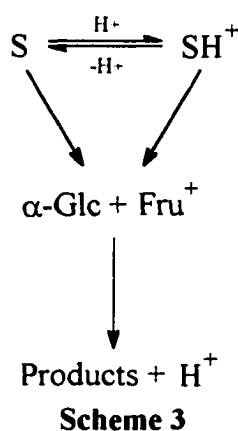
Sucrose Degradation in DMSO - The research in this section is not directly relevant to the current study; no mention is made of DFDA's. However, the fundamental significance lies in the contribution to our understanding of the non-aqueous chemistry of carbohydrates, mainly sucrose. These studies reinforce the concept of a fructofuranosyl cationic intermediate and provide evidence for the presence of anhydrofructose species.

Beginning in 1981, Moody and Richards published a series of papers⁴⁴⁻⁴⁷ describing the reactions that fructosyl-containing compounds, principally sucrose, undergo in hot dimethyl sulfoxide (DMSO). The authors had intended to explore the utility of thermolyzing sucrose in the presence of nucleophiles *e.g.* alcohols as a synthetic route to fructofuranosides. The work evolved, however, into a characterization of the factors affecting the hydrolysis of sucrose under these conditions. The first of the series⁴⁴ describes three separate fates for sucrose thermolysis in DMSO in the presence of alcohols: 1) alkyl-D-fructofuranosides, 2) non-specific degradation, and 3) 2,6-anhydro- β -D-fructose (**15**). The precursor intermediate in each case is the fructofuranosyl cation (**16**), which arises from the cleavage of the sucrose glycosidic bond. The anhydrofructose was never present in more than trace quantities, but



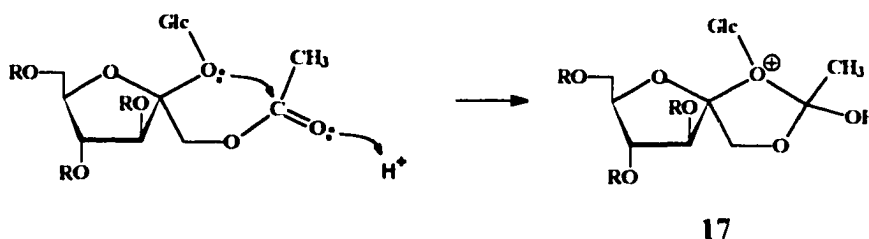
increased with steric interference of the larger alcohols.

The second paper of the series⁴⁵ revealed the critical role that traces of an acid impurity play in the thermolysis of sucrose. Sulfuric and *p*-toluenesulfonic acids both catalyzed the reaction while the weaker acetic acid did not. The mechanism shown in **Scheme 3** was proposed. Using known initial concentrations for sucrose and acid, and by observing the rate of disappearance of sucrose, the authors derived a first order rate expression and showed that all of the reaction proceeds *via* protonated sucrose (SH⁺).



Additional experiments using water or *N,N*-dimethylformamide as solvent, or using DMSO and adding water at varying intervals, confirmed the involvement of the protonated glycoside in the rate determining step. Also, small amounts of water (1%) added to an ongoing reaction caused only minor changes. This last discovery is relevant to the current study, in which the only water present during thermolysis is the small amount produced by dehydration of inulin and its oligomers.

In the third paper in the series,⁴⁶ partial or complete acetylation were shown to impart increased resistance to acid catalyzed degradation of sucrose in DMSO. Two of the factors thought to contribute to this effect were the electron-withdrawing nature of the acetyl group and competition for the proton catalyst by the carbonyl oxygen. Both of these factors would result in less efficient protonation of the glycosidic oxygen and slower rate of scission. A third contributing factor was thought to be the formation of a five-membered ring complex (17) that presumably would be more stable than the open form that is protonated at the glycosidic oxygen.



Shortly thereafter, Moody and Richards⁴⁷ measured the rates of glycosidation of fructose, sorbose, arabinose, and sucrose, and the rate of transglycosidation of various methyl and benzyl fructosides, in 1:1 alcohol:DMSO (alcohol = MeOH or EtOH) in the presence of sulfuric acid (10-100mM). Ketoses (fructose and sorbose) are glycosylated more easily than the aldose (arabinose) because they form a tertiary carbocation versus the secondary cation for the aldose. Therefore, only traces of acid are needed to produce them. This is important in controlling non-specific degradation to *e.g.* 5-(hydroxymethyl)-2-furaldehyde (HMF), which is favored by high concentrations of acid and high temperatures. The kinetic products of the transglycosidations have the same ring size as the starting material. They then slowly mutarotate to an equilibrium mixture of α - and β -D-fructofuranosides and β -D-fructopyranosides.[‡]

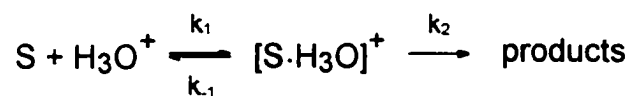
More importantly for the current study, the work includes experiments designed to gain insight into the mechanism of furanoside-pyranoside interconversion. These experiments determined the rates of glycosidation of the benzyl 2-thio-D-fructosides relative to their

[‡] Angyal and Bethell⁴⁸ showed α -D-fructopyranose to be highly disfavored due to synaxial interaction of the C2 hydroxyl with O3. Conformation inversion from ¹C₂ to ²C₅, instead of relieving this interaction, places the C2 hydroxymethyl group in the axial position and increases the *gauche* interaction between it and O3. Also, α -D-fructopyranose in ¹C₂ has three axial hydroxyls, two of which are cis-1,3, while β -D-fructopyranose has only two axial hydroxyls in either conformation. Moody and Richards found no evidence of α -D-fructopyranose in any of their experiments.

oxygen analogs. The elegant series of deductions that followed identified 2,6-anhydro- β -D-fructofuranose (**15**) as the key intermediate instead of acyclic D-fructose dialkyl acetals. This anhydride will play an important role in future mechanistic discussions of DFDA formation from inulin, since it provides a reasonable pathway between fructofuranose and fructopyranose.

Hydrolysis - Heyraud *et al.*⁴⁹ isolated the fructo-oligosaccharide components, from dp2 (sucrose) to dp7, from the juice of Jerusalem artichoke and measured the rate of hydrolysis of the individual components at 70°C in sulfuric acid (pH 2). The rate of disappearance of each oligosaccharide was assumed to follow pseudo first order kinetics. The glucose-fructose glycosidic bond was 4-5 times more resistant to hydrolysis than the fructose-fructose bond; scission of the glucose-fructose bond leads to the formation of a secondary carbocation while scission of the fructose-fructose bond leads to a tertiary carbocation.

Mandal *et al.*⁵⁰ determined rate constants of acid catalyzed hydrolysis of sucrose in aqueous mixtures of four solvents - protophobic protic glycerol, protophilic protic urea, aprotic dioxane, and dipolar aprotic DMSO. The kinetic behavior in all four solvents was similar to that in water and was therefore considered to be specific hydrogen ion catalysis following the general reactions depicted in **Scheme 4**. As the proportion of glycerol



Scheme 4

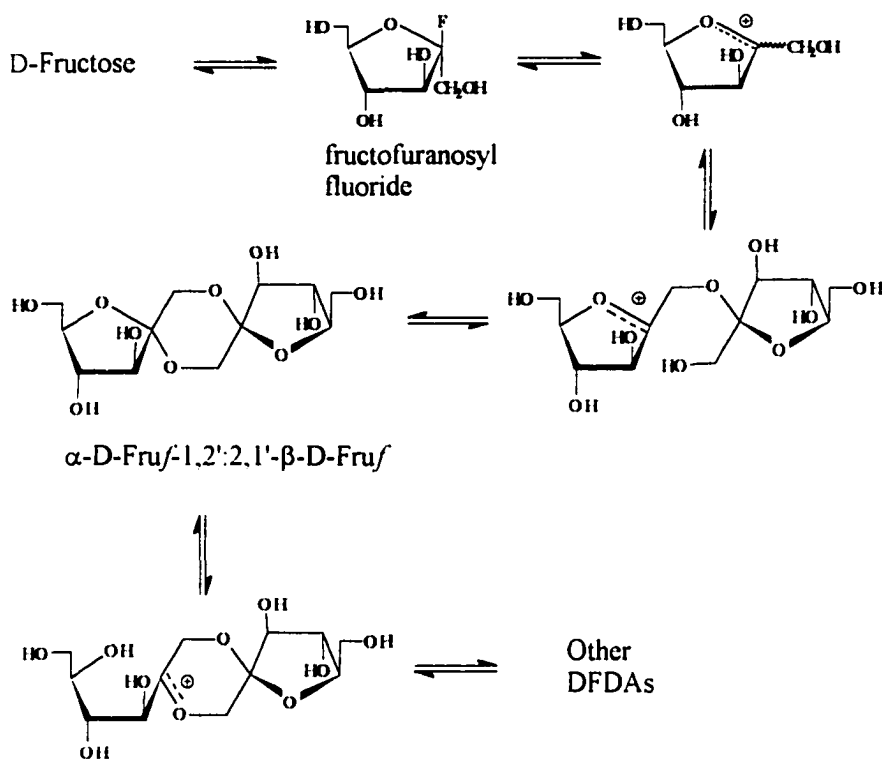
increased so did the observed rate constant because H^+ became less stabilized and more active as a catalyst. Hydrolysis rate relative to that in water showed a marked dependence on the basicity of the solvent. With the addition of the more basic solvents urea, DMSO, or up to 10 mol% dioxane, the observed rate constant decreased, H^+ becoming more solvated and less catalytically active. It is difficult to draw direct correlations between this behavior and the solvation of H^+ in anhydrous inulin/citric acid melts, in which inulin acts as a principal reactant and as solvent. It is fair to expect the many hydroxyl groups of inulin to effect some degree of solvation. As the thermolysis proceeds and the proportion of DFDA increases, so too does the number of free hydroxyl groups decrease, and we might expect solvation of H^+ to decrease. It is not clear, however, what effect acidic degradation products have on the availability of H^+ as a catalyst. Literature precedents do not exist.

DFDA Formation from Fructose-containing Substrates

Anhydrous HF - In 1985 Defaye *et al.*⁵¹ demonstrated the formation of DFDA from inulin and D-fructose upon treatment with anhydrous hydrogen fluoride at 20°C, and from D-fructose in sulfur dioxide at -78°C. These were the first non-aqueous systems employed to obtain DFDA. Under these conditions, inulin gave high yields of α -D-Frup-1,2':2,1'- β -D-Frup (**6**), α -D-Fruf-1,2':2,1'- β -D-Frup (**9**), β -D-Fruf-1,2':2,1'- β -D-Frup (**13**), β -D-Frup-1,2':2,1'- β -D-Frup (**14**), α -D-Fruf-1,2':2,1'- β -D-Fruf (**10**), and a previously unknown compound, β -D-Fruf-2,1':3,2'- β -D-Frup (**4**). The ratio of products varied with time, temperature, and initial concentration, suggesting equilibration among isomers.

The authors assigned a pair of ^{13}C signals to the anomeric carbons of fructofuranosyl

fluorides presumed to be in equilibrium with fructofuranosyl cation. They proposed a mechanism (**Scheme 5**) whereby α -D-Fruf-1,2':2,1'- β -D-Fruf (**10**) forms first, then isomerizes *via* ionic intermediates to other DFDA. Support for isomerization lies in the fact that α -D-



Scheme 5

Frup-1,2':2,1'- β -D-Frup (**6**) and β -D-Frup-1,2':2,1'- β -D-Frup (**14**) treated with HF produced the same product mixture as D-fructose under the same treatment. A subsequent study⁵² using L-sorbose confirmed this behavior and reinforced the furanosyl ion as central to the mechanism.

Originally, isomerization appeared to be a legitimate mechanistic path among DFDA in the current study. However, the low temperature HF systems employed by Defaye and

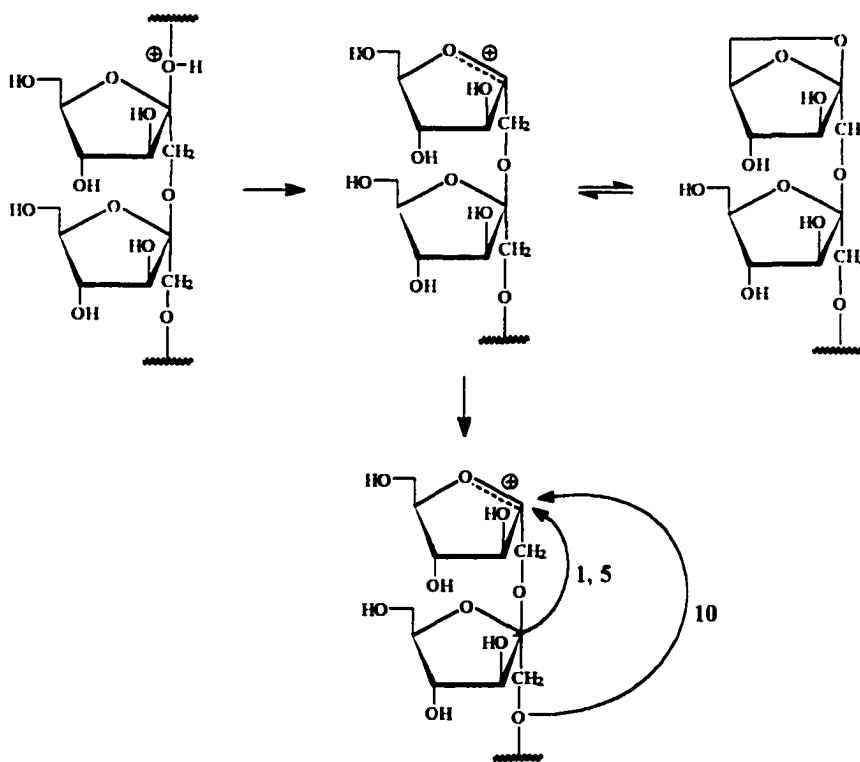
coworkers are fundamentally different than the high temperature inulin/citric acid systems. It was not known to what extent their findings may be applied to the high temperature treatments used in this study.

In 1988, Defaye *et al.*⁵³ extended their treatment with HF to inulin triacetate.[‡] Their proposed mechanism was expanded to include an inulobiosyl cation intermediate, as well as the fructofuranosyl cation, both of which were presumed to form the fluoride species before reacting further to form DFDA. The aforementioned ¹³C signals which were assigned to the anomeric carbons of fructofuranosyl fluorides appeared in all the crude product mixtures. It has been suggested³⁵ that in this system, the fluoride ion plays an important role in stabilizing cations that form in the reaction mixture. The solvent is a potent fluorinating agent. The fructofuranosyl fluorides that are presumed to form likely serve as reactive intermediates and provide lower energy pathways to such reactions as isomerizations, pathways that would not be available in inulin/citric acid melts.

Pyrolysis of Inulin - An investigation of the pyrolysis of inulin⁵⁸ revealed a rather high yield of DFDA. A subsequent detailed analysis of the products of inulin pyrolysis⁵⁹ revealed a mixture of products, the DFDA component of which contained predominantly di-D-fructofuranose dianhydrides. The trimethylsilyl derivatives of these compounds revealed seven peaks, three of which were positively identified as α -D-Fruf-1,2':2,1'- β -D-Fruf (**10**),

[‡] Defaye and coworkers have published many papers, several in collaboration with The Technical University of Denmark. A major focus has been formation of dianhydrides from carbohydrates and their derivatives in anhydrous HF and especially pyridinium poly(hydrogen fluoride), and the steric and electronic effects that govern product distributions under varying conditions of reaction time, temperature, etc. (See, for example, refs ⁵⁴⁻⁵⁷)

β -D-Fruf-1,2':2,3'- β -D-Fruf (**5**), and α -D-Fruf-1,2':2,3'- β -D-Fruf (**1**). Two others had mass spectra consistent with di-D-fructofuranose dianhydrides, and two minor peaks showed mass spectral evidence of the presence of furanose-pyranose dianhydrides. This is an important result in that the major DFDA products differ significantly from those obtained by the treatment of inulin with anhydrous HF.⁵¹ It was not possible to extend the pyrolysis times sufficiently to differentiate kinetic from thermodynamic products; at 200°C thermal degradation proceeds more rapidly than DFDA production. **Scheme 6** illustrates the mechanism proposed for DFDA formation from inulin. The first step is cleavage from the inulin chain of a fructo-oligosaccharide intermediate, which retains the \oplus charge as a terminal fructofuranosyl residue. Subsequent intramolecular attack by O-3' leads to either α -D-Fruf-



Scheme 6

1,2':2,3'- β -D-Fruf (1) or β -D-Fruf-1,2':2,3'- β -D-Fruf (5), depending on whether attack occurs α or β to the fructosyl carbon. If the glycosidic O-1' attacks the α side of the cation, the product is α -D-Fruf-1,2':2,1'- β -D-Fruf (10). The suggestion that an oligomer with a terminal anhydro unit is also present is based on analogy to similar pyrolysis experiments in the same laboratory using glucose as the substrate.⁶⁰ This mechanism is plausible given the extent to which the authors were able to isolate and positively identify the DFDA components of the reaction mixture. A subsequent investigation⁶¹ led to the identification of all 14 DFDA and the isolation and characterization of 13 of them.

DFDA Formation from D-Fructose - Only one study exists that attempts a detailed kinetic description of DFDA formation. In 1990, Chu and Berglund⁶² monitored DFDA formation in acidified, nearly saturated fructose solutions. Using HCl to adjust the initial pH (2.65, 4.35, 5.90), various solutions (65 to 92%) were held at constant temperature (30 to 60°C) for two weeks and the concentrations of four products - D1, D2, D3, D4 - were measured at intervals by integration of HPLC peaks. (See **Figure 4** for structures assigned by the authors to these products.)

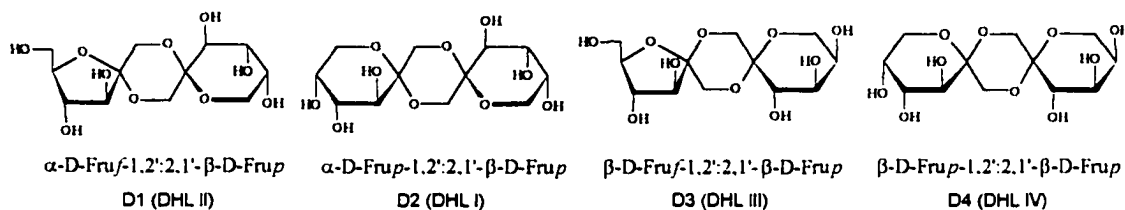


Figure 4 - The four DFDA products of Chu and Berglund.

The concentration versus time curves are reconstructed, using data from Chu's thesis,⁶³ in **Figure 5** for the experiment at 60°C and pH 2.65 with 80.3% initial fructose

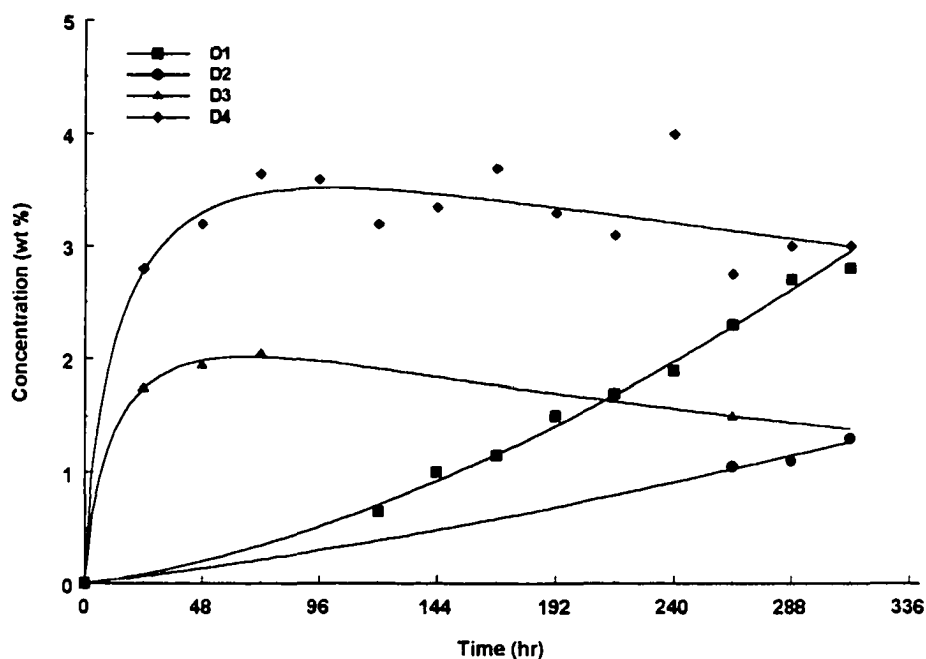
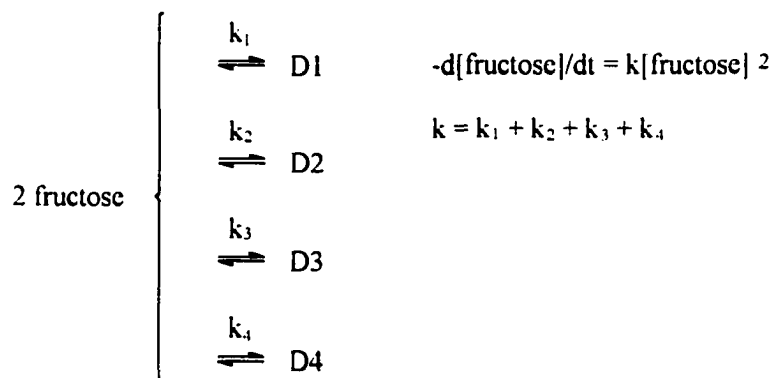


Figure 5 - Formation and decay of the four DFDA products of Chu and Berglund.

concentration. These data show D3 and D4 forming rapidly and reaching plateaus of ~2 and 3.5%, respectively, after about three days. Their concentrations then decline very slowly for the duration of the two week reaction time. The product D1 appears on day 5 at ~0.7% and increases to ~3% after two weeks. The rate of formation of D1 increases slightly as the reaction proceeds. The product D2 appears abruptly on day 11 at ~1% and remains more or less at that concentration.

The authors propose a simple, second-order rate equation (**Scheme 7**) of the form $-d[A]/dt=k[A]^2$, where each product forms directly from fructose and does not contribute, through isomerization or other processes, to the concentrations of the other products. This



Scheme 7

greatly simplifies the kinetic treatment. The authors cite the relative acid stability of DFDA's in general to justify this approach.

The second-order rate constants for total DFDA formation show an unexplained anomaly (**Figure 6**). The kinetic plot of the inverse fructose concentration versus time for pH 2.65 is relatively linear. The same plots for pH 4.35 and 5.90, however, show two separate linear regions with different slopes (rates). The authors fit the latter data with a two section broken line. Their explanation is that all four products contribute to the disappearance of fructose in the first section, while only D1 and D2 contribute in the second stage. No explanation is given for the straight line behavior at pH 2.65. In fact, the authors state specifically that, regardless of pH or temperature, the point at which D3 and D4

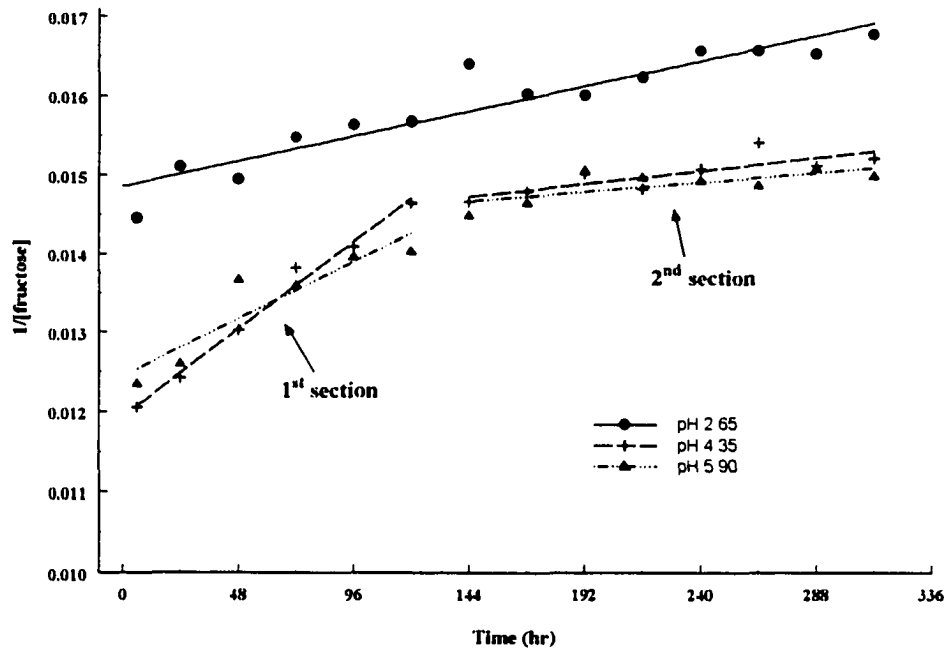


Figure 6 - Effect of pH on the rate of disappearance of fructose.⁶²

formation levels off coincides with the break point in the two section line. This does not appear to be true for pH 2.65. The data for formation of DFDA at pH 4.35 and 5.90 are even less conclusive; no data exists before five days.[‡]

Total DFDA formation increased with increasing acid concentration, but only for the first reaction section. The rate for the second reaction section was pH-independent (*i.e.* similar slope/rate for all pH). The authors postulate the change in rate to be the result of solvation of fructose at concentrations less than about 70%, which *selectively* [sic] inhibits the formation of D3 and D4, but not the formation of D1 and D2.

[‡] Data for these plots were excerpted from Chu's thesis.⁶³

The analytical techniques used to quantify DFDA in this study seem inappropriate. Firstly, the identity of two of the four HPLC peaks (excluding the fructose peak) is established solely on the basis of following the procedure of Hamada *et al.*^{64‡} for synthesizing α -D-Fruf-1,2':2,1'- β -D-Frup and α -D-Frup-1,2':2,1'- β -D-Frup (D1 and D2 in Chu and Berglund). The other two LC peaks are assumed by Chu and Berglund to be β -D-Fruf-1,2':2,1'- β -D-Frup and β -D-Frup-1,2':2,1'- β -D-Frup (DHLs III and IV; D3 and D4). The authors justify this assignment by stating that these two products each contain at least one β -pyranose moiety. There is no evidence given to support this statement.

In Chu and Berglund's analysis, the four DFDA in question show up as minor deflections of the baseline in both LC and GC traces. This inevitably results in considerable variation when integrating, which may be the source of some of the scatter observed. This low detector response probably also accounts for the paucity of early data, especially for D2, which is not detected until eleven days into the reaction. The authors used primarily HPLC to determine both DFDA and fructose concentrations. This works well for fructose, since it is unlikely that other monosaccharides will be present in the reaction mixture, and fructose is abundant at all stages of the reaction, but another technique should have been used to quantify DFDA. The use of GCMS for confirmation is quite acceptable, but the column used was inadequate (6 ft 3% OV-225). By using a short column the authors limited their ability

‡ Hamada *et al.*⁶⁴ incorrectly assigned the configuration of DHL I as the α - α anomer and DHL II as β -Fruf-1,2':2,1'- α -Frup. Hamada refers for confirmation to Binkley *et al.*,⁴³ who also misnamed both compounds. The correct assignments were published in 1985 by Defaye *et al.*⁵¹ Chu and Berglund listed the correct structures for these two DFDA but did not mention the discrepancies in earlier work. They also incorrectly listed the linkage of β -D-Fruf-1,2':2,3'- β -D-Fruf as 1,2':2,4' and included a still unknown DFDA in their table of "known" DFDA. (β -Frup-1,2':2,3'- β -Frup has never been isolated.) These errors exemplify typical problems with DFDA identification.

to resolve isomers. They state that, since difructose dianhydrides are nonreducing dimers, there is no chance of having anomeric isomers overlapped in the same peak. This statement is entirely false. GC analyses in this laboratory give baseline resolution for 14 DFDA, as well as other disaccharides, fructose and glucose anomers, and a range of trisaccharides, all at nearly ten-fold lower detection levels than Chu and Berglund achieved. It requires a 30 meter column, however, to achieve such resolution. Even so, two DFDA coelute and another appears on the leading edge of the sucrose peak. The authors also state that there were only four compounds formed in the reaction. In fact, experiments in this laboratory with fructose and HCl following Hilton⁶⁵ yielded predominantly DHLs I, II, III, and IV. But four other DFDA formed as well (α -D-Fruf-1,2':2,3'- β -D-Fruf (1), β -D-Fruf-1,2':2,1'- α -D-Frup (2), α -D-Fruf-1,2':2,1'- α -D-Fruf (8), and β -D-Fruf-1,2':2,1'- β -D-Fruf (12)).

In summary, we must read Chu and Berglund's wt% conversion data with caution. In looking at the DFDA conversion plot, it may be that the plateaus for D3 and D4 represent a steady state in which β -D-Fruf-1,2':2,1'- β -D-Frup (13) and β -D-Frup-1,2':2,1'- β -D-Frup (14) are being produced from fructose, likely in a second-order process. Their slow, steady decline might indicate they are reacting further to form the thermodynamically more stable α -D-Frup-1,2':2,1'- β -D-Frup (6) and α -D-Fruf-1,2':2,1'- β -D-Frup (9).[‡] The appearance of α -D-Fruf-1,2':2,1'- β -D-Frup (9) roughly coincides with the steady state. The data for α -D-Frup-1,2':2,1'- β -D-Frup (6) are inconclusive in this regard. Additionally, any conclusions we

[‡] The differences in stability are caused, in part, by the anomeric effect, which is discussed in more detail in the Results section. In accordance with the anomeric effect, the central dioxane ring will have substituent oxygens in the axial position. In the former compounds (13 and 14), this puts the central ring in a boat conformation. In the latter (6 and 9), the central ring is in the more stable chair conformation.

draw about the mechanism of formation must be tempered with the possibility of both interconversion between DFDA's and the presence in small amounts of other DFDA's. These possibilities each represent another layer of complexity in the mechanistic model.

The assertion that selective inhibition of the formation of D3 and D4 occurs due to solvation of fructose is puzzling. If, as the rate equation stipulates, each product forms directly from fructose, there seems no reason why solvation should inhibit D3 and D4 but not D1 and D2. If solvation were inhibiting formation of all DFDA's from fructose, D1 and D2 must be arising from the isomerization of D3 and/or D4, and the rate equation should reflect it. A study designed to determine the fate of each individual DFDA in the system might throw some light on this difficult question.

The second-order rate constants for the formation of total DFDA's were calculated from the slopes of the plots of inverse fructose concentration versus time.[‡] These plots were fitted with two section broken lines. This kind of behavior has been observed in at least two other cases, both of which were titrations.⁶⁶ The reactions proceeded at a specific rate until a reagent was consumed, at which point the rate slowed abruptly. A pH effect like this would seem to argue for the inclusion, or at least consideration, of hydronium ion concentration in the rate expression. Also, total DFDA's formed in Chu and Berglund's experiments increased with increasing acid concentration, but only for the first reaction section. The rate for the second reaction section was pH-independent, giving further cause to consider the role of $[H^+]$.

[‡] This assumes that DFDA's are the sole products that arise from fructose in these systems. Mass balance experiments could reveal non-specific degradation, perhaps to volatile products, in which case disappearance of fructose would not directly correspond to formation of DFDA's.

Acid Stability of DFDAs

Numerous studies³⁵ attest to the resistance of DFDA to acid hydrolysis compared to inulin, for example. Individual DFDA vary in their resistance to acid hydrolysis. Although a good portion of the work has been carried out on the per-*O*-methyl derivatives, there can be no doubt that DFDA are stable in acid solution relative to singly linked saccharides. (Additional detail on stability of DFDA in the presence of acid is given on page 70.) The current study provides some insight into DFDA stability in high temperature, anhydrous, acidified thermolyses.

Statement of Purpose for the Current Study

This study completes work[†] commenced in the Shafizadeh Center for Wood & Carbohydrate Chemistry at the University of Montana. The aims of that work were:

1. Isolate and characterize the individual components of thermally treated inulin and sucrose.
2. Extend the mass spectral library of the per-*O*-methylsilyl derivatives of DFDA's.
3. Determine the effects of variations in reaction conditions, including time, temperature, and the presence of additives, upon the relative proportions of the components in thermal product mixtures of DFDA's.

The work described herein consists of a thorough examination of thermolysis of inulin and 1.5wt% citric acid at 160°C. These experiments were then extended to higher temperatures and to varying citric acid concentrations. The end goal was to propose a reasonable mechanistic explanation for the formation of DFDA's from inulin using both empirical methods and computer modeling.

[†] Funding for this work was provided by the Cooperative State Research, Education and Extension Service, U.S. Department of Agriculture, under Agreement No. 95-37500-2098.

THERMOLYSIS RESULTS AND DISCUSSION

Chapter Introduction

Anhydrous melts of inulin/citric acid mixtures give high yields of di-D-fructose dianhydrides. The systems studied in this work contain from 1.0 to 2.9 wt% citric acid and yield up to 35 wt% DFDA after 30 minutes at 160°C. The focus of this chapter, which contains the majority of the thermolysis experimental work for this study, is to rationalize the relative distribution of individual DFDA at any point during the reaction.

The chapter begins with quality assurance procedures, followed by some preliminary experiments to confirm DFDA identities. The tools employed for this purpose were a combination of gas chromatography, NMR, and mass spectrometry. The primary quantitative tool for measuring DFDA conversion was capillary gas chromatography with flame ionization detector (GCFID). An explanation of the important characteristics of a typical chromatogram is given.

One of the first questions to arise concerns the chemical fate of DFDA after they have formed from inulin. Therefore, experiments were designed to isolate individual DFDA and test their fate by heating them in the presence of citric acid and measuring the products. Perhaps the simplest situation from a modeling standpoint would have all DFDA simply not degrade. In fact, some DFDA are thermally stable toward acid catalyzed degradation in these experiments. For others, their chemical fate is more complicated. A partial explanation for relative stability is offered based on structure.

The conversion data for individual DFDA during inulin thermolysis reveal a number of trends in relative abundance. A closer inspection of the structural similarities and

differences among DFDA's leads to a chemical mechanism that explains the formation from inulin of nine of the 14 DFDA's. Evidence for the source material for the other five DFDA's is provided by qualitative experiments that track the shift in inulin oligomers from higher to lower degree of polymerization during thermolysis.

The underlying theme throughout this and the next chapter is to provide a sensible explanation, in kinetic terms, of the reactions that inulin and its thermolysis products undergo. The data presented in this chapter, and the conclusions that are drawn, provide a foundation from which to build a suitable kinetic mechanism.

Quality Assurance and Preliminary Experiments

This section describes quality assurance measures taken early in the research to ensure accuracy and precision. Also presented here are the melting points of the inulin/citric acid powders used, a temperature equilibrium experiment to determine how much time elapses before the samples reach the prescribed reaction temperature, and a determination of response factors for individual DFDA's. The identities of the 14 DFDA's relevant to this study are confirmed by three separate instrumental techniques. Also included are a quantitative mass recovery experiment to expose any indeterminate loss of sample and a qualitative mass distribution experiment by Electrospray Mass Spectrometry (ESMS).

Purity of Reagents - During the course of this study, reagents had to be replenished. Each new bottle of *n*-hexane, pyridine, and Tri-Sil was tested for impurities by carrying out the complete sample workup procedure without any sample present. That is, the new reagent was used in the derivatization, cleanup, and analysis steps as outlined on page 153. At no point did impurities interfere with any peak of interest.

Precision of Weight and Volume Measurements - Weighing of xylitol and inulin/citric acid was accomplished with a high precision electronic balance as described. Gilson micro-pipetters (10-200 μ L and 200-1000 μ L) were used to dissolve the internal standard xylitol in a known volume of pyridine, then to deliver precise aliquots of that solution to each sample vial. The manufacturer serviced the larger pipetter shortly after this study began; its accuracy and precision were, therefore, recently certified. I tested the precision of the former, smaller

capacity pipetter, by repeatedly transferring the same volume of pyridine to a beaker on an electronic balance and recording the weight increase. Precision was excellent, as indicated in **Figure 7**.

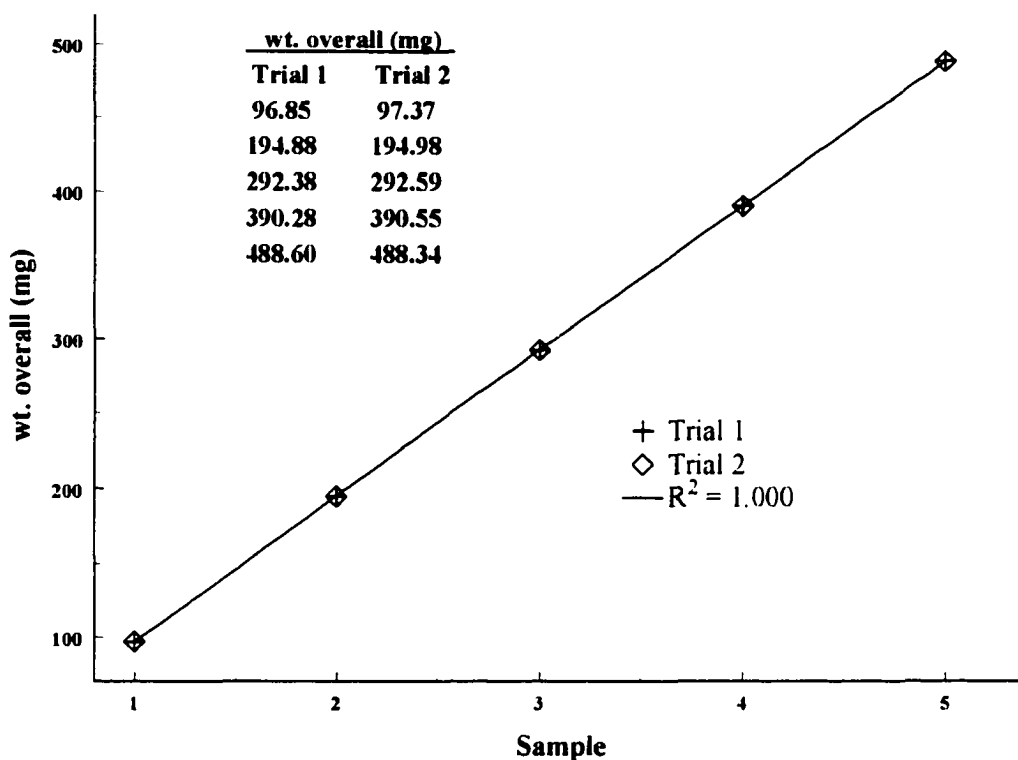


Figure 7 - Precision of 200 μ L Gilson pipetter.

Consistency of Detector Response - The GCFID was initially fitted with a split/splitless injector, which proved inadequate for quantifying samples of this type; repeated injections of the same sample gave wildly disparate quantitation of DFDAs. Split/splitless injectors contain glass injection port liners that must be carefully treated with silylating reagents to fully deactivate them. Poorly or incompletely deactivated liners adsorb and release analytes in

unpredictable ways and are the source of several chromatographic symptoms including poor peak shape, baseline deviations, and inconsistent detector response. The latter problem proved intractable and forced the installation of an on-column injector, which is much less susceptible to problems of this type.†

The on-column injector introduces liquid sample directly onto the column. This eliminates a major potential source for error. The limitations on contaminant levels imposed by the on-column system do not apply to the relatively clean samples that arise from thermolysis of inulin. That is, there are few if any non-volatile or marginally soluble compounds present and the on-column injector has proven reliable. **Table 3** compares the peak area ratios of α -D-Fruf-1,2':2,3'- β -D-Fruf (**1**) and α -D-Fruf-1,2':2,1'- β -D-Fruf (**10**) to

	DFDA 1/ xylitol	DFDA 10/ xylitol	DFDA 1/ DFDA 10
Injection 1	0.23	0.18	1.25
Injection 2	0.52	0.57	0.91
Injection 3	0.30	0.27	1.11
Injection 4	0.46	0.45	1.02
Injection 5	0.51	0.57	0.90
% RSD*	32	43	14

* relative standard deviation

Table 3 - Comparison of selected peak area ratios for repeated injections using split/splitless injector.

† The split mode of the split/splitless injector allows relatively large volumes of "dirty" samples to be analyzed by capillary GC. The majority of the volatilized sample, along with its contaminant element, bypasses the column to waste, while a small portion of relatively clean sample is introduced onto the column. The splitless mode of this injector introduces small amounts of relatively clean, volatilized sample directly onto the column, where it is recondensed, then subjected to some specific temperature program. Thus the same injector serves two different functions.

xylitol and to each other after five consecutive injections of the same sample using the split/splitless injector.[‡] These two DFDA's were chosen because they consistently give prominent, well resolved, symmetrical peaks.

The linear response range of the flame ionization detector (FID) is large.⁶⁷ As long as the weight of analyte does not exceed the column's ability to produce symmetrical peaks, the ratios of analytes to internal standard should be consistent to within a few percent from one injection to the next. As the table indicates, there was virtually no peak area consistency from one injection to the next using the split/splitless injector.

The new on-column injector alleviated the majority of this inconsistent response. A series of three consecutive injections of a sample from an early experiment yielded the peak area ratios in **Table 4** for α -D-Fruf-1,2':2,3'- β -D-Fruf (**1**), β -D-Fruf-1,2':2,3'- β -D-Fruf (**5**), and α -D-Fruf-1,2':2,1'- β -D-Fruf (**10**). RSD for peak area ratios are vastly reduced (0-3%).

	DFDA 1/ xylitol	DFDA 5/ xylitol	DFDA 10/ xylitol	DFDA 1/ DFDA 5	DFDA 1/ DFDA 10	DFDA 5/ DFDA 10
Injection 1	0.72	0.30	0.82	2.40	0.88	0.37
Injection 2	0.70	0.29	0.82	2.41	0.85	0.35
Injection 3	0.70	0.29	0.80	2.41	0.88	0.36
% RSD	2	2	1	0	2	3

Table 4 - Comparison of selected peak area ratios for repeated injections using on-column injector.

[‡] The sample was a 45 minute thermolysis of inulin/1.5% citric acid at 160°C. This and the other eight samples in this experiment showed inordinate scatter when converted to wt% conversion of inulin to DFDA's. This scatter is what prompted the test for consistency and subsequent change to an on-column injector. This and all previous sample sets were re-injected on the new system.

Melting Points of Inulin/Citric Acid Mixtures - At 200°C inulin changes from a white, granular powder to a white paste that slowly darkens and softens to a pale brown fluid,⁵⁹ after which the melt continues to darken and begins to foam considerably. Homogeneous mixtures of inulin and small weight percentages of citric acid undergo a glass transition at much lower temperatures (**Table 5**). There is no exact melting point for these mixtures. They appear as

	Wt% Citric Acid			
Trial	1.0	1.5	2.0	2.9
1	155	152	150	146
2	156	154	151	147
3	155	153	151	146
Avg.	155	153	151	146

Table 5 - Approximate melting points (°C) for inulin/citric acid mixtures.

solid foams having regions with sharp, angular, well defined edges. These edges begin to soften almost imperceptibly as the temperature increases (~2°C/min). The “melting point” readings in **Table 5** represent the point where the edges have unmistakably lost their crispness. This point occurs at 155°C for the 1.0% mixture, and decreases by ~9°C as the wt% of citric acid increases to 2.9. In all cases the aggregates appeared to liquify completely within several seconds.

Temperature Equilibration in Reaction Vials - Thermolysis of inulin samples was conducted by lowering 5 mL screw-cap vials containing ~10mg sample into silicon oil that was heated to a predetermined temperature. There is a short delay (**Figure 8**) from the time the reaction

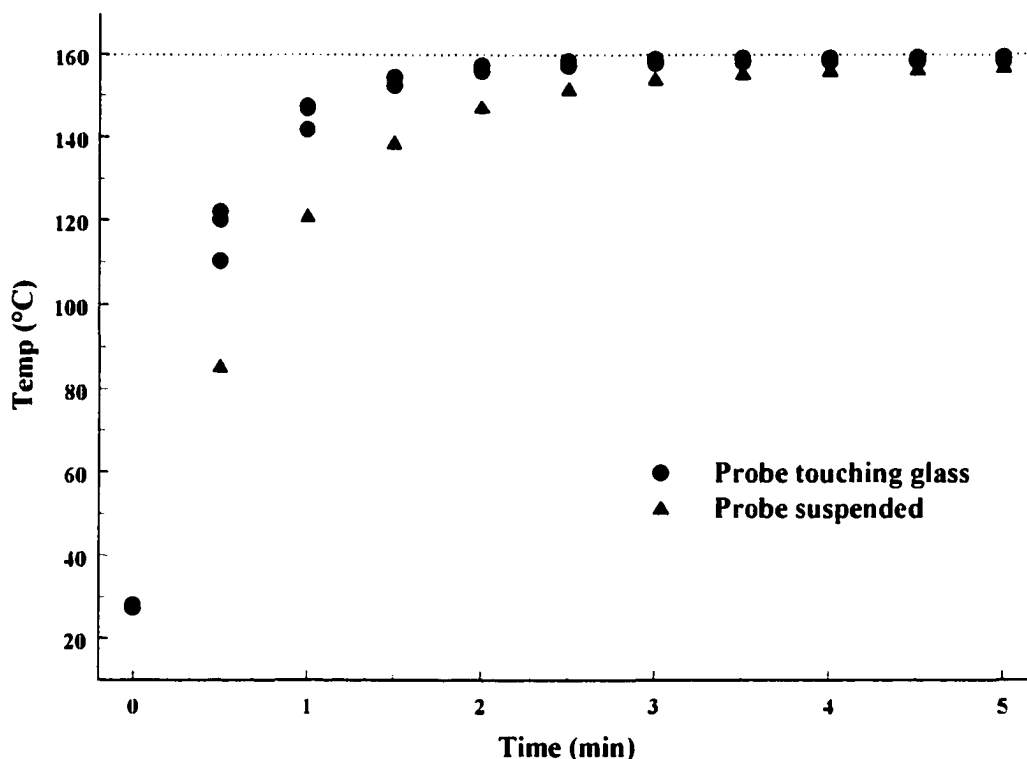


Figure 8 - Reaction vial equilibration time at 160°C.

vials are immersed in oil to the time after which the temperature within the vials remains constant. A thermocouple probe inserted through a septum at the top of a reaction vial and touching the inside, bottom edge showed this delay to be approximately two minutes. The graph shows three repetitions with the probe touching the inside of the vial and one experiment with the probe suspended ~1mm from the bottom. The glass equilibrates slightly

faster than the air within the vial. No adjustment to the treatment of data was made because of this delay.

Response Factors - The GCFID response factors (RF) for the per-*O*-trimethylsilylated derivatives of α -D-Fru μ -1,2':2,1'- β -D-Fru μ (**6**), α -D-Fru ν -1,2':2,1'- β -D-Fru μ (**9**), α -D-Fru ν -1,2':2,1'- β -D-Fru ν (**10**), and β -D-Fru ν -1,2':2,1'- β -D-Fru μ (**13**) are reported in **Table 6**.[‡]

	6	9	10	13	D-fructose	D-glucose	sucrose
RF	.61	.64	.57	.58	.90	.91	.79
Conc. in parentheses (mg/mL)	(.18)	(.17)	(.22)	(.17)	(.21)	(.20)	(.22)
	.62	.66	.58	.59	-	-	-
	(.075)	(.070)	(.088)	(.066)			
	.59	.62	.55	.56	.91	.88	.72
	(.019)	(.017)	(.022)	(.016)	(.021)	(.020)	(.022)
	.62	.66	.59	.59	.85	.86	.74
	(.0038)	(.0034)	(.0044)	(.0033)	(.0021)	(.0020)	(.0022)
Mean RF	0.61	0.65	0.57	0.58	0.89	0.88	0.75

Table 6 - Response factors of per-*O*-trimethylsilylated derivatives of **6**, **9**, **10**, **13**, fructose, glucose, and sucrose relative to internal standard xylitol.

Concentrations (mg/mL) are shown in parentheses. The data also include RF values for D-fructose, D-glucose, and sucrose. The xylitol concentration in all samples and standards was approximately equal. The concentrations of the standards ranged from 0.002 to 0.2 mg/mL, which elicited similar minimum and maximum detector response as actual samples. It was not practical, nor even possible given time constraints, to isolate all 14 DFDA in quantities sufficient to determine response factors. Therefore, an average RF of 0.60 was applied to all DFDA. These data are presented in **Figure 9** as a plot of RF versus concentration.

[‡] The isolation of these four DFDA is described in detail in a later section.

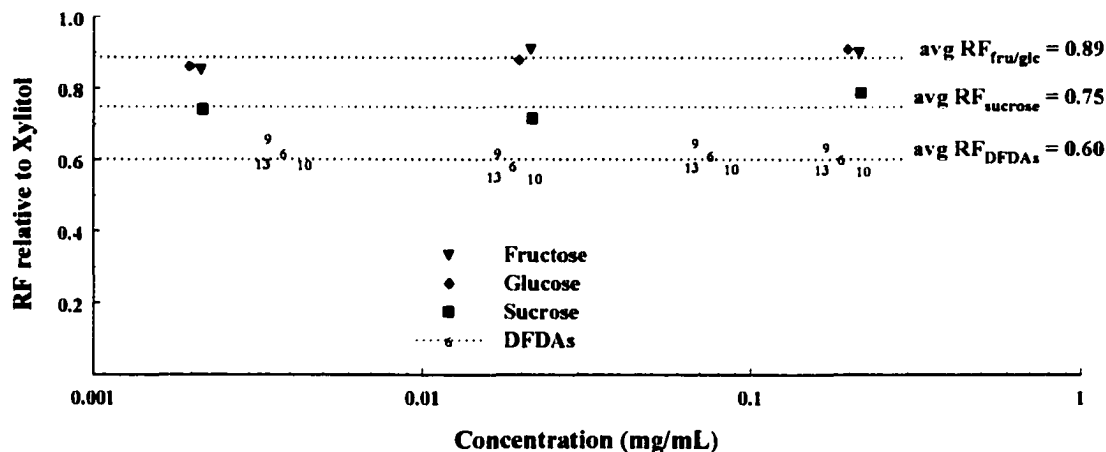


Figure 9 - Plot of response factor versus concentration for **6**, **9**, **10**, **13**; fructose and glucose; and sucrose.

Confirmation of DFDA Identities - DFDA identities were initially determined by comparison of relative retention times and abundances with previously established values.⁶¹ The schematic representation in **Figure 10** illustrates a near perfect GC/FID retention time correlation. Slight differences in column length and temperature program account for minor variations. The structure of α -D-Fruf-1,2':2,6'- β -D-Fruf (**3**), previously isolated from *Aspergillus fumigatus* and identified,⁶⁸ was confirmed in the laboratory of ref.⁶¹

The mass spectra of compounds **1-14** in the current study were also a close match to the database compiled by Manley-Harris and Richards.⁶¹ Slight variations in relative abundance which were observed between the two studies are attributable to the use of different instruments. The ¹³C spectra of α -D-Frup-1,2':2,1'- β -D-Frup (**6**), α -D-Fruf-1,2':2,1'- β -D-Frup (**9**), α -D-Fruf-1,2':2,1'- β -D-Fruf (**10**), and β -D-Fruf-1,2':2,1'- β -D-Frup (**13**) were compared with published values.^{54,61} **Table 7** lists chemical shifts obtained in the

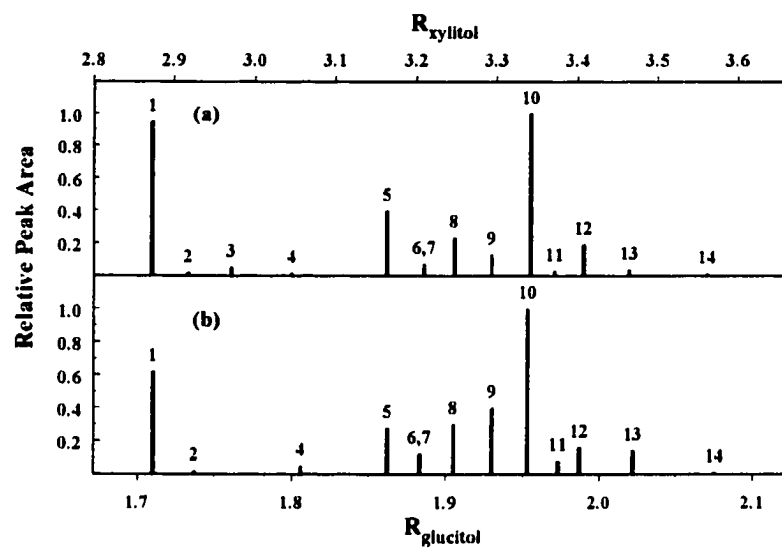


Figure 10 - DFDA peak areas and retention times relative to (a) xylitol, current study; and (b) glucitol.⁶¹

current study; published values are shown in parentheses. The down field shift of ~1.1 ppm in the current data relative to the published data is due to the use of different internal standards.

	Carbon Chemical Shifts (ppm)											
	C-2	C-2'	C-3	C-4	C-5	C-3'	C-4'	C-5'	C-6	C-6'	C-1	C-1'
α -D-Frnp-1,2':2,1'- β -D-Frnp (6)	97.5 (96.4)	96.5 (95.3)	71.0 (69.9)	72.7 (71.5)	66.0 (64.8)	70.5 (69.4)	72.6 (71.4)	71.0 (69.9)	61.7 (60.5)	62.6 (61.5)	62.9 (61.7)	65.5 (64.4)
α -D-Frnp-1,2':2,1'- β -D-Frnp (9)	104.3 (103.1)	97.7 (96.5)	83.9 (82.8)	79.8 (78.6)	85.5 (84.3)	70.6 (69.4)	71.0 (69.9)	71.0 (69.9)	63.2 (62.1)	63.2 (62.1)	63.5 (62.3)	65.5 (64.3)
α -D-Frnp-1,2':2,1'- β -D-Frnp (10)	104.5 (103.3)	100.8 (99.7)	83.9 (82.7)	79.7 (78.6)	85.5 (84.3)	79.0 (77.8)	76.6 (75.4)	83.2 (82.1)	63.2 (62.0)	64.7 (63.5)	63.7 (62.6)	64.5 (63.4)
β -D-Frnp-1,2':2,1'- β -D-Frnp (13)	102.7 (101.8)	98.8 (97.9)	81.8 (80.8)	77.0 (76.0)	83.8 (82.8)	73.0 (72.1)	71.4 (70.4)	71.0 (70.0)	64.4 (63.5)	66.2 (65.2)	64.2 (63.3)	66.8 (65.8)

Table 7 - ^{13}C chemical shifts for **6**, **9**, **10**, and **13**. Published values^{54,61} in parentheses.

Mass Balance and ESMS - Three separate ~100mg samples of inulin/1.5% citric acid were thermolyzed at 160°C for 20 minutes. The product from each experiment was weighed immediately after thermolysis, then dissolved in water and chromatographed using *LC Method (iv)*. **Figure 11** is a typical SEC chromatogram from these experiments and indicates the division of the eluant into six fractions.[‡] Each of the fractions was rotoevaporated and the

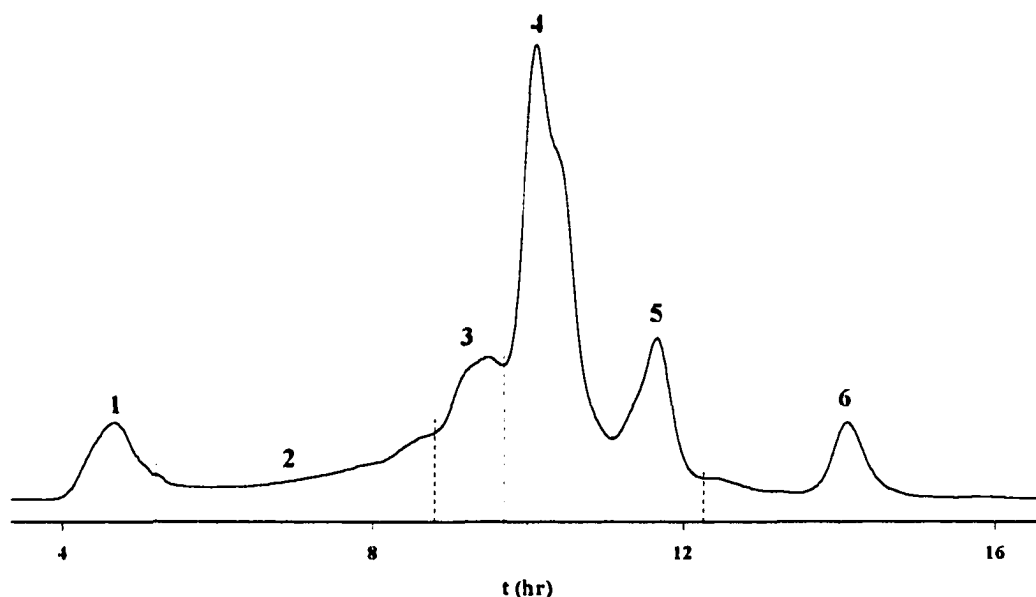


Figure 11 - SEC chromatogram of six fractions (1-6) collected for mass balance experiments.

residue weighed. Weights as percentage of total mass recovered for fractions 1-6 are reported in **Table 8**. Recovery of mass after thermolysis was nearly 100% for trials 1 and 2, but was not measured for trial 3. The relative amount of starting material recovered after SEC varied considerably in these three trials (91, 84, and 99%). HMF (5-(hydroxymethyl)-2-

[‡] This fractionation pattern was used in the last of three trials in order to further isolate thermolysis products for subsequent electrospray mass spectral analysis. In the first two experiments fractions 3 and 4 were collected as one.

		Trial 1	Trial 2	Trial 3
Total recovery after thermolysis (%)		99	97	nd
Total recovery after SEC (%)		91	84	99
Weight of fraction as percentage of material recovered after SEC (%)	Fraction 1	7.3	7.5	9.5
	Fraction 2	13.2	7.6	13.1
	Fraction 3			7.5
	Fraction 4	56.8*	63.1*	43.8
	Fraction 5	16.6	17.2	19.1
	Fraction 6	5.9	4.7	7.2

* Collected as two separate fractions in Trial 3. nd - not determined.

Table 8 - Recovery of product mass from 20 minute thermolysis of inulin/1.5% citric acid at 160°C.

furaldehyde) is a major degradation product^{58,69,70} with a relatively low boiling point (~115°C). Other minor products (*e.g.* H₂O, CO, CO₂, CH₂O, CH₃CHO, MeOH, EtOH) may form from secondary reactions of dehydration products.⁷¹ Some loss of these products during rotoevaporation is expected. Also, fractions were automatically dispensed into test tubes over the course of each 16 hour run (120 tubes x 8 min/tube). Some general loss of material is expected as a result of eluant transfer.

The dried fractions from trial 3 were dissolved in H₂O and subjected to Electrospray Mass Spectrometry (ESMS). Compositions of these fractions were similar to those of earlier investigations.^{59,61} For positive ion mode, samples were spiked with NaCl to aid ionization. Therefore, the reader must subtract 23 from the mass/charge value (Da/e) for each peak to obtain molecular weight.[‡] For example, a DFDA contains two fructose monomers (180 g/mol each), minus two glycosidic bonds (18 g/mol each), plus a sodium adduct (23 g/mol) and the

[‡] In the negative ion mode. Da/e values represent actual molecular weights.

ESMS positive ion peak for any DFDA occurs at 347. Oligomers show up as series of peaks incremented by 162 (fructose residue minus glycosidic linkage). The ESMS conditions used were developed using sucrose and other disaccharides as standards. The high cone voltage (180V) is intended to reduce hydrogen bonding among solutes and between solutes and the solvent.

The ESMS spectrum of fraction 1 is shown in **Figure 12**.[‡] Higher order polymers are excluded and should elute in fraction 1. But only small traces of material larger than 500 mass units appear in the spectrum. As determined by experimentation, citric acid ($C_6H_8O_7$)

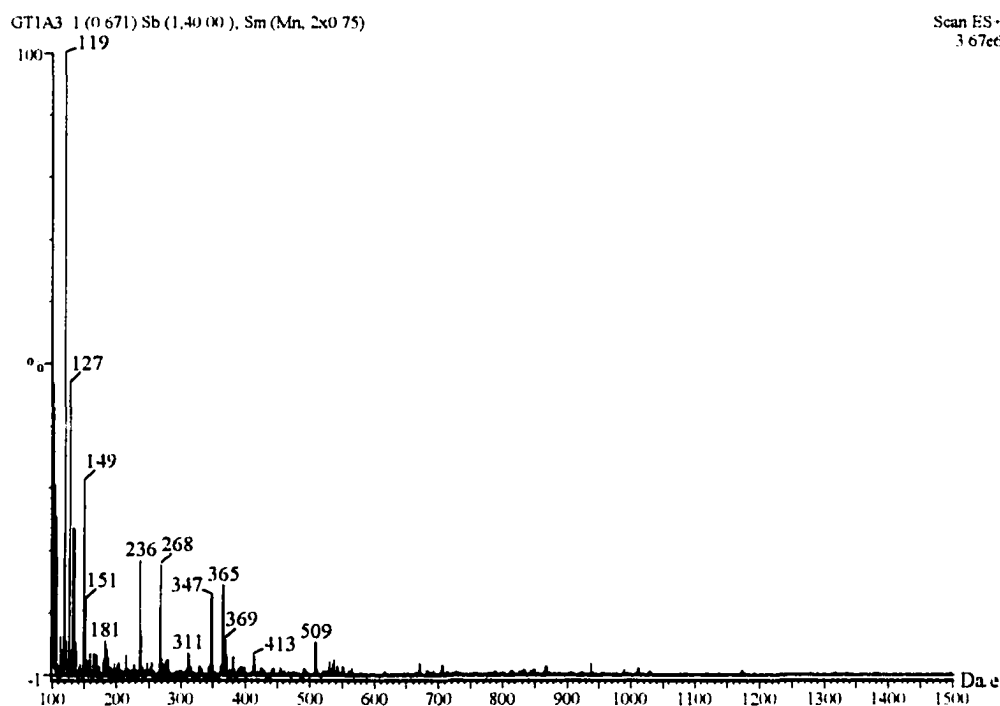


Figure 12 - ESMS spectrum of mass balance SEC fraction 1.

[‡] The header in this and subsequent ESMS figures contains sampling and processing information that includes a sample name, the number of the spectrum in the data file, the duration of the scan, and subtraction and smoothing parameters. The upper right corner shows the scan mode and the absolute intensity of the most abundant peak. All spectra are scaled to 100% of the most abundant peak, regardless of absolute intensity, and little correlation may be drawn between peak intensity and concentration.

is also excluded on BioGel P2. This means fraction 1 was probably acidic and rotoevaporation may have caused oligomeric material to hydrolyze.

Peaks 119 and 127 appeared in all six fractions. Peak 119 corresponds to furfural ($C_5H_4O_2 + 23$). All fractions were colored to some degree, indicating the presence of unsaturated degradation compounds. It is not known why furfural would elute in more than one fraction. The identity of 127 is not known. Peak 149 appeared in fractions 1, 5, and 6 and corresponds to HMF. Its presence in fraction 6 is expected - HMF elutes later than fructose monomers - and some HMF in fraction 5 may be expected since the resolution is poor between fractions; the dividing lines were chosen arbitrarily and "cross-contamination" is expected. The presence of HMF in fraction 1 may be the result of hydrolysis during rotoevaporation of hemi-acetal HMF polymers that formed during thermolysis.

The 347 and 509 peaks are presumed to be DFDA and DFDA + monomer. The peak at 365 is DFDA + H_2O , which corresponds to a singly-linked disaccharide.

Figure 13 shows the ESMS spectrum for fraction 2. Peaks 236, 268, 311, 347, 365, and 509 probably arise as a result of incomplete resolution between fractions. Peaks 509, 671, 833, and 995 represent a series of glycosylated DFDAs with one, two, three, and four glucose residues, respectively. Traces of DFDAs with five and six residues (1157, 1319) are evident when the y-axis is rescaled.

Fraction 3 (**Figure 14**), the "trimer" fraction, contains predominantly DFDA + glycosyl residue (509). This fraction also contains DFDA (347) and the glycosylated DFDA tetramers and pentamers at 671 and 833.

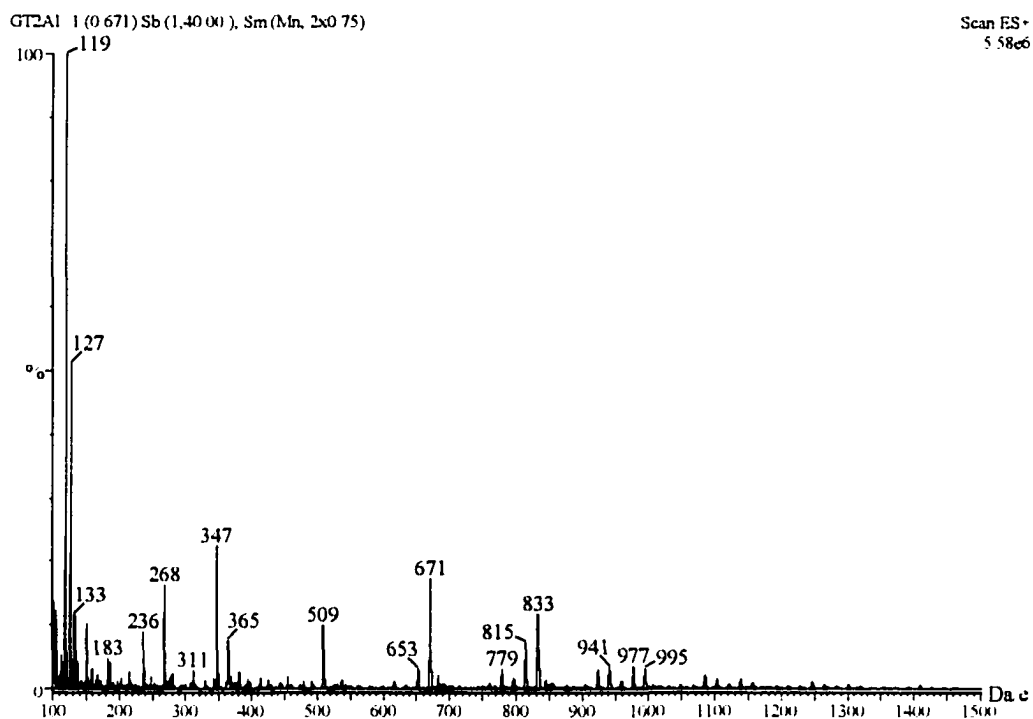


Figure 13 - ESMS spectrum of mass balance SEC fraction 2.

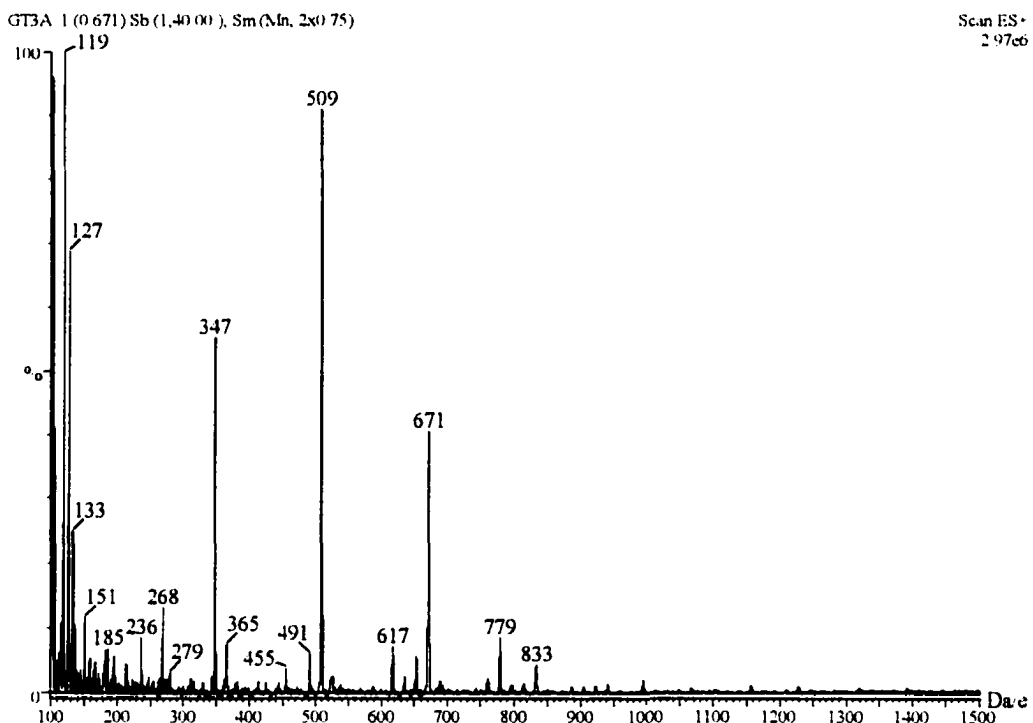


Figure 14 - ESMS spectrum of mass balance SEC fraction 3.

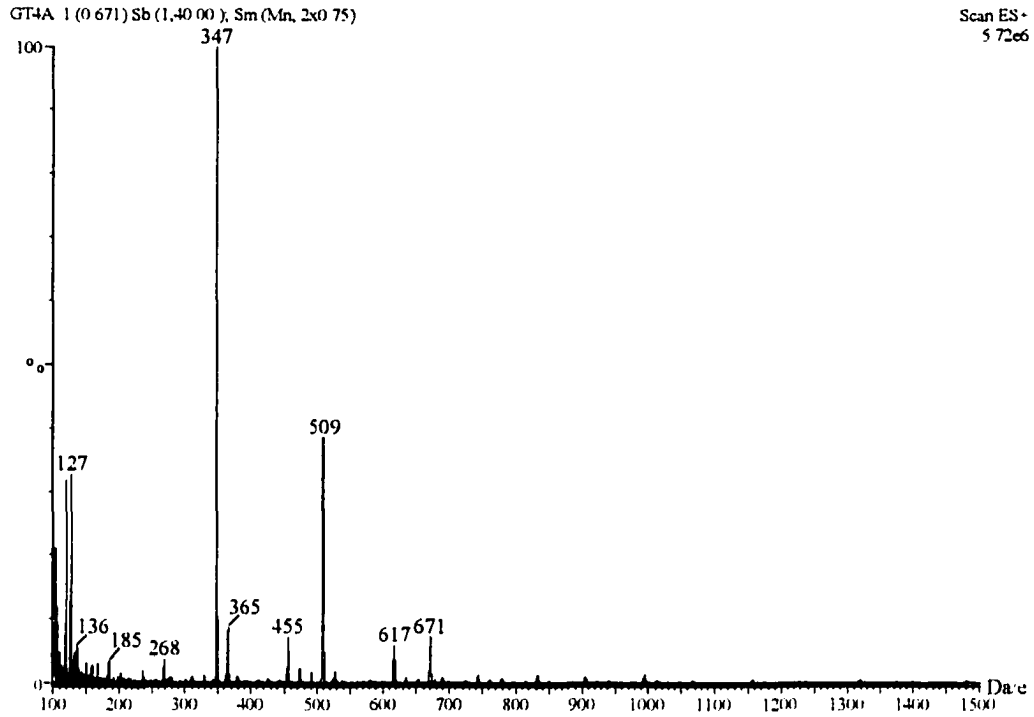


Figure 15 - ESMS spectrum of mass balance SEC fraction 4.

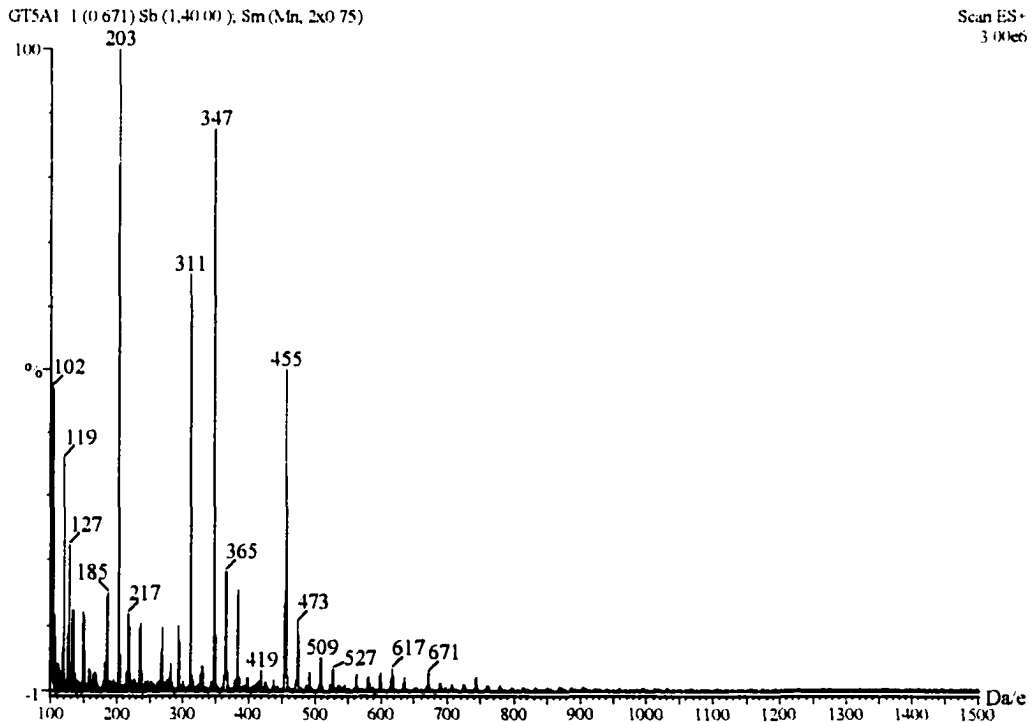


Figure 16 - ESMS spectrum of mass balance SEC fraction 5.

Fraction 4 (**Figure 15**) is the "dimer fraction" and contains predominantly DFDA's (347), but the 509 and 671 peaks are also present. Fraction 5 (**Figure 16**) elutes late from the SEC system and contains predominantly monomers and dimers. The peak at 203 is assumed to be fructose, and the peak at 185 is assumed to be anhydrofructose.

The latest eluting fraction is 6 (**Figure 17**), which contains mostly HMF (149). The peak at 181 could conceivably be HMF + methanol. There is a small monomer peak (203) from overlap between fractions.

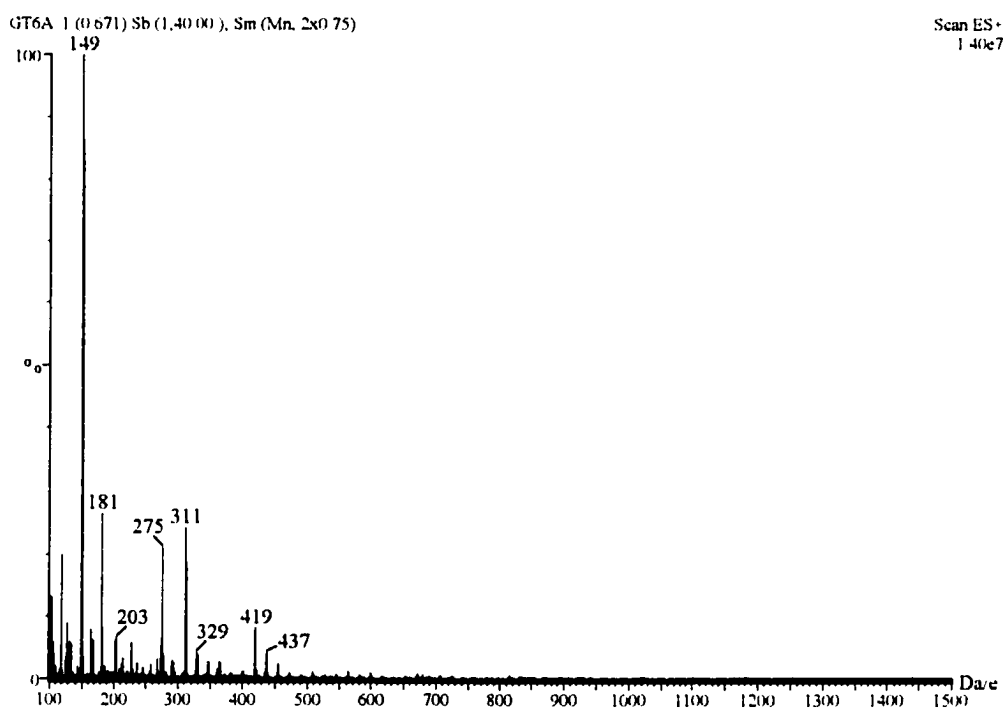


Figure 17 - ESMS spectrum of mass balance SEC fraction 6.

The basic composition, then, for SEC fractions 1-6 is as expected. But the spectra reveal an interesting phenomenon. Each glycosylated DFDA peak is accompanied by one or more peaks that correspond to the loss of H_2O molecules. For example, in fraction 5 (**Figure 16**) the 491 (not labeled), 473, and 455 peaks may represent the loss of one (M-18), two (M-

36), and three (M-54) H₂O from a DFDA + monomer peak (509). The 311 peak in fraction 5 could arise from the loss of three H₂O from the singly linked disaccharide at 365. In fraction 2 (**Figure 13**) the peaks for DFDA + 2, 3, and 4 fructose residues (671, 833, and 995) are each accompanied by M-18, M-36, and M-54 peaks.

Although the high cone voltage used in this analysis may be responsible for some loss of H₂O from samples within the instrument, the spectra provide evidence that the majority of dehydration occurred during thermolysis. For example, in fraction 4 the 365 peak is many times more abundant than the 311 peak, which is buried within the baseline. In fraction 5 the 311 peak is several times more abundant than 365. The same is true for 455 and 509. The 455 peak is smaller than 509 in fraction 4 and much larger than 509 in fraction 5. If loss of H₂O were occurring solely within the instrument the relative abundances of the M-54 peaks to their respective parent peaks would be consistent across the fractions. This lack of consistency points to loss of H₂O during thermolysis and subsequent fractionation of M-54 compounds according to molecular weight.

Further confirmation is provided by the spectra of sucrose, 1-kestose, and nystose. Under ESMS conditions identical to the above, the singly-linked disaccharide sucrose does not dehydrate (**Figure 18a**). It does, however, partially hydrolyze and revert, as evidenced by traces of monomer (203) and singly-linked trimer (527).

The spectrum of a mixture of 1-kestose and nystose was obtained at two different cone voltages. The lower voltage (80V) spectrum (**Figure 18b**) contains predominantly 1-kestose (527) and nystose (689). Traces of singly-linked pentamer (851) appear as a result of the enzymatic origin of the sample. There are M + methanol peaks at 397 (sucrose or

inulobiose + 32), 559 (1-kestose + 32), and 721 (nystose + 32). The only possible dehydration peak is 347. The high voltage (180V) spectrum of 1-kestose and nystose

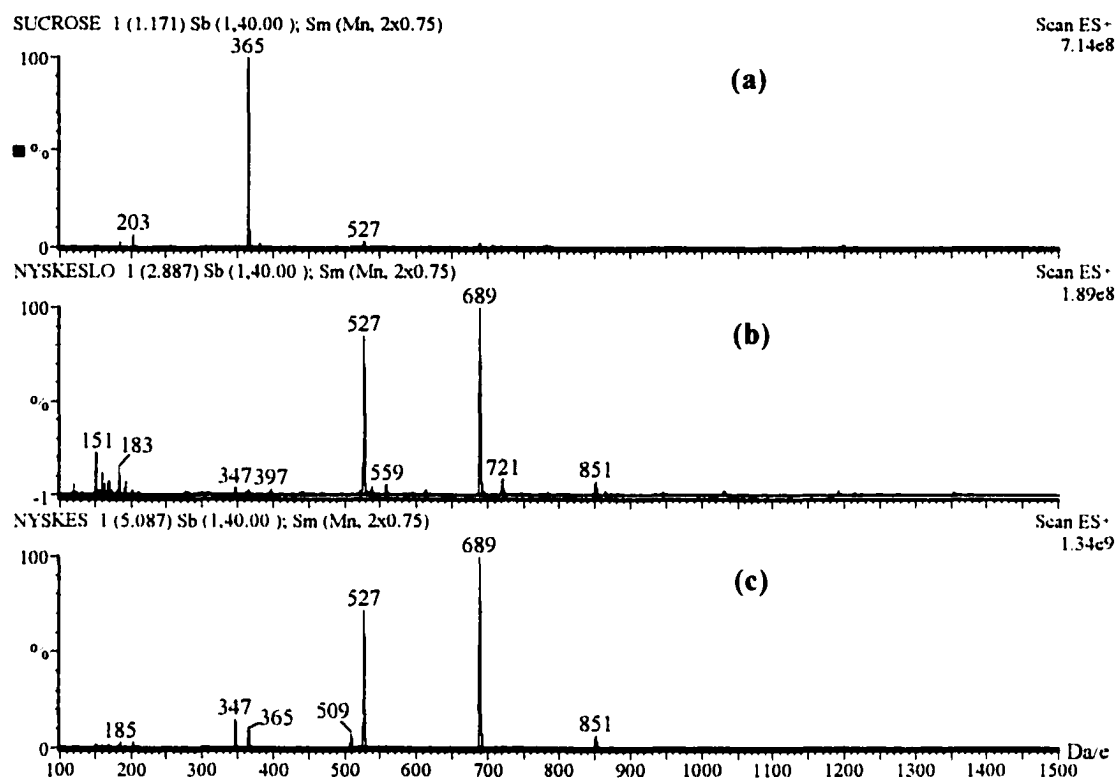


Figure 18 - ESMS spectra of sucrose (a), and a mixture of 1-kestose and nystose at cone voltages of 80V (b) and 180V (c).

(Figure 18c) contains M-18 peaks for the singly-linked disaccharide and for 1-kestose, but not for nystose or the pentamer. Obviously, the higher cone voltage is sufficient to cause loss of H₂O to some extent. However, the abundances of the M-H₂O peaks in the thermolysis samples are many times greater than what can be expected from high cone voltage. They could not have arisen solely as a result of the electrospray analysis.

DFDAs do not appear to lose H₂O as a result of electrospray analysis. **Figure 19a**

shows the spectrum of α -D-Fruf-1,2':2,1'- β -D-Frup (**9**) at 180V. The spectra of α -D-Fruf-1,2':2,1'- β -D-Fruf (**10**) at 180V and 80V are shown in **Figure 19b** and **c**. The 671 peak is

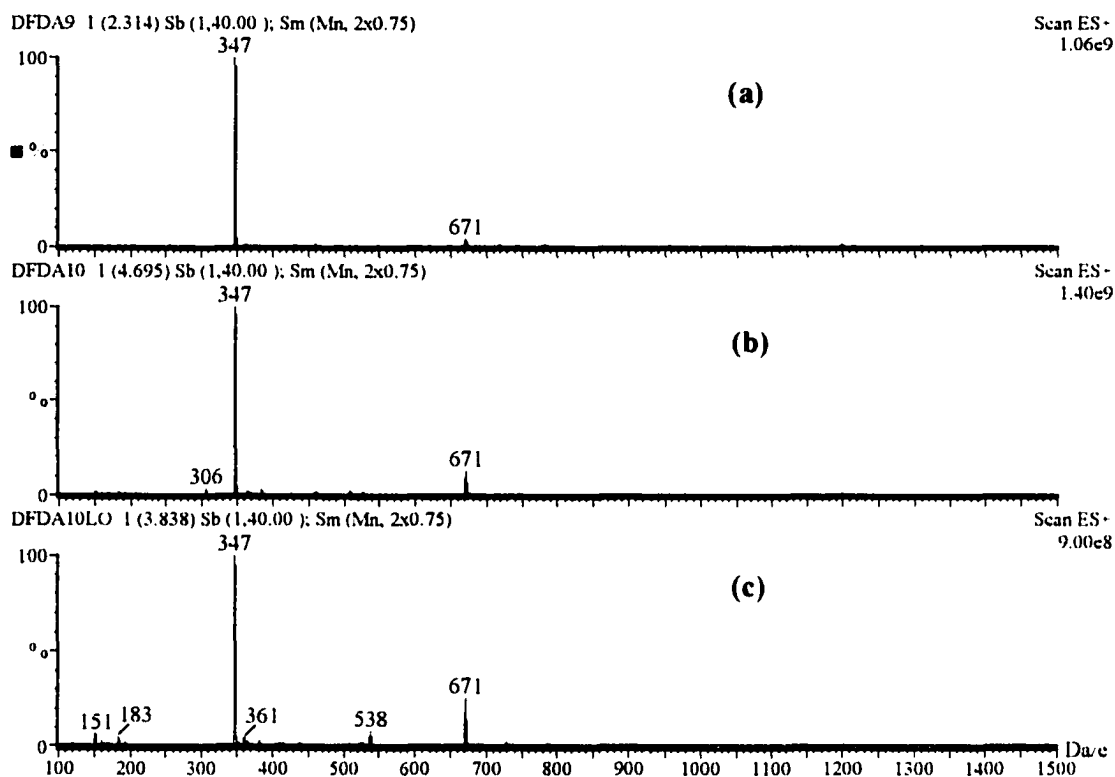


Figure 19 - ESMS spectra of (a) α -D-Fruf-1,2':2,1'- β -D-Frup (**9**) and of α -D-Fruf-1,2':2,1'- β -D-Fruf (**10**) at cone voltages of 180V (b) and 80V (c).

present in all three spectra and probably arises as a result of intermolecular hydrogen bonding. Therefore, a portion of the 671 peaks that were assumed to be glycosylated DFDA tetramer in the thermolysis fractions may actually be DFDA that has dimerized in the electrospray mass spectrometer. M+32 peaks appear with the lower voltage setting. But there is no indication of loss of H₂O from either of these two DFDA.

The abundance of M-54 peaks in the thermolysis fractions is unlikely to be due to the degradation of the singly linked fructose residue of a glycosylated DFDA to HMF. The

mechanism by which HMF forms from fructose⁷⁰ includes keto-enol tautomerism at the anomeric carbon. The authors of ref ⁷⁰ cite the ease with which HMF forms from both fructose and the fructosyl moiety of sucrose. It is reasonable to expect the fructosyl moiety of glycosylated DFDA to form monomeric HMF as well. However, this does not explain the M-54 peaks since the formation of HMF *via* the mechanism given in ref ⁷⁰ is not compatible with retention of the glycosidic bond. Therefore, it is unlikely that the M-54 peaks are glycosylated DFDA with an HMF somehow bonded to the end of the chain and more likely they are caused by random dehydrations.

ESMS of fractions 1-6 in the negative ion mode revealed only peaks that could be classified as background. The six fractions were virtually indistinguishable from one another.[†] **Figure 20** compares the negative ion spectra of citric acid (a), SEC fraction 1 (b), and the typical background at the time of the analysis (c). The small cluster at 383 in the citric acid spectrum is probably citric acid dimer in various ionic states. The 191 citric acid peak was missing from all SEC fractions. The concentration of citric acid expected in fraction 1 can only be estimated. Assuming citric acid is a true catalyst in this system, that it does not degrade (m.p. 153 °C) during thermolysis and is not consumed in side reactions, that the overall mass recovery is 70%, and that all citric acid elutes in fraction 1, the concentration in the ESMS sample should have been ~0.6 mg/mL.^{**} This is above the concentrations recommended by the instrument manufacturer⁷² for calibration with a mixture of corn syrup

[†] Carbohydrates do not ionize easily. High cone voltage in the positive mode gives reasonable results. No carbohydrates in these samples appeared in the negative mode. This "selectivity" provides a convenient method of searching for acidic species.

^{**} 1.5mg citric acid (100mg x 1.5%) before thermolysis. Final dried fraction re-dissolved in 2.0 mL H₂O.

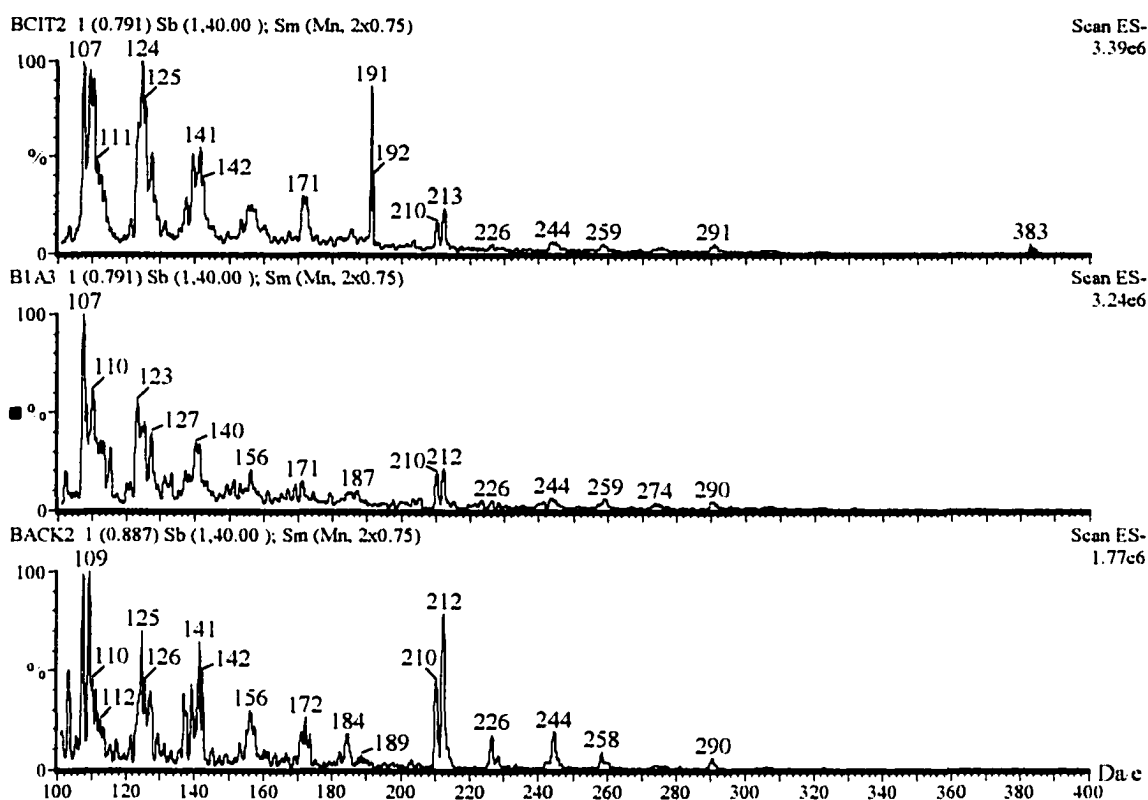


Figure 20 - ESMS spectra of (a) citric acid, (b) SEC fraction 1, and (c) the typical background at the time of the analysis.

(0.5 mg/mL), maltose (0.02 mg/mL), raffinose (0.1 mg/mL), and maltotetraose (0.02 mg/mL). These recommendations are for operation in ES- mode at 30V. However, the chromatogram pictured in the user guide contains only some of the expected peaks from this mixture. Also, as mentioned above, carbohydrates in the current study were not detected in any fraction in ES- mode. It is conceivable that citric acid has formed citrate esters, in which case it would be distributed among the SEC fractions.

General Features of GCFID Chromatograms

The chromatogram shown in **Figure 21** is typical of the per-*O*-trimethylsilyl derivatives of inulin/citric acid thermolysis samples. There are four specific regions corresponding to molecular size, as previously established.⁶¹ The monomer region (9-17 minutes) consists primarily of anomers of fructofuranose, fructopyranose, and glucopyranose. (HMF elutes before 9 minutes.) The dimer region (26-38 minutes) is predominantly di-*D*-fructose dianhydrides. The trimer region (44-53 minutes) has been partially characterized⁶¹ and contains substantial amounts of glycosylated DFDA. Trace quantities of trimers remain in inulin samples heated for 12 hours or more. Tetramers and higher oligomers (dp 4+) elute

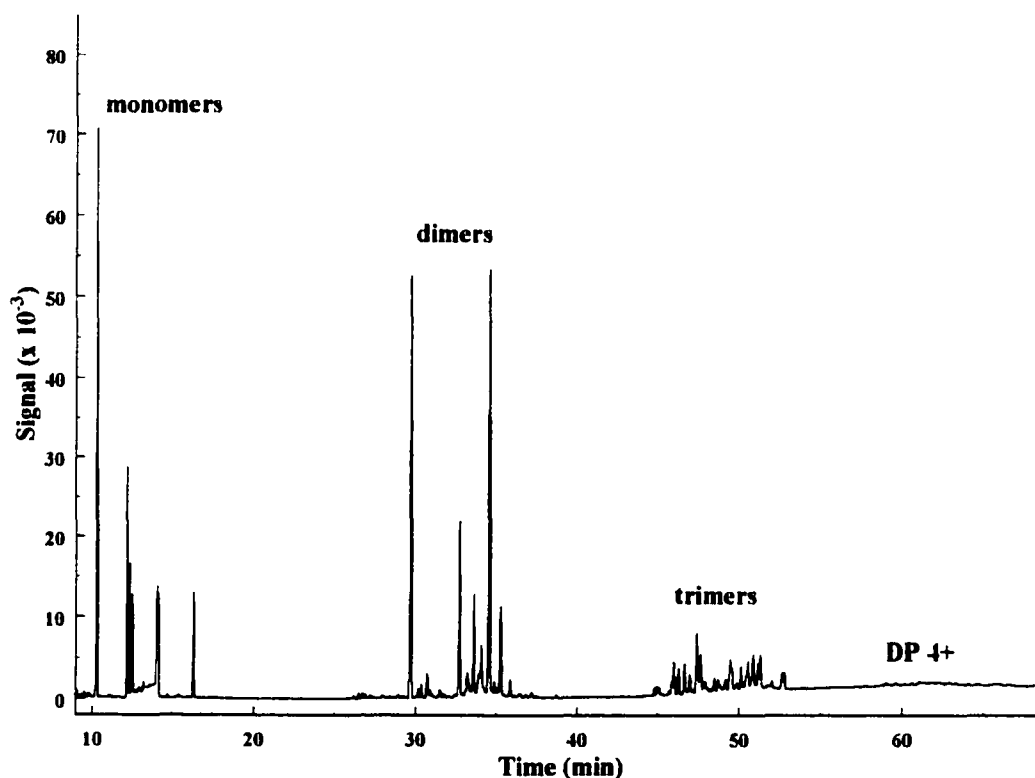


Figure 21 - GCFID chromatogram of 8 minute thermolysis of inulin/1.5% citric acid.

at the end of the run when column temperature reaches 300°C and greater. Samples thermolyzed for 20 minutes or more do not contain detectable tetramers or higher oligomers.

Figure 22 is an expanded view of the monomer region showing the internal standard xylitol, as well as fructose and glucose isomers. For all samples, xylitol is a single, well-

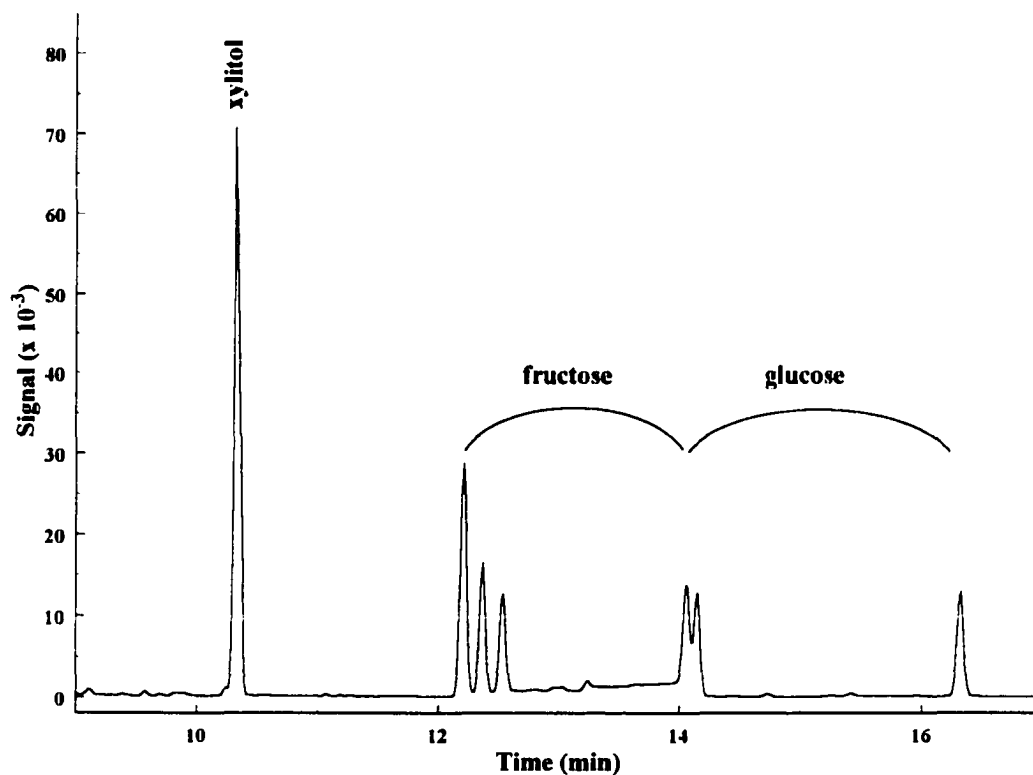


Figure 22 - Monomer region of 8 minute thermolysis of inulin/1.5% citric acid.

resolved peak. A small impurity peak sometimes appears as a shoulder on the leading edge of the xylitol peak. This impurity was removed from peak integrations by manually drawing the baseline and splitting the impurity vertically from the xylitol peak. Fructose and glucose formed in relatively large abundance within the first few minutes and disappeared gradually

over the course of several hours. For example, after 8 minutes fructose and glucose combined made up ~8% by weight of the inulin, ~2% after 40 minutes, and <1% after 2 hours.

The primary area of interest is the dimer region, in which 14 DFDA's elute (**Figure 23**). Several unidentified compounds also appear in this region. After 8 minutes at 160°C,

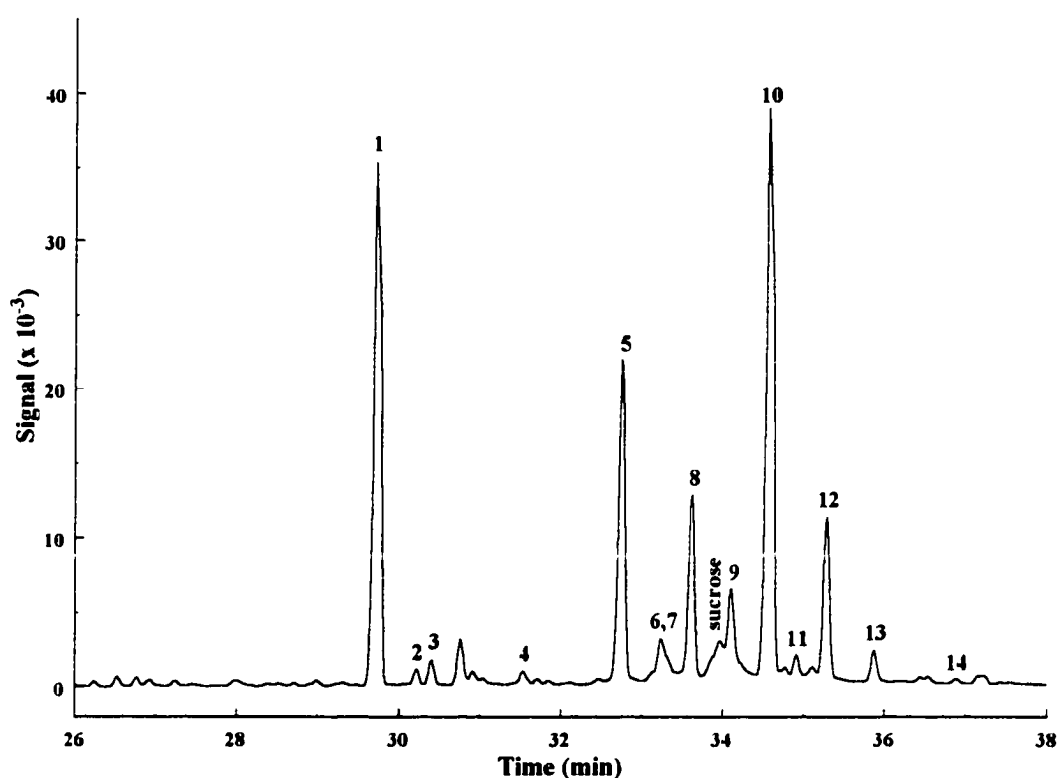


Figure 23 - Dimer region, showing 14 DFDA's, of 8 minute thermolysis of inulin/1.5% citric acid.

all 14 DFDA's have formed from inulin/1.5% citric acid. All but three are baseline resolved; α -D-Fru p -1,2':2,1'- β -D-Fru p (6) and β -D-Fru f -1,2':2,1'- α -D-Fru p (7) coelute on this column

and α -D-Fruf-1,2':2,1'- β -D-Frup (9) elutes on the trailing edge of sucrose.[‡]

Throughout the study, α -D-Frup-1,2':2,1'- β -D-Frup (6) and β -D-Fruf-1,2':2,1'- α -D-Frup (7) are quantified as a single peak. The formation and decay data for each DFDA that arises from repeated thermolysis experiments had to be applied to these two together, rather than individually. This is unfortunate because α -D-Frup-1,2':2,1'- β -D-Frup (6) is a difructopyranose compound and β -D-Fruf-1,2':2,1'- α -D-Frup (7) is a furanose-pyranose. Conclusions based on structure that appear later in this work will make reference to the stability and/or rate of formation and decay of these two DFDA “types”, and additional data would have been helpful.

The fact that α -D-Fruf-1,2':2,1'- β -D-Frup (9) cannot be resolved from sucrose is a problem only while sucrose is present in the reaction mixture. Integration of α -D-Fruf-1,2':2,1'- β -D-Frup (9) in samples heated for 15 minutes or less was approximated by splitting the sucrose/DFDA 9 peak vertically into two “shoulders”. Using this technique may cause the integrator to underestimate the area for both peaks because the true peak shape is less than vertical on most chromatography systems. The trailing edge of the sucrose peak and the leading edge of α -D-Fruf-1,2':2,1'- β -D-Frup (9) would not be included in the integration of their respective peaks.^{**} Sucrose, however, degrades almost completely after ~15 minutes, so the wt% conversion data for α -D-Fruf-1,2':2,1'- β -D-Frup (9) after 15 minutes are reliable.

Two other integration effects are worth mentioning. In some samples heated for 10-

[‡] Each inulin chain ends in glucose (Figure 1); the glucose-fructose bond is 4-5 times more resistant to hydrolysis than the fructose-fructose bond (see discussion on page 15 and ref⁴⁹). Therefore, sucrose appears in limited quantities.

^{**} The error introduced by vertical peak splitting is small for capillary GC relative to packed column GC or to most LC systems because the peaks are much sharper.

20 minutes, the two small peaks (**Figure 23**) to either side of α -D-Fruf-1,2':2,1'- α -D-Frup (**11**) interfered with integration enough to cause more than the usual variation.[‡] This effect was presumably amplified by the low abundance of **11**, which never rises above 1% by weight of total inulin. A similar interference occurred for β -D-Fruf-2,1':3,2'- α -D-Frup (**2**) in the 10-20 minute samples. The abundance of **2** is even lower (<0.5wt%) and the variation is accordingly greater.

[‡] Presentation of the data, with error bars, for formation and decay of DFDA appears later. Those data are a direct result of integration of DFDA peaks in chromatograms of the type presented above. Any anomalies that occur during integration are incorporated into the data.

Isolation of Individual DFDA's

There were at least two compelling reasons to isolate significant quantities of individual DFDA's for this study. DFDA response factors relative to xylitol can only be determined using known compounds. Ideally, the study would have included response factors for all 14 DFDA's. This was not practical, nor even possible given time constraints, so an average RF was applied under the assumption that the flame ionization detector responds similarly to all DFDA's.

Also, it became obvious early in the study that the fate of individual DFDA's could profoundly impact whatever kinetic mechanism was proposed. If isomerization was occurring, the mechanism would need to account for it. Data on isomerization of DFDA's in these thermolysis systems are not available. It is possible to extract and plot (from total conversion data) the concentrations of individual DFDA's at any time during the reaction. It is not possible to predict from these data to what extent isomerization contributes to those concentrations.

One main goal of this research is to describe the rates at which DFDA's form from inulin under the conditions tested. Any proposed mechanism must conform to two criteria: it must fit the data, but it must also make chemical sense. Without knowing what, if any, isomerizations occur, the number of permutations required to reveal reaction mechanisms that satisfy both these criteria would be too great. It would be far more economical to characterize isomerizations first and incorporate them into a more limited set of possible reaction mechanisms - *i.e.* narrow down the choices. So the attempt to prove or disprove isomerization through thermolysis of individual DFDA's was essential.

DFDA 10 from Inulin/citric acid - The glassy residues (~11g overall) from 20 consecutive thermolyses of ~0.5g inulin/1.5% citric acid were dissolved in water, combined, and chromatographed using *LC Method (i)*. The column capacity for this LC system ranges from ~0.25g to ~0.5g, depending on the condition of the column, degree of contamination, number and variety of analytes, etc. **Figure 24** shows a typical preparative LC chromatogram from these experiments. The peaks labeled A-K represent eluant fractions collected manually at

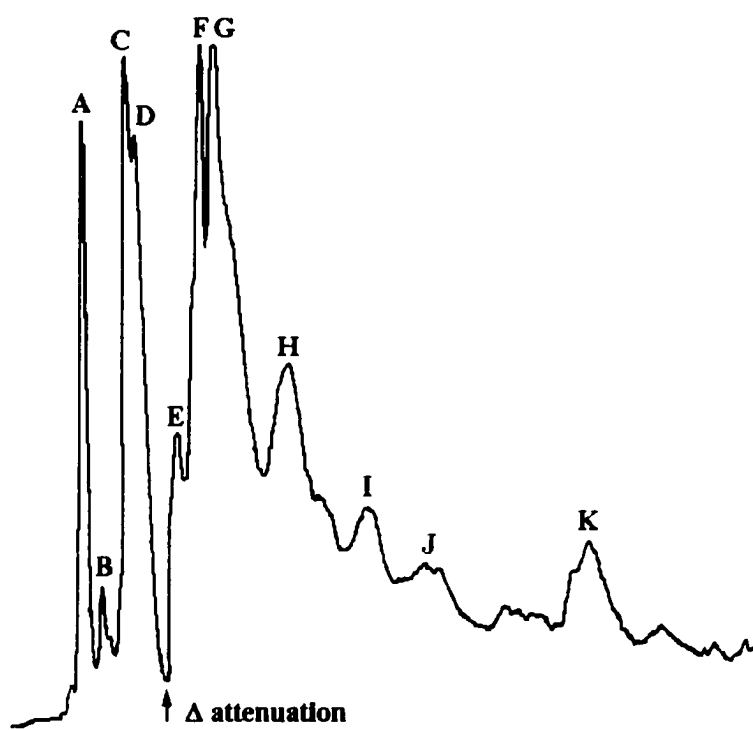


Figure 24 - Typical preparative LC chromatogram from 20 minute thermolysis of inulin/1.5% citric acid at 160°C.

the detector outlet port into a series of flasks. The arrow indicates the point in each run at which the signal attenuation was decreased in order to highlight start and stop times of small, late eluting peaks. Run time was approximately 90 minutes per injection.

Each fraction was rotoevaporated to dryness and analyzed for DFDA content by

silylation and GCFID. Estimates of percent composition for each fraction were based on peak areas under the assumption that response factors for monomers, dimers, and trimers are similar. This is not a valid assumption, but sufficed for the purpose of judging which fractions were worthy of further purification.

All but one DFDA (α -D-Fruf-1,2':2,6'- β -D-Fruf) appeared in at least one fraction.[‡] Only fraction D contained a single DFDA in sufficient purity to pursue as a potential source of starting material for degradation studies. This fraction contained 76% α -D-Fruf-1,2':2,1'- β -D-Fruf (**10**), 14% α -D-Fruf-1,2':2,3'- β -D-Fruf (**1**), a few percent of β -D-Fruf-2,1':3,2'- β -D-Frup (**4**), β -D-Fruf-1,2':2,3'- β -D-Fruf (**5**), α -D-Frup-1,2':2,1'- β -D-Frup (**6**) and/or β -D-Fruf-1,2':2,1'- α -D-Frup (**7**), α -D-Fruf-1,2':2,1'- β -D-Frup (**9**), and traces of trisaccharides. It was not known at this point in the study whether the presence of other DFDA's would affect degradation. I suspected that isomerization did not contribute significantly to the mechanism and that the presence of a small amount of other DFDA's should not matter. Therefore, fraction D was subjected to another round of preparative LC. Trimethylsilylation and GC analysis of the final product showed 88% α -D-Fruf-1,2':2,1'- β -D-Fruf (**10**), 11% other DFDA's, and a small amount of trisaccharide. The disaccharide structures were confirmed by GCMS and by co-injection with an inulin/citric acid thermolysis sample.

This thermolysis and fractionation of gram quantities of inulin/1.5% citric acid was repeated at a later date in order to obtain more α -D-Fruf-1,2':2,1'- β -D-Fruf (**10**). The major difference in the procedure was in the method of heating the starting material. In the latter

[‡] α -D-Fruf-1,2':2,6'- β -D-Fruf (**3**) is unstable because it contains an eight-membered central ring and degrades rapidly. **3** was no longer present in these 20 minute cooks.

case, ~20g inulin/1.5% citric acid was heated in an oven at 160°C for 20 minutes and the glassy product dissolved in water. A more detailed preparative LC separation of the product into 20 fractions still yielded only one fraction worthy of further purification. That fraction corresponded to fraction D from the earlier experiment. The combined yield of α -D-Fruf-1,2':2,1'- β -D-Fruf (**10**) from these two experiments, after extensive freeze drying, was ~900 mg of a dry, solid foam.

DFDAs 6, 9, and 13 from Fructose/HCl - The treatment of crystalline D-fructose with cold, concentrated HCl produces a thick black liquor. Fractionation by preparative LC, after ion exchange, of this digestion product yielded six peaks (**Figure 25**). The residues from each fraction (A-F) were rotoevaporated and analyzed by GCFID of the per-*O*-trimethylsilyl derivatives. Approximate wt% compositions for each fraction are given in **Table 9**. Fractions A and B contained predominantly monomers and low molecular weight degradation products and were discarded.

Fraction C contained 95% α -D-Frup-1,2':2,1'- β -D-Frup (**6**), 3% dimers other than DFDAs, and 1% trimers. Fraction D contained 92% α -D-Fruf-1,2':2,1'- β -D-Frup (**9**) and 8% dimers other than DFDAs, and Fraction F contained 96% β -D-Fruf-1,2':2,1'- β -D-Frup (**13**) and 3% trimers. These three fractions were rotoevaporated and extensively freeze dried to yield respectively 580mg, 600mg, and 75mg dry foam. I did not consider the presence of dimers other than DFDAs in fractions C and D to be detrimental. It was not possible to identify the trimers in fractions C and F, and it was not practical to remove them. Fraction

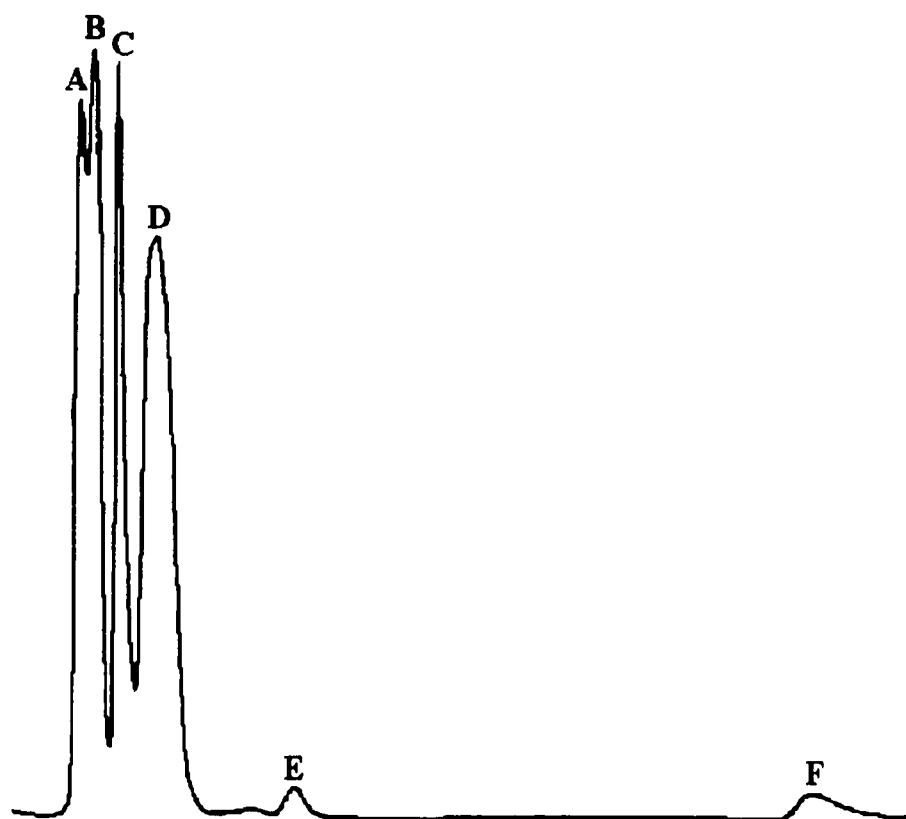


Figure 25 - Typical preparative LC chromatogram from fructose/HCl digestion.

E contained six DFDAs, none in high relative abundance, and was discarded. The only difuranose dianhydrides to form in this experiment (α -D-Fruf-1,2':2,1'- α -D-Fruf (**8**) and α -D-Fruf-1,2':2,1'- β -D-Fruf (**10**)) eluted within this fraction. The presence of a β -D-fructopyranose moiety in all three major products of this acid digestion reflects the fact that crystalline D-fructose is β -D-fructopyranose.

Compound ID	Fraction					
	A	B	C	D	E	F
monomers	98	95	1	-	1	1
α -D-Fruf-1,2':2,3'- β -D-Fruf 1	-	-	-	-	-	-
β -D-Fruf-2,1':3,2'- α -D-Fruf 2	-	-	-	-	-	-
β -D-Fruf-2,1':3,2'- β -D-Fruf 4	-	-	-	-	-	-
β -D-Fruf-1,2':2,3'- β -D-Fruf 5	-	-	-	-	-	-
α -D-Fruf-1,2':2,1'- β -D-Fruf 6	-	-	95	-	5	-
β -D-Fruf-1,2':2,1'- α -D-Fruf 7	-	-	-	-	-	-
α -D-Fruf-1,2':2,1'- α -D-Fruf 8	-	-	-	-	4	-
α -D-Fruf-1,2':2,1'- β -D-Fruf 9	-	-	-	92	21	-
α -D-Fruf-1,2':2,1'- β -D-Fruf 10	-	-	-	-	1	-
α -D-Fruf-1,2':2,1'- α -D-Fruf 11	-	-	-	-	-	-
β -D-Fruf-1,2':2,1'- β -D-Fruf 12	-	-	-	-	-	-
β -D-Fruf-1,2':2,1'- β -D-Fruf 13	-	-	-	-	12	96
β -D-Fruf-1,2':2,1'- β -D-Fruf 14	-	-	-	-	54	-
dimers	2	5	3	8	1	-
trimers	-	-	1	-	1	3

Table 9 - Percentage composition of preparative LC fractions A-F from fructose/HCl digestion.

Thermolysis of Individual DFDA_s

Degradation studies were carried out separately on α -D-Fru μ -1,2':2,1'- β -D-Fru μ (**6**), α -D-Fru ν -1,2':2,1'- β -D-Fru μ (**9**), and α -D-Fru ν -1,2':2,1'- β -D-Fru ν (**10**).[‡] Note that this group includes a dipyrano μ , a furanose-pyrano μ , and a difuranose dianhydride. Each was thermolyzed individually in the presence of 1.5wt% citric acid at 160°C and the products analyzed by GC/FID of the per-*O*-trimethylsilyl derivatives.

Degradation of DFDA 6 - The relative concentration of the dipyrano μ dianhydride α -D-Fru μ -1,2':2,1'- β -D-Fru μ (**6**) remained greater than ~95% over a reaction period of five hours (**Figure 26**). The starting material contained small amounts of a dimer and two trimers. The insert shows the relative concentrations of these impurities on an expanded y-axis. The thermally stable dimer (\blacktriangle) had the same retention time as α -D-Fru ν -1,2':2,1'- β -D-Fru μ (**9**). In the preparative LC separation of the fructose/HCl digest from which these individual DFDA_s were obtained, **6** and **9** are not fully resolved and some cross contamination occurred, despite repeated fractionations. The two trimers (\blacksquare , \blacklozenge) show some scatter, and the least abundant of the two (\blacklozenge) might be perceived as degrading slightly. It is improbable, however, that the small amount of product from the decay of this trimer goes specifically toward the formation of α -D-Fru μ -1,2':2,1'- β -D-Fru μ (**6**), and at a rate equal to the rate of disappearance of **6**. The more likely conclusion from this experiment is that α -D-Fru μ -1,2':2,1'- β -D-Fru μ (**6**) is thermally stable.

[‡] There was insufficient material (75 mg) to conduct thermolysis experiments on β -D-Fru ν -1,2':2,1'- β -D-Fru μ (**13**).

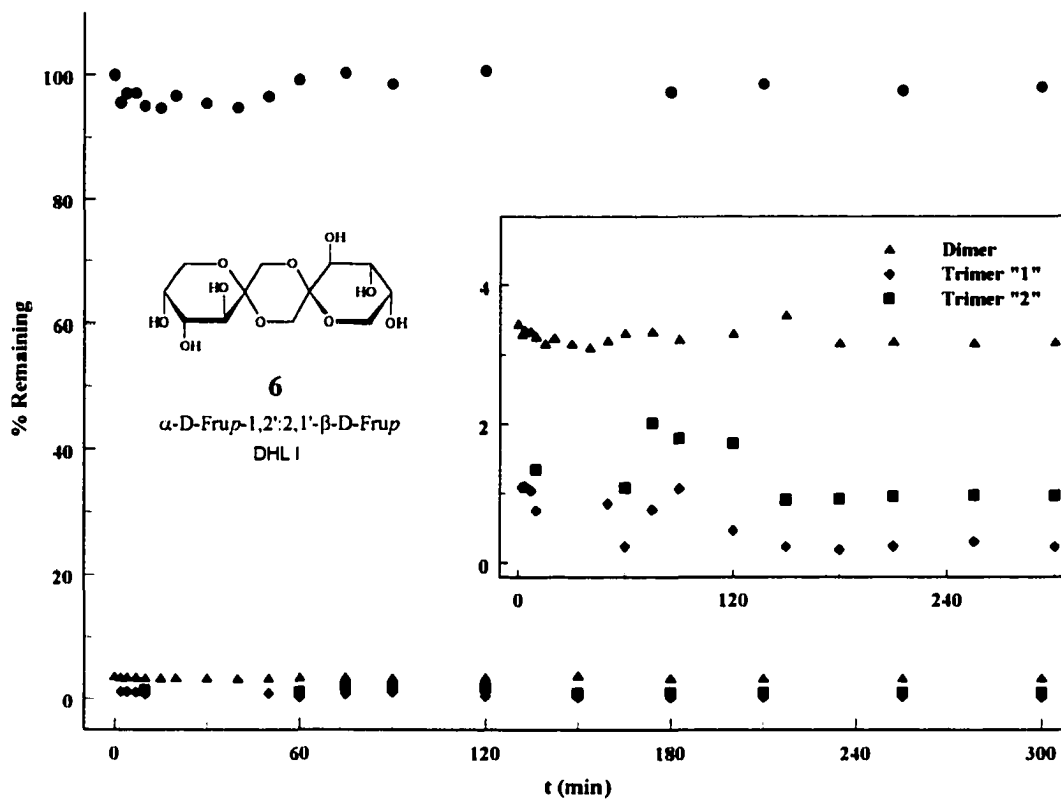


Figure 26 - Thermolysis of α -D-Fru-p-1,2':2,1'- β -D-Frup (**6**) at 160°C in the presence of 1.5% citric acid.

Degradation of DFDA 9 - Thermolysis of the furanose-pyranose dianhydride α -D-Fru-f-1,2':2,1'- β -D-Frup (**9**) gave similar results (**Figure 27**); **9** did not decay after five hours at 160°C. The starting material in this case contained no detectable trimers. The four dimers that were present in the starting material are shown in the insert. The two least abundant dimers (◆, ▼) decayed to non-quantifiable levels within the first 45 minutes. The retention time of the most abundant dimer impurity (▲) did not correlate to any of the 14 known

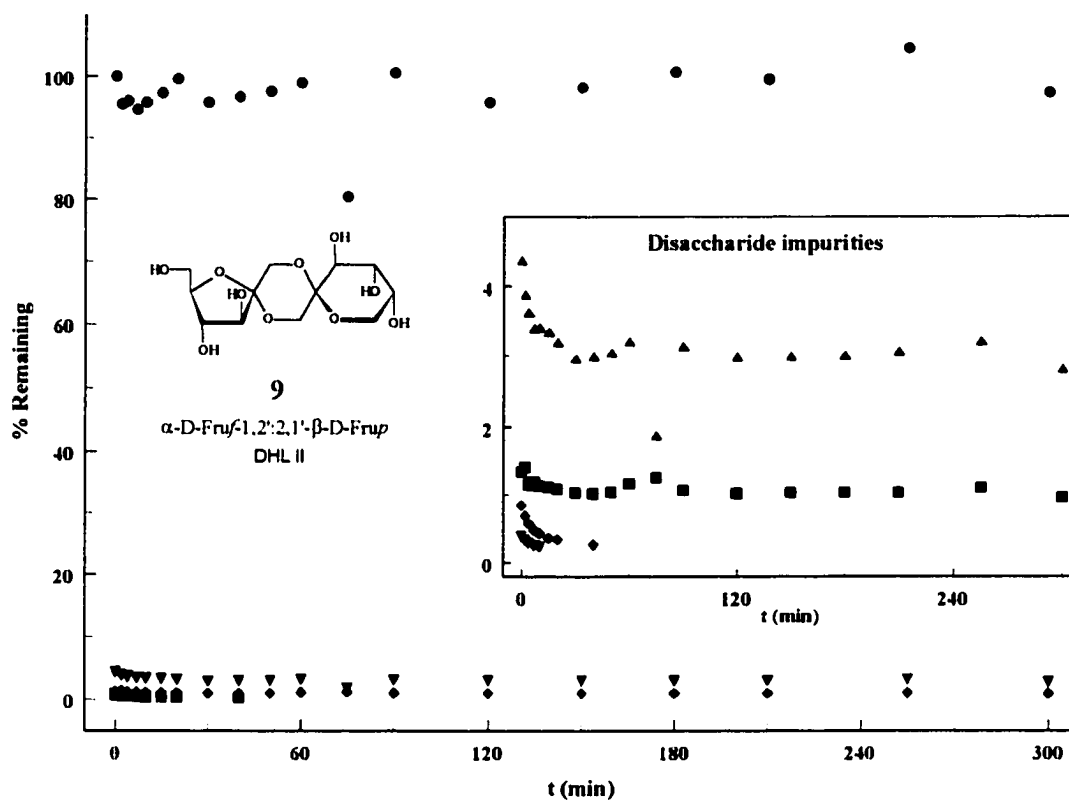


Figure 27 - Thermolysis of α -D-Fruf-1,2':2,1'- β -D-Frup (**9**) at 160°C in the presence of 1.5% citric acid.

DFDAs. The dimer of intermediate abundance (■) had the same retention time as α -D-Fruf-1,2':2,1'- β -D-Frup (**6**) and is present as a result of cross contamination from preparative LC fractionation. As before, it is unlikely that impurities have degraded specifically to **9**, and at a rate equal to the degradation of **9**. Therefore, α -D-Fruf-1,2':2,1'- β -D-Frup (**9**) may be considered thermally stable.

Degradation of DFDA 10 - The behavior of α -D-Fruf-1,2':2,1'- β -D-Fruf (**10**) was decidedly different from **6** and **9** (Figure 28); **10** degraded steadily over the five hour reaction time. At

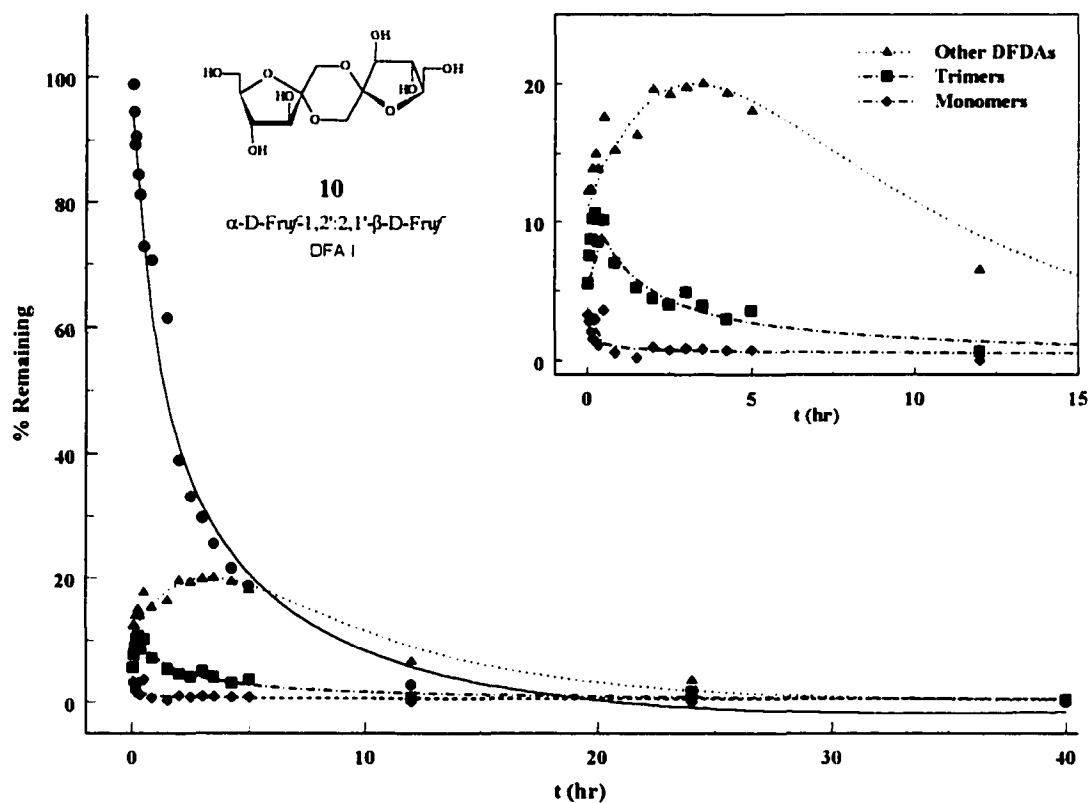


Figure 28 - Thermolysis of α -D-Fruf-1,2':2,1'- β -D-Fruf (**10**) at 160°C in the presence of 1.5% citric acid.

least five other DFDA (page 60) were present in the starting material, and after 30 minutes at least 12 of the 14 DFDA were still present or had formed. The reaction time was extended to 40 hours. Note in the insert the increased relative abundance of DFDA other than α -D-Fruf-1,2':2,1'- β -D-Fruf (**10**). Note also that the time scale is hours instead of minutes. As α -D-Fruf-1,2':2,1'- β -D-Fruf (**10**) degrades, the combined concentration of other DFDA (\blacktriangle) in the reaction mixture increases out to four hours, after which all DFDA

gradually decay to very low abundance.

These data are presented in the form of a bar graph in **Figure 29**. The vertical axis (Wt% Conversion) reflects the approximate proportion of the recovered starting material that is monomers, trimers, other DFDA's, and α -D-Fruf-1,2':2,1'- β -D-Fruf (**10**). The time axis is

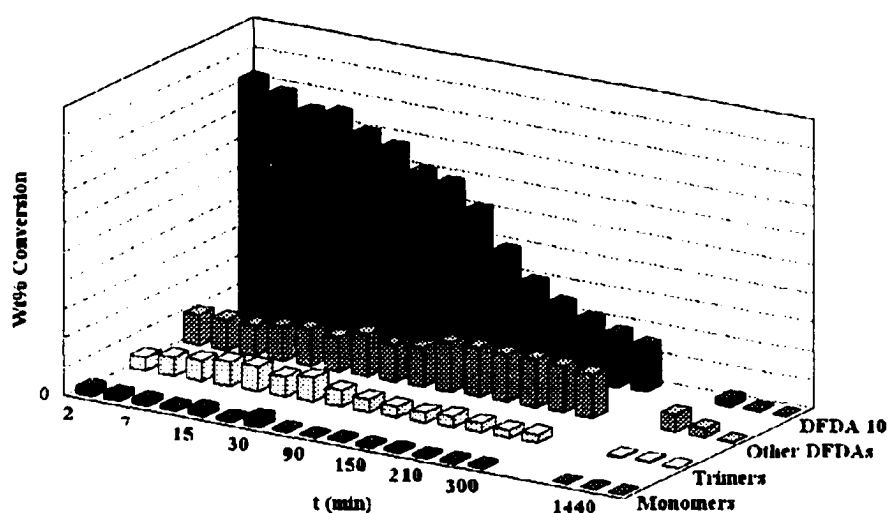


Figure 29 - Mono-, di-, and trisaccharides accompanying degradation of α -D-Fruf-1,2':2,1'- β -D-Fruf (**10**).

not to scale and contains a gap solely to emphasize the delay between 5 and 12 hour sample times (300-720 min). Once the concentration of α -D-Fruf-1,2':2,1'- β -D-Fruf (**10**) falls to a certain level (~5 hrs or 300 min.), the concentrations of all DFDA's decline steadily. It is possible that α -D-Fruf-1,2':2,1'- β -D-Fruf (**10**) isomerizes to other DFDA's, or that it decays to products which react further to form other DFDA's, or both. The trisaccharides increase

slightly in abundance for the first 30 minutes then decrease slowly, though not to the same extent as the other DFDA. The monomer component arises from degradation to yield fructose. Some non-specific degradation products^{58,71,73} (e.g. H₂O, CO, CO₂, CH₂O, HMF, furfural) presumably elute with the solvent or are lost as volatiles. Also, as a result of polymerization of degradation products, the long cooks - 12 hours and greater - contained small amounts of black char that were eliminated during sample workup. The relative abundance of the monomer component remained low and declined steadily throughout the 40 hour reaction period.

The data for these degradation experiments indicate that α -D-Fruf-1,2':2,1'- β -D-Frup (6) and α -D-Fruf-1,2':2,1'- β -D-Frup (9) are thermally stable. Although several of the impurities in the starting materials degrade, it does not seem feasible that 6 and 9 degrade into products which then react to re-form the same two DFDA. It also seems improbable that 6 isomerizes to 9 and vice versa. Bond breaking is required in these scenarios, and other DFDA would form, yet no other DFDA were identified in these two degradation experiments.

The degradation of α -D-Fruf-1,2':2,1'- β -D-Fruf (10) is accompanied by formation of other DFDA. The combined mass of other DFDA in the reaction mixture at no time accounts fully for the loss of α -D-Fruf-1,2':2,1'- β -D-Fruf (10); 10 does not degrade solely to DFDA. Still, the mechanism of formation of DFDA from inulin must incorporate "side reactions" to account for some isomerization of α -D-Fruf-1,2':2,1'- β -D-Fruf (10) to other DFDA. By analogy we can expect other difuranose dianhydrides to behave similarly.

Also, it should be noted that the decline in the concentration of trimers (**Figures 28**

and **29**) coincides with the initial increase then decline in the concentration of DFDA's other than α -D-Fruf-1,2':2,1'- β -D-Fruf (**10**). This implicates trimers as sources for DFDA's. The composition of the trimer fraction was shown⁶¹ to contain a high proportion of glycosylated difuranoses as opposed to pyranose-containing trimers. As such they are susceptible to degradation themselves and their contribution to DFDA concentration from hydrolysis of the glycosyl residue will be somewhat limited.

The general acid stability of DFDA's was documented early⁷⁴ in a study showing that DFDA's were 25 times more resistant than inulin to acid hydrolysis. Related studies^{75,76} showed α -D-Frup-1,2':2,1'- β -D-Frup (**6**) to be more than twice as resistant as α -D-Fruf-1,2':2,1'- β -D-Fruf (**10**) to hydrolysis at 60°C in N H₂SO₄. A more recent study⁵⁹ noted a higher resistance to acid hydrolysis of the 2,3-linked difuranoses α -D-Fruf-1,2':2,3'- β -D-Fruf (**1**) and β -D-Fruf-1,2':2,3'- β -D-Fruf (**5**) relative to the 1,2-linked difuranose α -D-Fruf-1,2':2,1'- β -D-Fruf (**10**). The furanose-pyranose α -D-Fruf-1,2':2,1'- β -D-Frup (**9**) also showed acid stability.

The current study suggests that the presence of one or two D-fructopyranose rings imparts significant stability toward acid in anhydrous melts. The experiments presented in the following section support this hypothesis; all seven pyranose-containing DFDA's that form from inulin reach a maximum concentration after ~30 minutes and do not decay appreciably. The kinetic mechanism will be slightly less complex as a result of this stability because some isomerization steps can be eliminated.

Thermolysis of Inulin/1.5% Citric Acid at 160°C

The majority of the data presented in this work were acquired from thermolysis of inulin/1.5% citric acid at 160°C. This was the first set of inulin thermolysis conditions tested, mainly because it was a logical continuation of previous work.⁶¹ (See also Statement of Purpose for the Current Study, page 28.) It was important to establish a reliable and relatively extensive set of data for one system before moving on to variations in temperature and/or citric acid concentration.

Total DFDAs from Inulin 1.5% Citric Acid/160 °C - The data for inulin/1.5% citric acid thermolysis at 160°C are the result of 18 experiments[†] composed of 127 data points and 13 outliers. These data are presented in **Figure 30**. The first four experiments included a “zero time” sample that was not thermolyzed, but that was derivatized and analyzed for DFDAs.^{**} Conversion of inulin to total DFDAs reaches a maximum of approximately 35wt% after about 30 minutes. (Conversion is expressed as the percentage weight of DFDAs relative to the starting weight of inulin. Total conversion is the sum of wt% conversion values for all DFDAs in a sample.) This rapid conversion is followed by a much slower degradation, which appears to end after ~30 hours.

Nine of the outliers came from only two experiments. Notably, the four perceived outliers at 15 and 40 hours all arose from one experiment using the standard screw cap vials. There was some doubt about the ability of these caps to protect against loss or to resist

[†] The reader is reminded that each “experiment” is comprised of up to 9 individual samples, each in its own vial. The vials were thermolyzed simultaneously and analyzed separately for DFDAs.

^{**} None of the zero time samples contained DFDAs.

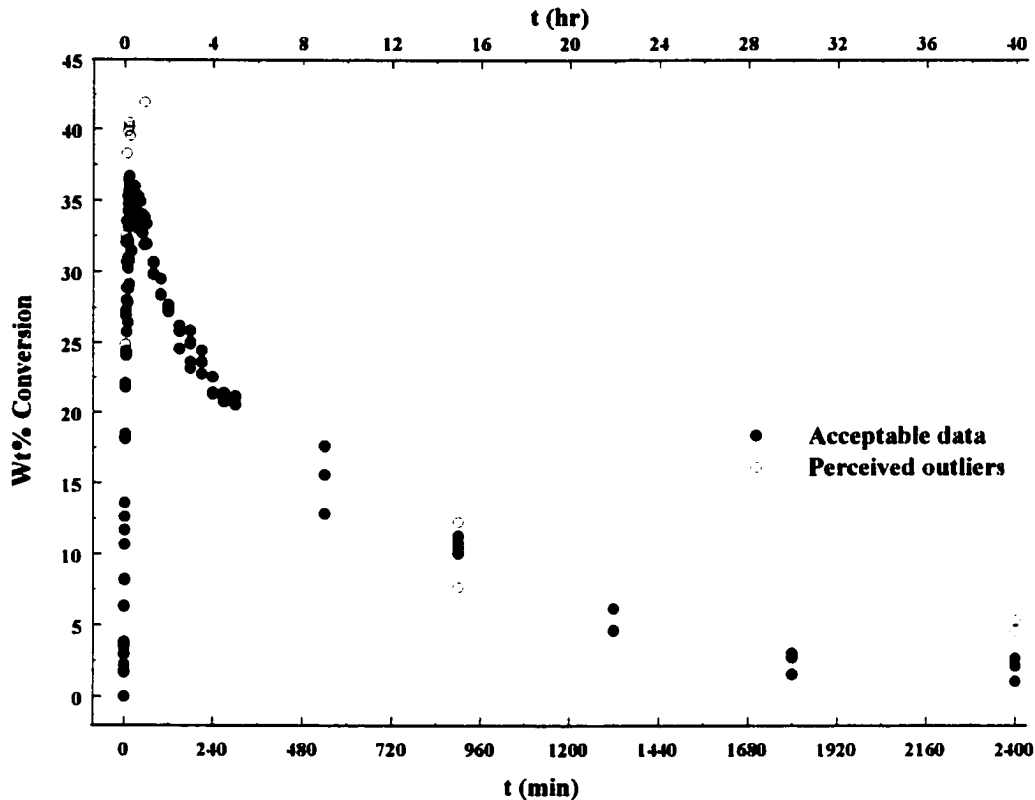


Figure 30 - Conversion (0-40 hr) of inulin/1.5% citric acid to DFDAs at 160°C.

breakdown after extended heating at high temperatures. The “reliable” data points in **Figure 30** for 15 and 40 hours came from experiments using sealed glass tubes in place of screw cap vials. This reduced the scatter considerably.

Closer inspection of the data for the first hour reveals the inherent difficulty of repeating the shorter thermolyses without undue variation (**Figure 31**). Nine of the 13 outliers occur from 8-16 minutes. Five of these nine came from one experiment. This suggests a problem with that experiment, rather than some systematic error. The remaining four outliers in this region arose one or two at a time from three separate experiments and may be attributed to random error.

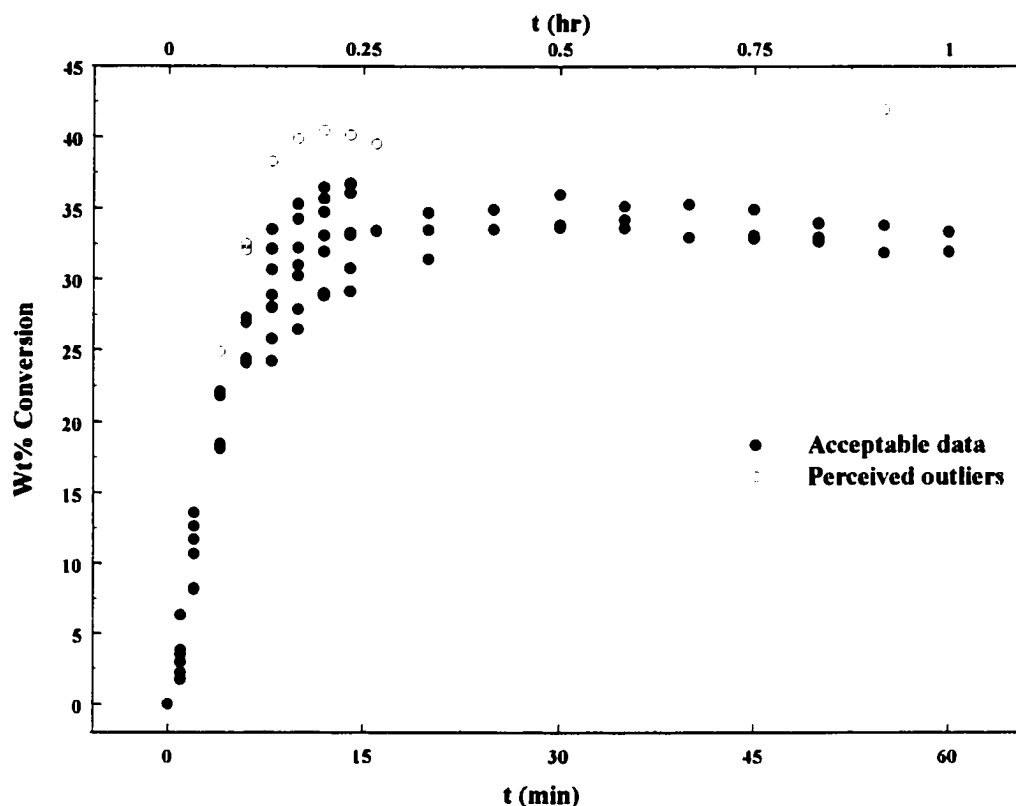


Figure 31 - Conversion (0-60 min) of inulin/1.5% citric acid to DFDA's at 160°C.

The data from 0-16 minutes are relatively scattered. As mentioned (page 36), it takes about two minutes for the vials to reach reaction temperature, and doubtless slightly longer for the sample. Presumably, it takes some time for the vial and sample to cool from reaction temperature after submersion in ice water. Therefore, the sample spends a substantial proportion of the total reaction time at some temperature other than 160°C. This might explain some of the observed variation. It may have been possible to slow the reaction by lowering the temperature to *e.g.* 155°C. This would extend the reaction times and reduce the error introduced by unavoidable temperature changes. However, the inulin/1.5% citric

acid mixture melts around 153°C and any advantage gained by lowering the reaction temperature might well be offset by inconsistencies arising from incomplete or uneven melting.

The scatter may also be related to the chronological order in which the data were acquired. The 0-16 minute thermolyses were the first six experiments conducted and the degree of operator inexperience may have been high. The experimental procedures had become straightforward and routine by the time the next group of experiments commenced. The reaction times for this next group begin at 20 minutes. Processing and viewing the data from both groups of experiments revealed inordinate variation, so the 8, 10, 12, and 14 minute thermolyses were repeated in duplicate. These eight new data points fell in the mid and lower region of the existing early data and provided assurance that the experimental procedure was capable of effecting a smooth transition between the 15 and 20 minute data.

Individual DFDAs from Inulin/1.5% Citric Acid/160 °C - The relative distribution of DFDAs throughout the thermolysis of inulin/1.5% citric acid at 160°C is shown in **Figure 32**. The data result from integration of individual GC peaks from thermolyzed inulin/citric acid

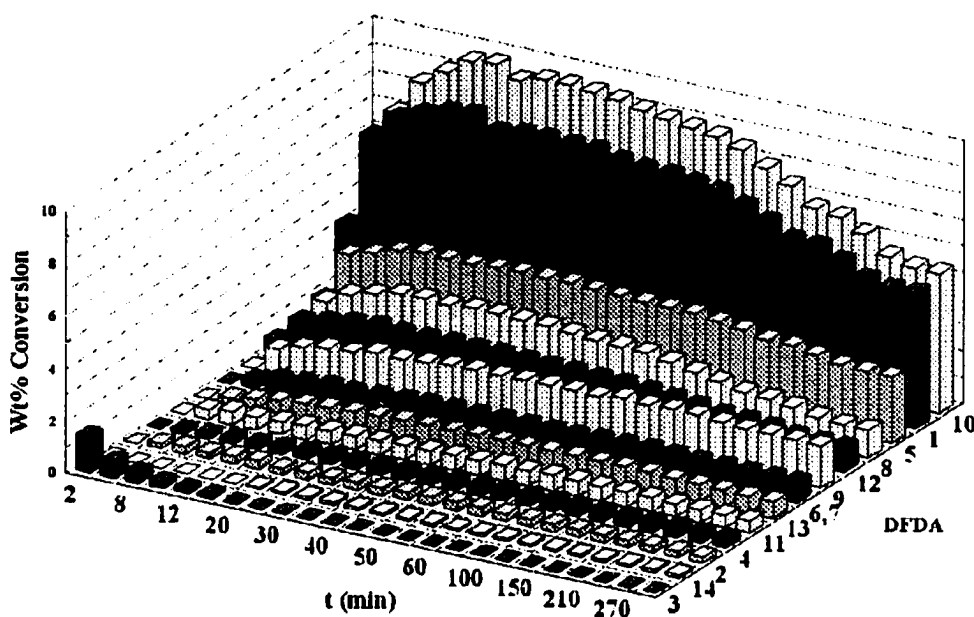


Figure 32 - Wt% individual DFDAs from thermolysis of inulin/1.5% citric acid at 160°C.

samples.† DFDAs are sorted in this figure, for convenience only, from front to back in order of least abundant to most abundant at 30 minutes into the reaction. The right hand axis, labeled “DFDA”, reflects this sorting. It is important to note again that α -D-Frup-1,2':2,1'- β -

† Separate wt% versus time plots for all 14 DFDAs are presented in the kinetics discussion which appears later.

D-Fru_p (6) and β-D-Fru_f-1,2':2,1'-α-D-Fru_p (7) are listed together because they were not resolved on the GCFID.

General Trends in Individual DFDA Conversion Data - **Table 10** shows the changes in DFDA abundance relative to each other at 2, 6, 30, 80, and 300 minutes for inulin/1.5% citric acid at 160°C. The table is divided into four groups of columns (sections a, b, c, d) for purposes of discussion.

	← Higher abundance ————— Lower abundance →													
	a		b		c				b		d			
2 min	1	10	3	5	12	8								
6 min	10	1	-	5	8	12	9	3	11	6,7	13	2	4	14
30 min	10	1	-	5	8	12	9	-	6,7	13	11	4	2	14
80 min	10	1	-	5	8	9	12	-	6,7	13	11	4	2	14
300 min	10	1	-	5	9	8	12	-	6,7	13	11	4	2	14

Table 10 - Relative abundance of DFDA's - highest to lowest from left to right - at 2, 6, 30, 80, and 300 minutes. (Inulin/1.5% citric acid/160°C).

The two columns in section **a** show that, except for early in the reaction (2 min), α-D-Fru_f-1,2':2,1'-β-D-Fru_f (10) is the most abundant DFDA. The mean wt% conversions for α-D-Fru_f-1,2':2,3'-β-D-Fru_f (1) and α-D-Fru_f-1,2':2,1'-β-D-Fru_f (10) were similar and the reversal at six minutes is not overly important. It is important to note that these are the two major products throughout the reaction.

Sections **b** illustrate the labile nature of α-D-Fru_f-1,2':2,6'-β-D-Fru_f (3), an unstable product that forms early. (The spaces in the **b** columns are for convenience in comparing trends in neighboring sections and do not represent gaps in the data.) At two minutes α-D-Fru_f-1,2':2,6'-β-D-Fru_f (3) is the 3rd most abundant DFDA. After six minutes it is only the

7th most abundant, at 20 minutes (**Figure 32**, page 75) it the least abundant, and after 30 minutes it has disappeared altogether.

Two interesting phenomena occur in section c. First, at two minutes β -D-Fruf-1,2':2,1'- β -D-Fruf (**12**, 0.51wt%) is more than twice as abundant as α -D-Fruf-1,2':2,1'- α -D-Fruf (**8**, 0.21wt%), but **8** becomes more abundant at six minutes and remains so for five hours. Second, α -D-Fruf-1,2':2,1'- β -D-Frup (**9**) "overtakes" first **12**, then **8**, and does not degrade throughout the five hour reaction period. These three products must have similar rates of formation in the early stages, but α -D-Fruf-1,2':2,1'- β -D-Frup (**9**) remains stable while the other two are susceptible to thermal degradation.

At first glance, the abundances of β -D-Fruf-2,1':3,2'- α -D-Frup (**2**) and α -D-Fruf-1,2':2,1'- α -D-Frup (**11**) (section d) appear to change relative to β -D-Fruf-2,1':3,2'- β -D-Frup (**4**), β -D-Fruf-1,2':2,1'- β -D-Frup (**13**), and β -D-Frup-1,2':2,1'- β -D-Frup (**14**). But recall (page 57) that the integration data for these two in the first 10-20 minutes are unreliable. Each occurred in small abundance and each eluted with "contaminant" peaks that caused inordinate integration error. With this in mind, there are no detectable changes in relative abundance between these five DFDA's. No accurate determination is possible for α -D-Frup-1,2':2,1'- β -D-Frup (**6**) and β -D-Fruf-1,2':2,1'- α -D-Frup (**7**), except that as a pair their relative abundance is constant.

Structural Properties as Partial Explanation for Relative Abundance - Some correlation exists between DFDA structure and relative abundance. The most obvious example is the lability of α -D-Fruf-1,2':2,6'- β -D-Fruf (**3**), presumably because it contains an eight-membered

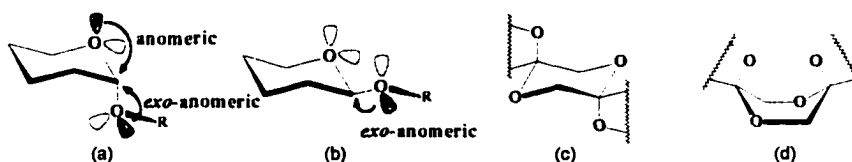
central dioxane ring, which breaks apart easily under the reaction conditions employed. But other, less obvious correlations exist. This section points out several of these in an attempt to understand the factors controlling DFDA formation and decay in anhydrous, high temperature environments.

Table 11 lists ring configuration, dianhydride linkage, and central ring conformation[‡]

DFDA	Anomer	Ring Size	Linkage	Anomer	Ring Size	Central Ring Conformation	Wt% @ 30 min
10	α	fur	1,2':2,1'	β	fur	chair	9.55
1	α	fur	1,2':2,3'	β	fur	boat	8.05
5	β	fur	1,2':2,3'	β	fur	chair	3.52
8	α	fur	1,2':2,1'	α	fur	boat	2.51
12	β	fur	1,2':2,1'	β	fur	boat	1.75
9	α	fur	1,2':2,1'	β	pyr	chair	1.70
6,7	-	-	1,2':2,1'	-	pyr	chair	0.79
13	β	fur	1,2':2,1'	β	pyr	boat	0.77
11	α	fur	1,2':2,1'	α	pyr	boat	0.56
4	β	fur	2,1':3,2'	β	pyr	chair	0.31
2	β	fur	2,1':3,2'	α	pyr	boat	0.26
14	β	pyr	1,2':2,1'	β	pyr	boat	0.09
3	α	fur	1,2':2,6'	β	fur	flexible	0.00

Table 11 - Anomeric configuration, dianhydride linkage, and central ring conformation of individual DFDA's.

[‡] With the exception of α -D-Fruf-1,2':2,6'- β -D-Fruf (3), the central ring formed by the dianhydride linkage of DFDA's is a six-membered 1,4-dioxane. The anomeric and *exo*-anomeric effects⁷⁷⁻⁷⁹ control which conformation this central ring adopts. Both effects arise when a lone electron pair of one oxygen in an O-C-O system is arranged antiperiplanar to the σ^* anti-bonding orbital of the carbon. The *exo*-anomeric effect may operate from either the axial (a) or equatorial (b) position. By contrast, the anomeric effect applies when the

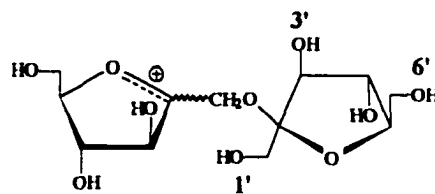


electronegative substituent is axially disposed (a). In DFDA's, the most important consequence is to force the anomeric oxygens of each D-fructose residue into the axial position on the central ring. For the 1,2':2,1' (continued...)

for each of the 14 DFDA. They are sorted in order of relative abundance (highest to lowest) after thermolysis for 30 minutes at 160°C, the same sort order used in **Figure 32**. The complete structures of **6** and **7** are known, but are not included since it is not known how much each one contributes to wt% conversion data. We can combine structural properties from **Table 11** with our general knowledge of the mechanisms of formation (**Scheme 5**, page 17 and **Scheme 6**, page 19) to explain partially the distributions of DFDA during thermolysis.

At 2 minutes α -D-Fruf-1,2':2,3'- β -D-Fruf (**1**), α -D-Fruf-1,2':2,6'- β -D-Fruf (**3**), β -D-Fruf-1,2':2,3'- β -D-Fruf (**5**), α -D-Fruf-1,2':2,1'- β -D-Fruf (**10**), and β -D-Fruf-1,2':2,1'- β -D-Fruf (**12**) are the most abundant DFDA. All contain a β -D-fructofuranose, and none contain fructopyranose. The inulin chain, except the terminal α -D-glucopyranose, is made up entirely of β -D-fructofuranose and it is not surprising that this moiety predominates in the major thermolysis products. The three most abundant products after 2 minutes (**1**, **3**, **10**) also contain α -furanose rings, and could form as follows: The β -1,2-linkage is already present in abundance. All that is needed is cleavage of the glycosidic bond to give a cationic dimer (**19**)

D-fructofuranosyl-(1 \rightarrow 2)- β -D-fructofuranose



19

‡ (...continued)

linked dianhydrides, the central ring is a chair (c) if the fructose residue anomeric configurations are different (α,β or β,α), and a boat (d) if they are the same (α,α or β,β). The reverse is true for 1,2':2,3' and 2,1':3,2' linked dianhydrides (boat for α,β or β,α ; chair for α,α or β,β).

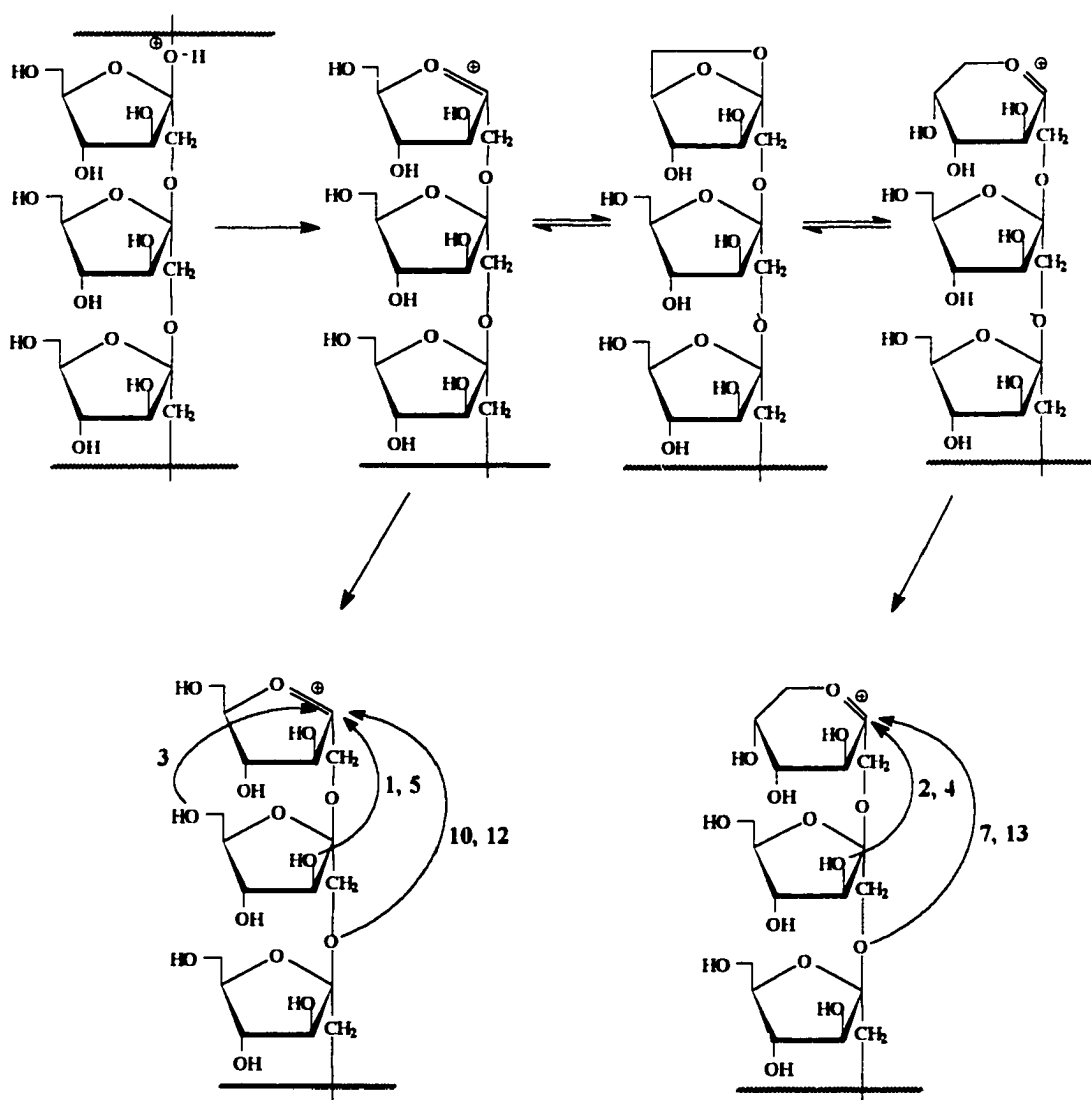
with a β -D-fructofuranose linked 1 \rightarrow 2 to a D-fructofuranosyl cation. The anomeric carbon of the cationic residue is planar sp^2 and susceptible to attack from either side. The β -side, however, may be sterically hindered to some degree by the C-3 hydroxyl group, which would make attack slightly more favored from the α -side. This would account for the three aforementioned products. (α -attack by O-1' \rightarrow α -D-Fruf-1,2':2,1'- β -D-Fruf (**10**); by O-3' \rightarrow α -D-Fruf-1,2':2,3'- β -D-Fruf (**1**); by O-6' \rightarrow α -D-Fruf-1,2':2,6'- β -D-Fruf (**3**)) β -attack by each of the hydroxyl oxygens O-1' and O-3' gives the two remaining products β -D-Fruf-1,2':2,1'- β -D-Fruf (**12**) and β -D-Fruf-1,2':2,3'- β -D-Fruf (**5**), respectively.[‡] Cleavage of the dimer from the inulin oligomer may occur before or after DFDA formation.

The absence of pyranose in these early products is also not surprising. The partial mechanism of **Scheme 6**, page 19, illustrates an important pathway to D-fructopyranose. In addition to being attacked immediately by neighboring hydroxyl groups, a terminal fructofuranosyl cation can adopt a 2,6-anhydro- β -D-fructofuranose form. This anhydro form is in equilibrium, not only with the furanosyl cation, but with a pyranosyl cation, which is slower to form than the furanosyl. Attack on this pyranosyl cation by O-1' or O-3' leads to the pyranose containing DFDA's.⁸⁰ (α -attack by O-1' \rightarrow β -D-Fruf-1,2':2,1'- α -D-Frup (**7**); by O-3' \rightarrow β -D-Fruf-2,1':3,2'- α -D-Frup (**2**); β -attack by O-1' \rightarrow β -D-Fruf-1,2':2,1'- β -D-Frup (**13**); by O-3' \rightarrow β -D-Fruf-2,1':3,2'- β -D-Frup (**4**)). Thus, formation of the pyranose-containing DFDA's requires an additional step and proceeds through a less stable intermediate.

These reactions are summarized in **Scheme 8**, in which an inulin polymer is

[‡] β -D-Fruf-1,2':2,6'- β -D-Fruf, which is the DFDA that would result from β -side attack by O-6', has never been identified. It is transient if it forms at all. Also, O-4' cannot approach the anomeric C-2 without severe bond strain; 1,2':2,4' di-D-fructose dianhydrides do not appear to form.

cleaved to form an oligomer with a terminal D-fructofuranosyl cationic residue. The cation is in equilibrium, *via* the anhydro species, with a D-fructopyranosyl cation. Either of these cations may react with neighboring hydroxyl groups or the glycosidic oxygen to form DFDA. The mechanism accounts for all the DFDA that contain one or more β -D-fructofuranose rings. It is important to note, however, that five DFDA (α -D-Frup-1,2':2,1'- β -D-Frup (6),



Scheme 8

α -D-Fruf-1,2':2,1'- α -D-Fruf (**8**), α -D-Fruf-1,2':2,1'- β -D-Frup (**9**), α -D-Fruf-1,2':2,1'- α -D-Frup (**11**), and β -D-Frup-1,2':2,1'- β -D-Frup (**14**) are still unaccounted for and must arise from starting material other than inulin oligomers. We have seen (page 55) that D-fructose and glucose are present for up to two hours. Evidence is presented in the following section that further supports D-fructose as starting material for DFDA formation.

Disappearance of Inulin by HPLC - A quantitative determination of the rate of disappearance of inulin was not feasible because inulin consists of a range of oligomers and polymers. However, a qualitative understanding can be gained from HPLC analysis of thermolysis samples using *LC Method (iii)*. **Figure 33** compares an unreacted sample of inulin/1.5% citric acid with samples that have been thermolyzed at 160°C for one and three minutes. Inulin oligomers and polymers differ only in the number of fructose residues; they elute on the

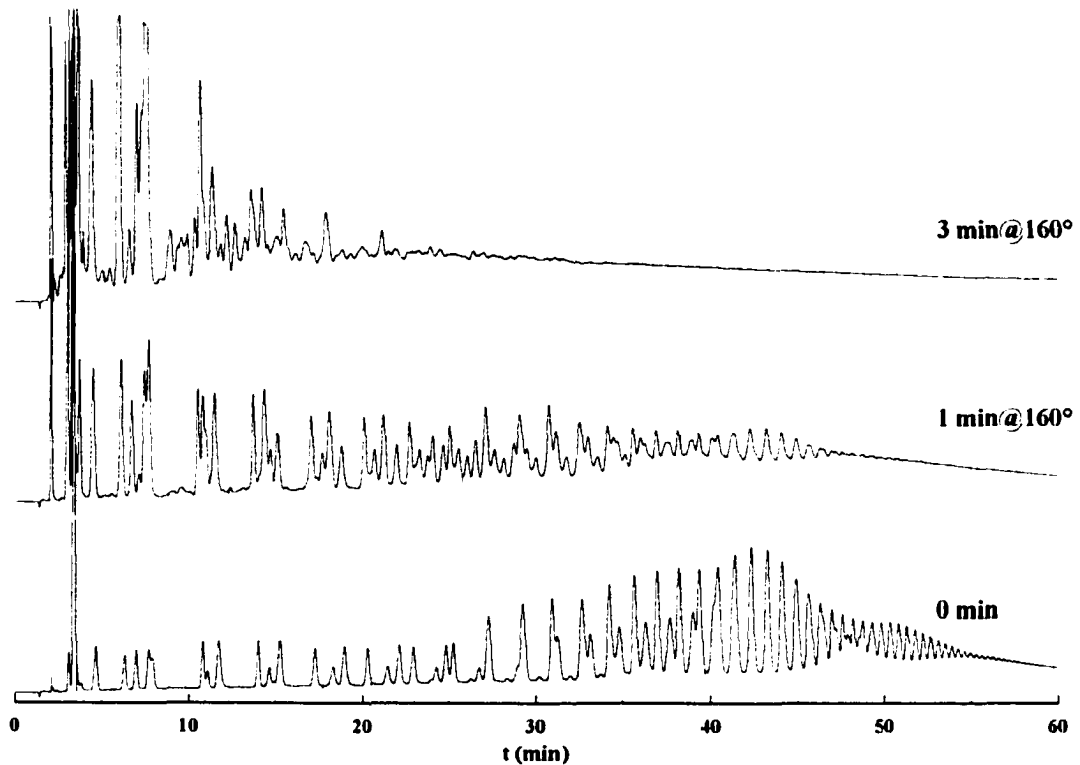


Figure 33 - Comparison of HPAE-PED chromatograms of inulin/1.5% citric acid after 0, 1, and 3 minutes at 160°C.

Dionex LC system in order of increasing chain length.^{81,82} Assuming an initial maximum dp of approximately 70 (page 1), it is apparent that inulin fragmentation is extensive and occurs

rapidly. The large peak at ~3 minutes in the 0 minute sample has the same retention time as D-fructose.

The 5, 10, and 15 minute samples are shown in **Figure 34**. The rapid disappearance of inulin - nearly complete, on a qualitative basis, after 15 minutes - does not coincide with the maximum concentration of DFDA, which occurs after about 25 minutes (**Figure 31**,

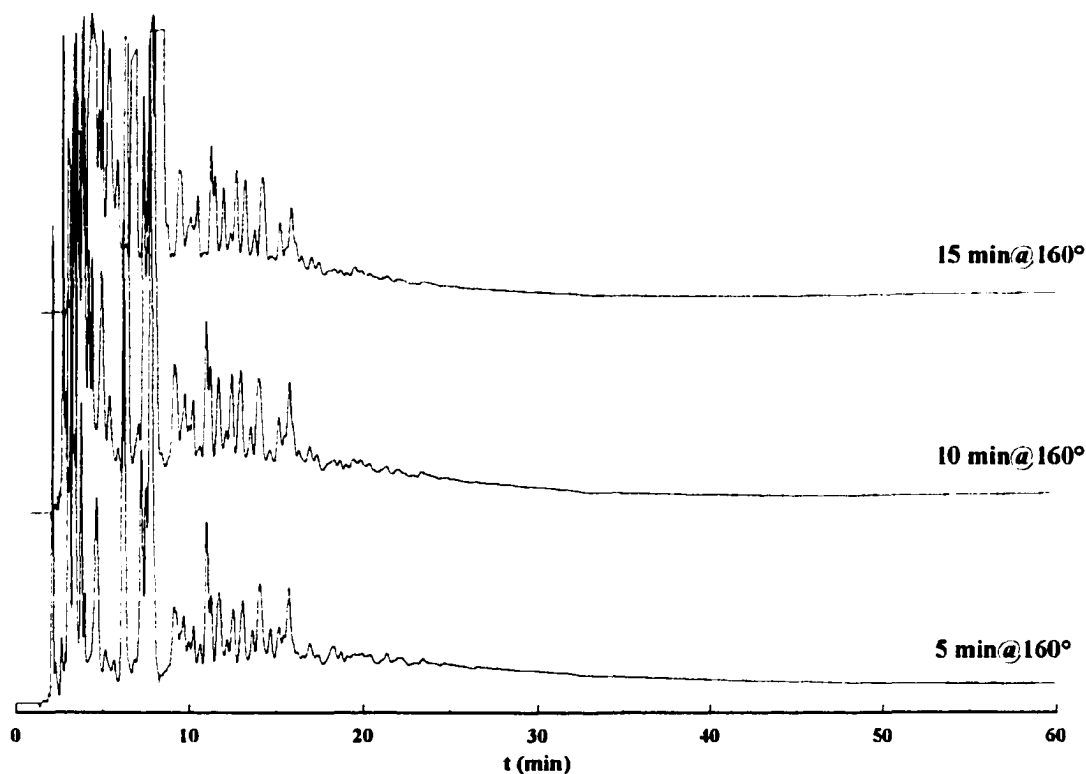


Figure 34 - Comparison of HPAE-PED chromatograms of inulin/1.5% citric acid after 5, 10, and 15 minutes at 160°C.

page 73). The discrepancy between the apparent disappearance of oligomeric starting material and the time after which DFDA decay occurs more rapidly than formation suggests a route to DFDA formation that does not include inulin oligomers.

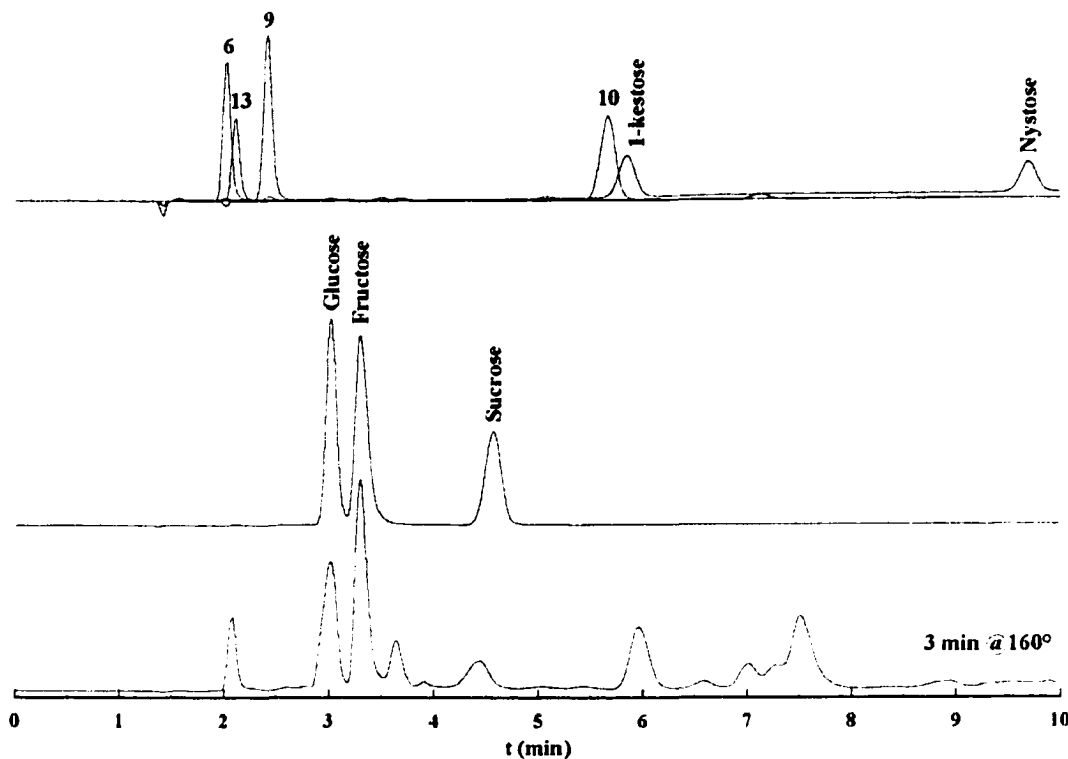


Figure 35 - Comparison of HPAE-PED chromatograms of a 3 minute thermolysis sample with glucose, fructose, sucrose, 1-kestose, nystose, and DFDA standards.

Figure 35 compares the first ten minutes of a three minute thermolysis sample with the retention times of various individual compounds. The chromatograms for α -D-Frup-1,2':2,1'- β -D-Frup (**6**), α -D-Fruf-1,2':2,1'- β -D-Frup (**9**), α -D-Fruf-1,2':2,1'- β -D-Fruf (**10**), and β -D-Fruf-1,2':2,1'- β -D-Frup (**13**) were obtained individually and are overlain for convenience. 1-kestose and nystose[‡] were co-injected, as were glucose, fructose, and sucrose. There is a correlation among the four DFDA between elution order and number

[‡] The structures of 1-kestose (GF₂) and nystose (GF₃) are given on page 154. They were confirmed by comparison of ¹³C chemical shifts with published data.⁸³

of primary hydroxyl groups. α -D-Fru μ -1,2':2,1'- β -D-Fru μ (**6**) does not contain primary OH groups and elutes first; α -D-Fru f -1,2':2,1'- β -D-Fru μ (**9**) and β -D-Fru f -1,2':2,1'- β -D-Fru μ (**13**) each contain one primary OH and elute next; α -D-Fru f -1,2':2,1'- β -D-Fru f (**10**) contains two primary OH groups and elutes last. Also, the disaccharide **10** nearly co-elutes with the trisaccharide 1-kestose. By analogy, glycosylated DFDA trimers and tetramers could be expected to elute in the same regions as inulin-derived tetramers and pentamers, respectively. Therefore, at least a portion of the peaks with retention times between 10 and 20 minutes in **Figure 34** are likely to represent the more stable glycosylated DFDAs and not the more labile inulin oligomers.

Separate thermolysis experiments using nystose in the presence of citric acid further reinforced this assumption. At 160°C and 1.5% citric acid, nystose had completely disappeared within 2 minutes and a range of DFDAs had formed. A ten-fold decrease in citric acid concentration to 0.17% did not change this result. Only when the reaction temperature was lowered to 130°C did nystose react slowly enough for the rate of disappearance to be measured. Thus, the conditions during inulin thermolysis in this study were sufficient to cause complete and almost immediate removal of low dp inulin oligomers.

Three peaks in each of the thermolysis samples correspond, by retention time, to glucose, fructose, and sucrose (**Figure 36**). Although retention time alone does not prove these assignments, they are supported by GCFID analysis (page 53). Glucopyranose, fructopyranose, and fructofuranose are present early in relatively large abundance and

disappear gradually.[‡] Sucrose forms to a lesser extent and is all but gone after 15 minutes. The same patterns appear in **Figure 36** and it is logical to believe that the three peaks at 3.0, 3.3, and 4.0 minutes are glucose, fructose, and sucrose.

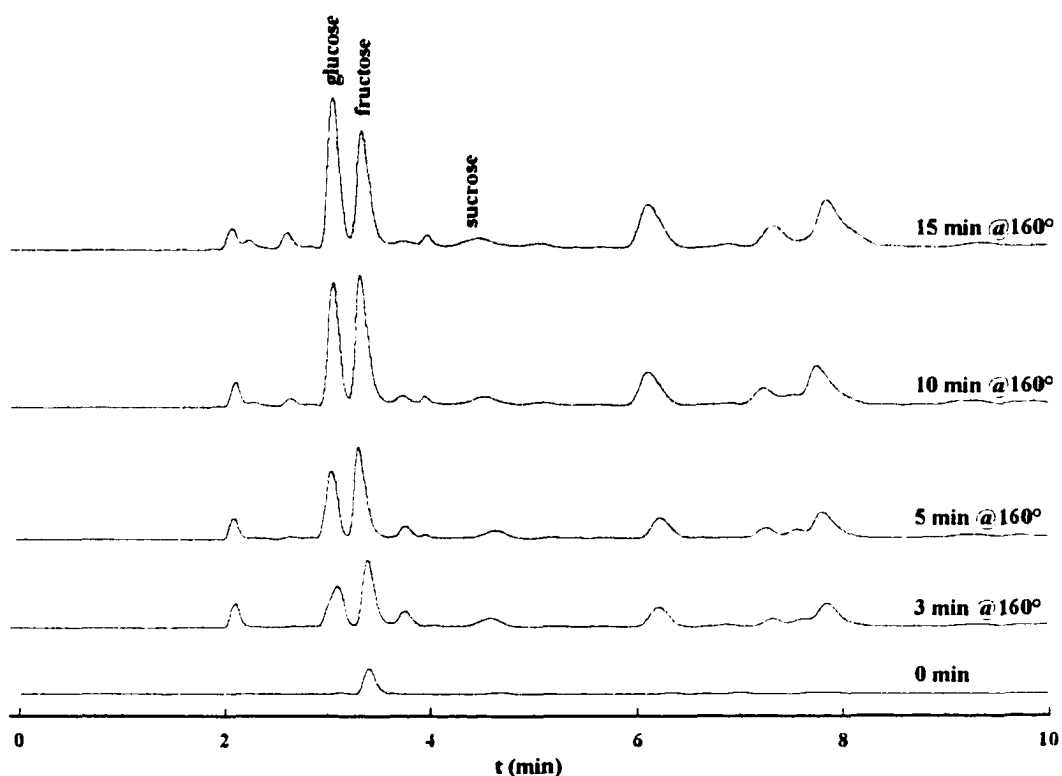


Figure 36 - Glucose, fructose, and sucrose in inulin/1.5% citric acid thermolysis samples.

The presence of D-fructose - and sucrose to a limited extent - makes it a candidate for source material for the five DFDA's whose mechanism of formation is still unaccounted for.

[‡] Glucose-fructose dianhydrides did not form in this study, nor did they occur in similar studies with inulin.^{59,61} The 3° fructosyl cation that results from protonation of the anomeric OH and subsequent loss of H₂O is more stable than the analogous 2° glucosyl cation.⁸⁴ Therefore, fructose plays a more critical role in DFDA formation. Glucose is ~35 times more abundant in sucrose than in inulin (assuming avg inulin dp~35) and at least one glucose-fructose dianhydride has been identified in sucrose caramels.⁶¹

These five - α -D-Frup-1,2':2,1'- β -D-Frup(6), α -D-Fruf-1,2':2,1'- α -D-Fruf (8), α -D-Fruf-1,2':2,1'- β -D-Frup (9), α -D-Fruf-1,2':2,1'- α -D-Frup (11), and β -D-Frup-1,2':2,1'- β -D-Frup (14) - do not contain β -linked fructofuranose and cannot form directly from inulin. Instead, they can arise from the attack of fructopyranose or fructofuranose OH groups on a monomeric fructosyl cation. This cation may also contribute to the formation of the other nine DFDA, in addition to their formation directly from inulin oligomers.

KINETICS RESULTS AND DISCUSSION

Chapter Introduction

The mechanism that describes the reactions that inulin and its oligomers undergo in the current conditions is complex. According to the partial mechanism of **Scheme 8**, page 81, some DFDA's may form directly from inulin, some *via* the anhydrofructose intermediate, and the remainder through one or more unknown pathways. Degradation studies revealed secondary sources - from interconversion or cleavage of trimers or both - of at least some DFDA's. Decay of DFDA's appears to be divided into at least two classes. The thermally stable DFDA's contain one or two pyranose rings and decay slowly if at all. The difuranoses are more labile and may lead to other DFDA's *via* isomerization. The overall order of these reactions is not immediately apparent.

Inulin cannot easily be quantified since it consists of a continuum of fructose oligomers, the distribution of which begins changing immediately upon heating. There was no quantitative tool available during this study to monitor inulin concentration. Citric acid is equally difficult to track in this system. I found no method of measuring pH in thermal melts *in situ* and citric acid is not amenable to silylation and GC/FID analysis with the same reliability as conventional carbohydrates. Therefore, one of the most common and powerful kinetic tools - measurement of reactant concentrations - was unavailable from the start.

With the exception of degradation studies on individual DFDA's, the quantitative empirical evidence for the proposed reaction mechanisms presented here was obtained by measuring product concentrations. Linear and nonlinear least squares curve-fitting provided a preliminary means of validating possible mechanisms on the basis of how well the predicted

curves fit the data. The nonlinear least squares routine provided initial estimates for individual DFDA growth and decay rate constants. These were then used in numerical simulations of more detailed mechanisms. Slight changes in "goodness of fit" between the data and simulated curves were easy to identify by visual inspection.

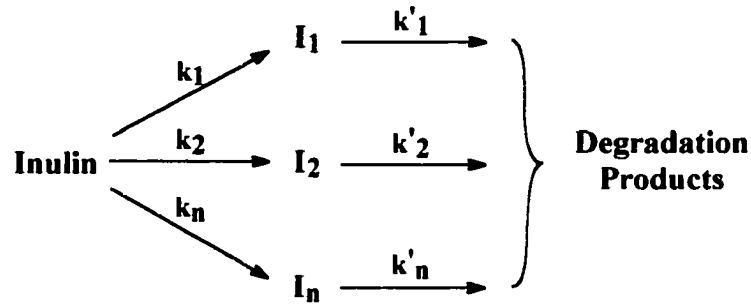
The "final" reaction mechanism is a product of refinements to a simple, first order approximation that does not fail too seriously to mimic the data. It is beyond the scope of this work to insinuate the "true" mechanism for thermolysis of inulin/citric acid mixtures. Instead the following series of adjustments and refinements are offered as logical steps toward a reasonable set of reactions that makes chemical sense.

Estimating Individual DFDA Rate Constants

The Livermore Solver for Ordinary Differential Equations (LSODE) will be used later in this chapter to predict concentrations of reactants and products for various reaction mechanisms. This modeling tool requires as input a complete breakdown of the mechanism into individual reactions, including a list of all reactants and products, and a rate constant for each reaction. It is these rate constants that present the most immediate challenge, since virtually none of them could be determined purely by empirical methods. Instead, nonlinear least squares curve-fitting was used to gain insight into the overall order of certain reactions and to provide initial estimates of the growth and decay rate constants of individual DFDA.

Derivation of 1st Order Parallel-Consecutive Rate Equation - A simple mechanistic explanation for inulin/citric acid thermolysis is a set of first order parallel-consecutive reactions^{85,86} of the type $A \rightarrow B \rightarrow C$. In this scenario inulin (A) gives rise to DFDA (B) which decay to unspecified products (C). Growth and decay in this model are first order or pseudo first order. There is no compensation for isomerization between DFDA and no consideration for specific versus general acid catalysis. Also, fructose as source material is neglected for the time being.

The following derivation results in an expression for the concentration of any individual DFDA at any point in the reaction. In this treatment, all of the oligomers of inulin are grouped together as Inulin. Each DFDA is represented by I_n , where n is the number of the DFDA as used throughout this work. The formation rate constant is k_n , the degradation rate constant is k'_n . **Scheme 9** gives the overall mechanism.



Scheme 9

According to this reaction scheme, the disappearance of inulin can be written as:

$$-\frac{d[inulin]}{dt} = (k_1 + k_2 + \dots + k_n)[inulin] \quad (1)$$

and integration gives:

$$[inulin] = [inulin]_0 e^{-kt} \quad \text{where } k = \sum k_n \quad (2)$$

Substituting Eq. (2) into the expression for the formation of I gives:

$$\frac{d[I_n]}{dt} = k_n [inulin]_0 e^{-kt} \quad (3)$$

But each I decays to non-specific products at some rate k'_n . Adding this degradation of I to the expression for formation of I gives:

$$\frac{d[I_n]}{dt} = k_n [inulin]_0 e^{-kt} - k'_n [I_n] \quad (4)$$

Eq. (4) can be rearranged and multiplied by an integrating factor to give the following:

$$\left(\frac{d[I_n]}{dt} + k'_n[I_n]\right) e^{k'_n t} = k_n[\text{inulin}]_0 e^{(k'_n - k)t} \quad (5)$$

The left side of Eq. (5) can be simplified using the product rule to give:

$$\frac{d}{dt}(e^{k'_n t}[I_n]) = k_n[\text{inulin}]_0 e^{(k'_n - k)t} \quad (6)$$

Finally, Eq. (6) can be directly integrated and the constant of integration defined at time $t=0$.

The result is the integrated rate expression:

$$[I_n] = \frac{k_n[\text{inulin}]_0}{k'_n - k} (e^{-kt} - e^{-k'_n t}) \quad (7)$$

Eq. (7) can then be fitted to the data using nonlinear least squares. The figures on the following pages depict wt% conversion for each DFDA from inulin/1.5% citric acid at 160°C. Mean wt% conversion data are plotted with error bars to show standard error. The line in each plot is the curve predicted by the nonlinear least squares algorithm. In this treatment all three rate constants - inulin disappearance, DFDA growth, and DFDA decay - were floated in the calculation, *i.e.* the program was allowed to converge iteratively on the best fit to the data by adjusting all three rate constants. The individual plots are presented in pairs of similar relative abundance. The y-axis maximum (wt%) is the same in each pair and decreases from 10wt% in the first pair to 1wt% in the last.

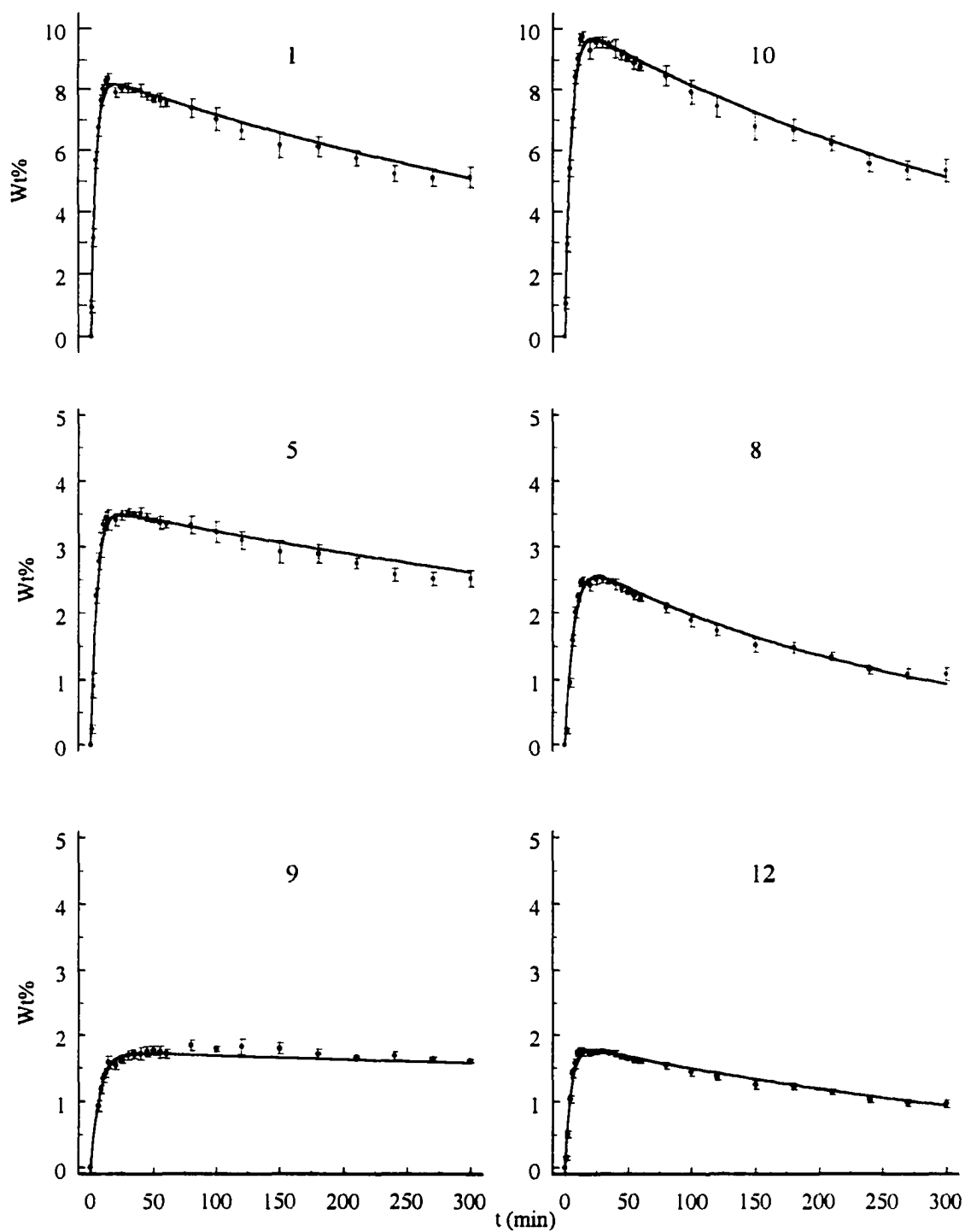


Figure 37 - Nonlinear least squares curve-fitting to DFDAs 1, 10, 5, 8, 9, and 12.

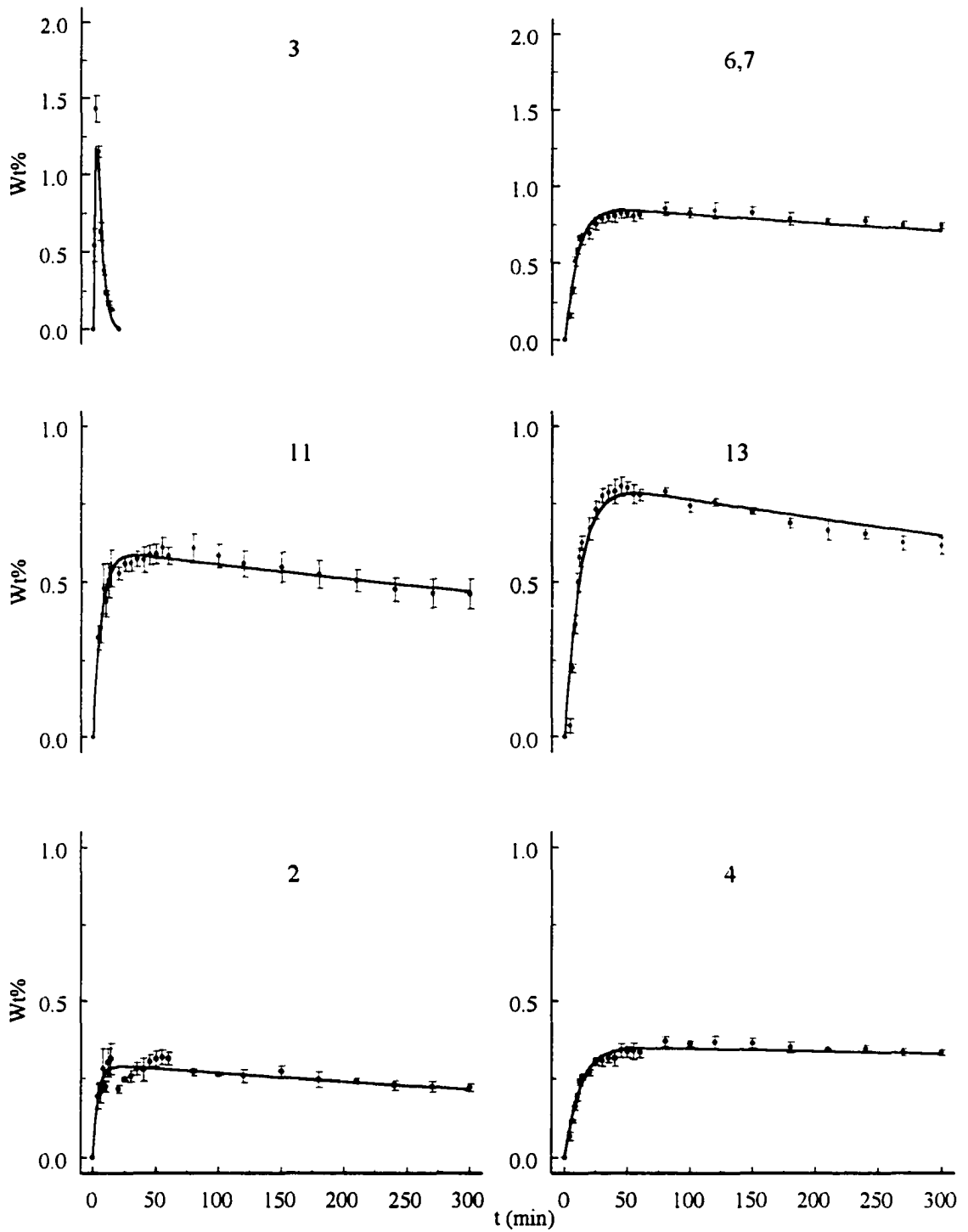


Figure 38 - Nonlinear least squares curve-fitting to DFDAs 3, (6)7, 11, 13, 2, and 4.

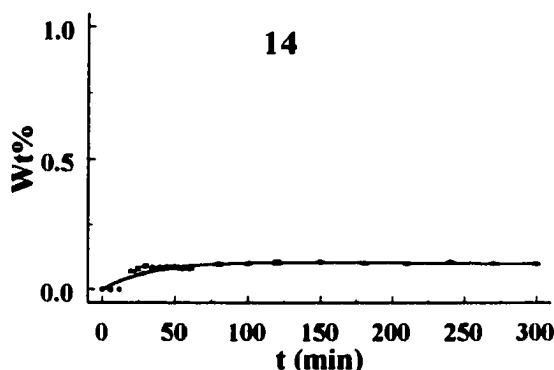


Figure 39 - Nonlinear least squares curve-fitting to DFDA 14.

The predicted curves fit the data reasonably well in the first 30 minutes of the reaction. Eq. (7) seems capable of estimating DFDA formation rates, which implies that formation is first order. The estimated rate constants for this preliminary round of curve fitting are shown in **Table 12**. Inulin disappears by a number of pathways and this simple mechanism can in no way account for them all. This limitation is reflected in the ten-fold variation for the inulin

	DFDA													
	1	2	3	4	5	6,7	8	9	10	11	12	13	14	
k	0.25	0.26	0.38	0.08	0.21	0.11	0.15	0.14	0.20	0.16	0.21	0.07	0.03	
$k_n (\times 10^3)$	26	0.913	15.3	0.346	9.2	1.08	4.94	2.96	24.7	1.17	4.73	0.785	0.0397	
$k'_n (\times 10^3)$	2.03	0.892	400	0.0927	1.45	0.425	3.89	0.341	2.59	0.842	2.61	1.35	0.487	

Table 12 - First estimates of rate constants from nonlinear least squares curve fitting to 1st order parallel-consecutive mechanism.

disappearance rate constant k . The formation and decay rate constants (k_n and k'_n) have been multiplied by 10^3 for convenience. They mirror the trends in the data for relative abundances and provide "order of magnitude" starting points for more serious modeling.

All of the partial reaction mechanisms presented so far were constructed under the assumption that the reactions were acid catalyzed. In keeping with that history, it is

appropriate to infer at this point that the rate of DFDA formation is dependent on hydrogen ion concentration and that the hydrogen ion concentration is constant throughout the thermolysis. This inference will be re-examined in a later section.

After ~30 minutes DFDA decay is the dominant process and the rate equation fails to mimic the data, especially for the difuranose DFDA α -D-Fruf-1,2':2,3'- β -D-Fruf (**1**) and α -D-Fruf-1,2':2,1'- β -D-Fruf (**10**), β -D-Fruf-1,2':2,3'- β -D-Fruf (**5**) and α -D-Fruf-1,2':2,1'- α -D-Fruf (**8**), and β -D-Fruf-1,2':2,1'- β -D-Fruf (**12**) (**Figure 37**). Decay of these difuranoses occurs more rapidly than the predicted values out to ~150 minutes, after which it slows more rapidly than the predicted values. The first order parallel-consecutive model cannot quite duplicate the "curvature" of the data. Degradation studies have already shown that isomerization of **10** occurs. By inference, the other difuranoses probably also isomerize. This does not explain the discrepancy since the model specifies only that decay occurs and does not rely on the nature of the decay products. If decay and isomerization are first order processes, their contribution to the decay rate could be summed and the model would remain valid.

Isomerization might supply a secondary source of the difuranose DFDA, in which case a new rate expression would be required. Based on degradation studies, these processes represent a small contribution to wt% conversion, but that contribution might be more noticeable in the later stages, when the initial rapid formation has ceased. The 1st order parallel-consecutive model would also be expected to fail if decay were occurring *via* 2nd order or higher processes.

Each of the curves in **Figures 37-39** was generated by allowing the least squares algorithm to assign a unique value for the rate constant for disappearance of inulin. If the curve-fitting is repeated with this constant fixed, the match between the data and the predicted curve becomes unacceptable. In **Figure 40** the nonlinear LS fit to Eq. (7) is compared to the data for α -D-Fruf-1,2':2,1'- β -D-Fruf (10) with the inulin disappearance rate constant (k) fixed

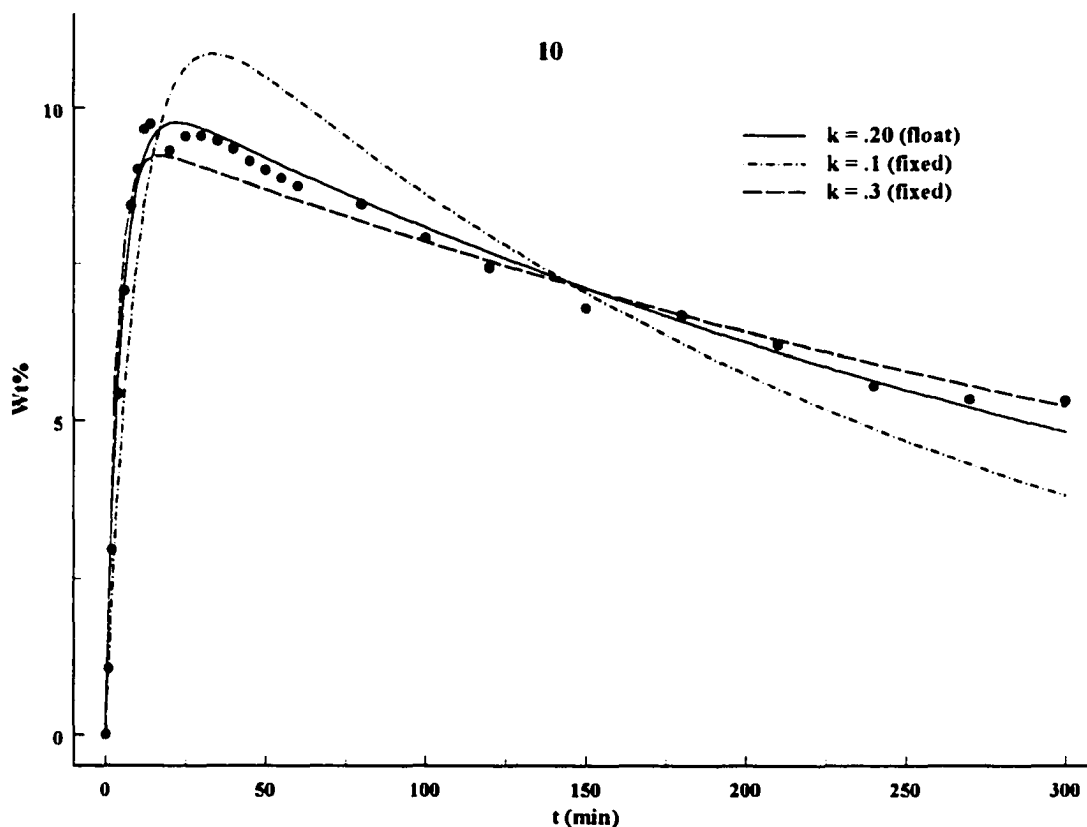


Figure 40 - Effect of varying the inulin disappearance rate constant on nonlinear least squares curve for α -D-Fruf-1,2':2,1'- β -D-Fruf (10).

at 0.10 and 0.30. The resulting curves are compared to that predicted by nonlinear LS when the rate constant is floated. (The error bars are removed for convenience.) When the rate constant is decreased from .20 (float) to .10 (fixed), the maximum predicted wt% conversion

increases. The maximum occurs later in the reaction and the decay gradient becomes steeper. When the rate constant is increased from .20 (float) to .30 (fixed), the maximum predicted conversion is reduced and occurs sooner, and decay is slower than the data. The same effect was exhibited by all 14 DFDA's.

This sensitivity may be a consequence of the simplicity of the reaction mechanism used to generate the curves. The value of the nonlinear LS approach lies in its ability to provide rough estimates of rate constants. The curve shapes for the first 30 minutes of reaction match the data well and the corresponding formation rate constants are suitable as initial estimates. The decay stages, especially for difuranoses, need to be inspected more closely.

Curve-fitting Treatments of DFDA Decay - Degradation rates for thermally stable DFDA's are slow and should have little impact on the overall mechanism. DFDA's that decay rapidly will begin doing so immediately upon formation and the mechanism and rate constants must reflect that fact. The mechanism must also provide "cross links" between DFDA's to account for isomerization, which provide secondary sources for DFDA formation. Each of these additional pathways adds a level of complexity. In addition, the above curve-fitting treatment of a set of first order parallel-consecutive reactions indicates it may be safe to assume a first order mechanism for DFDA formation, but the mechanism for decay, for the difuranoses at least, may be of higher order.

To address this question of decay order, nonlinear LS plots of standard rate equations were compared to wt% conversion data for individual DFDA's. The rate equations under consideration are:

- $v=k[A]$
- $v=k[A]^2$
- $v=k[A][B]$

A prerequisite for comparing the data in this way is that the variables must be reactant concentrations, either directly determined or as determined through their stoichiometric relationship to product concentrations. It is not possible to express DFDA concentration in terms other than wt% conversion, which negates the use of data obtained while inulin is still present and forming DFDA. To circumvent this problem, the comparison was confined to data after 30 minutes reaction, the assumption being that formation of a particular DFDA from inulin has ceased and the dominant process is degradation.[‡] This makes the DFDA the sole reactant in a 1st order treatment. The following graphical treatments were conducted on each of the five difuranoses that persist beyond 30 minutes reaction.^{**} The results were virtually identical for each; α -D-Fruf-1,2':2,1'- β -D-Fruf (10) is used here to demonstrate the principles.

- 1st Order Decay of DFDA 10 ($v=k[A]$) - If degradation occurs *via* a 1st order process, the rate law and its integrated solution are:

$$-\frac{d[A]}{dt}=k[A] \rightarrow [A]_t=[A]_0e^{-kt} \quad (8)$$

[‡] The degradation data for individual DFDA are not applicable. The initial *molar* ratio of DFDA to citric acid in those experiments was ~39. The same molar ratio in thermolysis samples, assuming M_w inulin = 5000 (dp 31), is ~2.5.

^{**} One method for graphical treatment of reaction mechanisms is linear least squares,⁸⁶ in which the integrated rate law is rearranged algebraically in order to write it in the form of the equation of a straight line. This method tends to overemphasize variance in the later stages. Nonlinear least squares avoids this problem because the quantity being plotted is $[A]$, which usually has a constant variance.⁸⁷

The nonlinear least squares treatment of this equation for the inulin/1.5% citric acid/160°C thermolysis data for α -D-Fruf-1,2':2,1'- β -D-Fruf (**10**) is given in **Figure 41**. This rate equation overestimates the extent of degradation in the later stages (a) and

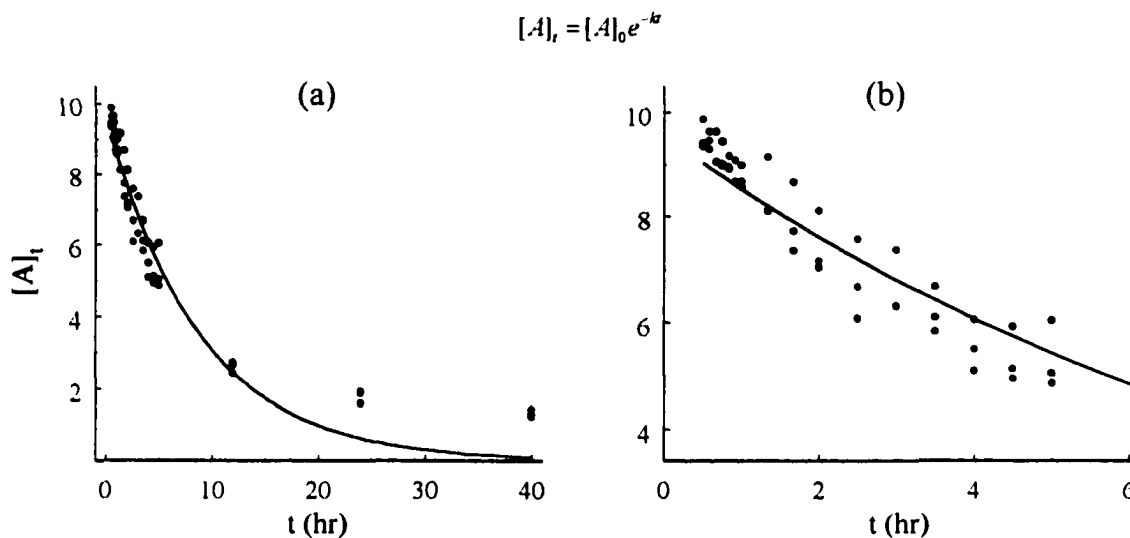


Figure 41 - 1st order nonlinear least squares curve-fitting to decay of α -D-Fruf-1,2':2,1'- β -D-Fruf (**10**).

underestimates the rate of degradation in the early stages (b). The nonlinear LS algorithm converges on a rate constant value that provides the best fit to the data based on initial concentration. For α -D-Fruf-1,2':2,1'- β -D-Fruf (**10**) the initial concentration $[A]_0$ is 9.55, the mean wt% conversion at 30 minutes.

If the initial concentration of **10** is increased from 9.55 to 10.2, the fit to the later data (6-40 hrs) is relatively unaffected while the fit to the early data (0-6 hrs) improves significantly (**Figure 42**). One of the original assumptions for this 1st order treatment was that α -D-Fruf-1,2':2,1'- β -D-Fruf (**10**) is the only reactant. If there are components present in the melt that

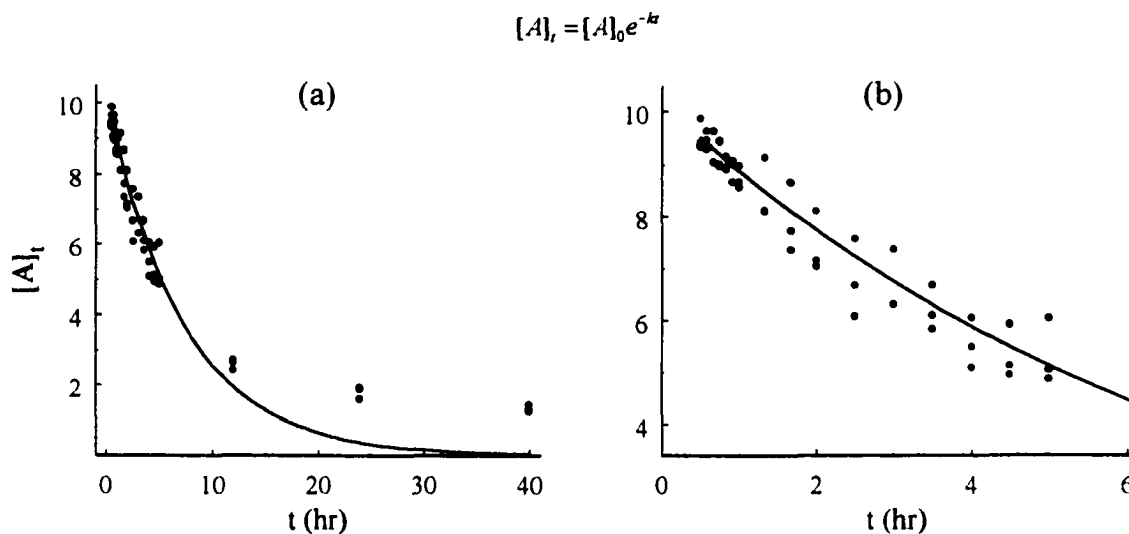


Figure 42 - 1st order nonlinear least squares curve-fitting to decay of α -D-Fruf-1,2':2,1'- β -D-Fruf (10) with $[A]_0 = 10.2$ wt%.

provide a secondary source of 10, the actual rate of decay will be somewhat greater than that reflected by the data. Recall that trimers and other DFDA's (page 67), and D-fructose (pages 55 and 87) are likely candidates for this role. This argument lends validity to a 1st order or pseudo 1st order decay mechanism for α -D-Fruf-1,2':2,1'- β -D-Fruf (10).

- **2nd Order Decay of DFDA 10 ($v=k[A]^2$)** - This equation states that the rate of decay is proportional to the square of the DFDA concentration. For this to be true, the DFDA must either react with another molecule of itself, or with something else that is present at the same initial concentration. In keeping with the chemical mechanisms reviewed in this work that involve the fructosyl cation, DFDA self reaction might involve protonation, opening of an anhydride linkage to form a glycosylated fructosyl, and attack by a hydroxyl group from another DFDA of the same type. But it seems unlikely, given the variety of DFDA's present,

that attack by the same species would predominate over attack by several different species. Also, once the cation formed, the likelihood of intramolecular hydroxyl attack is also high.

Based once again on the mechanisms reviewed in this work, the most likely candidate for a 2nd order DFDA decay mechanism that is not self reacting is citric acid. But citric acid could not have been present at 30 minutes at the same concentration as α -D-Fruf-1,2':2,1'- β -D-Fruf (10). Each sample weighed ~10mg, of which 1.5% or .15mg was citric acid. The weight of 10 present at 30 minutes was ~1mg (~10wt% maximum conversion). Converting these amounts to moles gives 8×10^{-7} mol citric acid and 3×10^{-6} mol α -D-Fruf-1,2':2,1'- β -D-Fruf (10), which is a four-fold excess of DFDA. If all the difuranose DFDAs present in the melt at 30 minutes are included in the calculation (~25wt% conversion) there is a ten-fold excess over citric acid at 30 minutes. The likelihood of any other species being present at the same initial concentration and reacting only with α -D-Fruf-1,2':2,1'- β -D-Fruf (10) is remote.

Nevertheless, the graphical treatments from the previous section were applied to the 2nd order rate law $v=k[A]^2$. The integrated form of this equation is:

$$\frac{1}{[A]_t} = \frac{1}{[A]_0} + kt \quad (9)$$

Solving Eq. (9) for $[A]_t$ gives:

$$[A]_t = \frac{[A]_0}{1 + [A]_0 kt} \quad (10)$$

Nonlinear least squares curve-fitting to Eq. (10) is shown in **Figure 43**. This equation

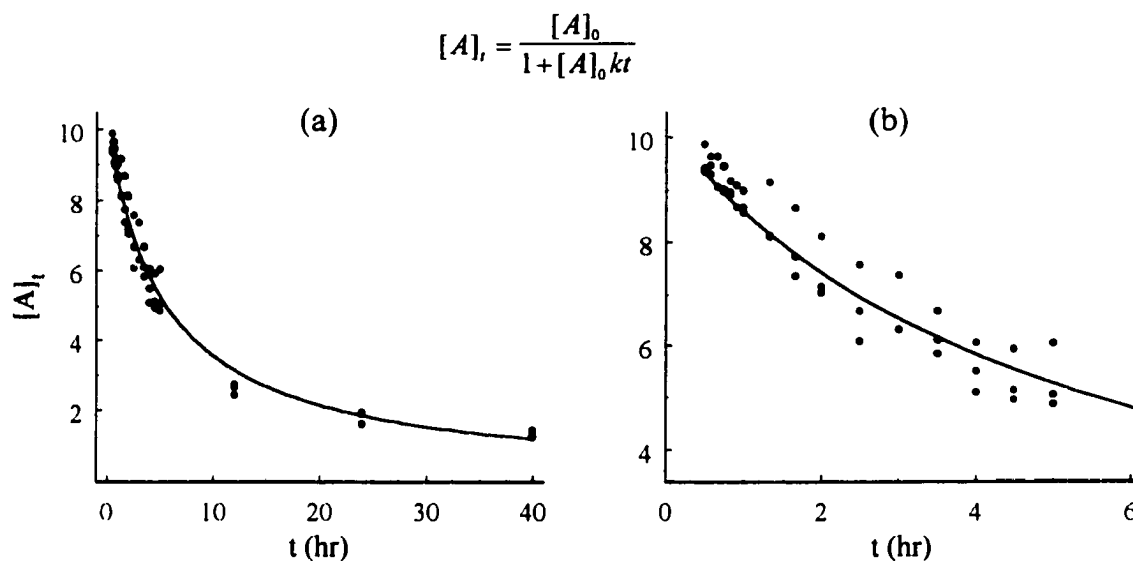


Figure 43 - 2nd order nonlinear least squares curve-fitting to decay of α -D-Fruf-1,2':2,1'- β -D-Fruf(10) with $[A]_0 = 10.2$ wt%.

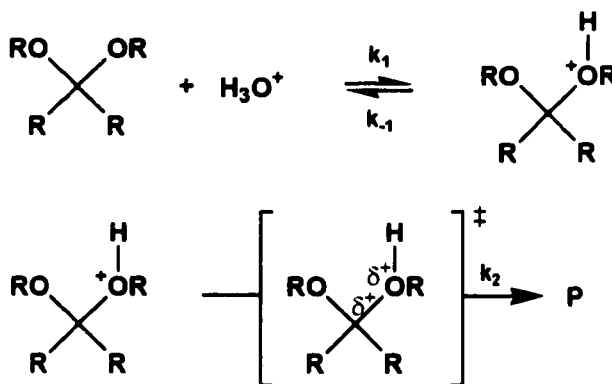
more closely approximates the data after ~ 20 hours (a), indicating that 2nd order processes may be of greater importance in the later stages of thermolysis. The fit to the first five hours of reaction (b) is not as good as that for the 1st order plot (**Figure 42**) where $[A]_0 = 10.2$. Using $[A]_0 = 9.55$ in the 2nd order plot (not shown) considerably worsens the predicted fit in the 0-5 hour region.

- 2nd Order Decay of DFDA 10 ($v = k[A][B]$) - This form of 2nd order kinetics is widely encountered, yet its application to the current study is far from straightforward. The nature of the analysis does not allow the identification of the second reactant. Known possibilities include citric acid, which was added to the mixture, and inulin thermolysis products such as fructose, other DFDA, glycosylated DFDA, and non-specific degradation products *e.g.* HMF. But the concentration of each of these is small relative to the difuranose DFDA,

which comprise 25.4% by weight of the reaction mixture at 30 minutes. The pattern of decay for the five difuranoses (α -D-Fruf-1,2':2,6'- β -D-Fruf(3) excluded) is similar (Figure 37, page 94) and a rate law applied to one of these should be valid for the other four. This assumption is based on the structural and behavioral similarities among these five difuranoses.

If one of the above thermolysis products were involved, it would be the limiting reagent and 2nd order decay would only continue until that reactant had been consumed. But difuranose decay continues for 40 hours until the combined mean concentration of the five difuranoses falls to 4.4 wt%. No single compound appears in the analytical methods used to track products in this study that is present in high enough amounts to react for 40 hours on a 1:1 basis with five different DFDA's. Even if a general class of compound, *e.g.* trimers or monomers, were responsible for 2nd order decay, there doesn't appear to be enough material present to account for this loss. At least a portion of difuranose decay is probably non-specific in the sense that collision with any of various classes of compound in the mixture results in a reaction. This might account for the apparent 2nd order nature of the decay curve after 12 or so hours. But with the current knowledge of the contents of the melt during thermolysis, a sensible graphical treatment of the rate equation $v=k[A][B]$ is not possible.

The Role of Citric Acid in DFDA decay - As mentioned above, DFDA decomposition might involve protonation and opening of an anhydride bond to form a carbocation (fructofuranose singly-linked to a fructosyl cation). The general features of this mechanism are common to



Scheme 10

acetals,⁸⁶ and are extrapolated here to the fructose-based ketals. In **Scheme 10** the cation is a distinct species and the rate equation in the steady state is:

$$v = \frac{k_1 k_2 [A][H^+]}{k_{-1} + k_2} \quad (11)$$

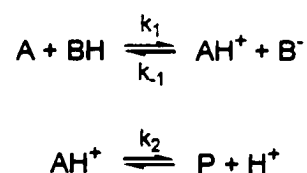
where A is the ketal.[‡] If the reaction is acid catalyzed $[H^+]$ is constant, being regenerated as a product, and the expression for the observed reaction rate is $v = k_{\text{obs}}[A]$. The observed rate

[‡] If the cation is not a distinct species and the reaction proceeds by a concerted pathway, the rate equation becomes: $v = k_2[A][H^+]$. These two reaction pathways are kinetically indistinguishable because they show the same dependence on concentration. But in both cases the rate depends upon hydrogen ion concentration.

constant will be dependent on hydrogen ion concentration.

It is important to remember during the course of this discussion that DFDA growth and decay take place in anhydrous melts. The situation in aqueous chemistry in which H₂O is in large excess and constitutes an abundant supply of a conjugate acid/base pair does not apply. The sole initial proton donor is citric acid. Carbohydrate OH groups are poor proton donors (*c.f.* conditions required for methylation). As the reaction proceeds other proton donors may become available. For example, aqueous acidified solutions of sucrose or D-fructose (0.05M sugar, 2mM H₂SO₄) heated to 250°C yield acidic products that include levulinic, lactic, formic, and acetic acid.⁷⁰ Also, the predominant decomposition product of anhydrous sucrose at 150-250°C is H₂O.⁷¹ These products must be considered as possible by-products of inulin thermolysis.

The ketal mechanism can be incorporated into a general scheme for acid catalyzed degradation of DFDA:



Scheme 11

where A and AH⁺ are the ketal and the protonated ketal (a difuranose DFDA in this case), BH an organic acid, and B⁻ the conjugate base. The opening of AH⁺ to a carbocation and subsequent reaction to form products (P) are incorporated into the second step of **Scheme 11** under the assumption that the carbocation is more reactive than the protonated ketal. If

the first reaction in **Scheme 11** is the rate controlling step the rate equation is:⁸⁶

$$v = k_1[A][BH] \quad (12)$$

The system will show *general* acid catalysis and the rate will increase not with increasing hydrogen ion concentration, but with the concentration of the acid. The concentrations of acidic by-products of inulin thermolysis will influence the rate.

If the second reaction in **Scheme 11** is the rate controlling step the rate equation is:⁸⁶

$$v = \frac{k_2}{K_a^{AH}} [A][H^+] \quad (13)$$

The system will show *specific* acid catalysis and the rate will depend on hydrogen ion concentration regardless of the source of hydrogen ion. Aqueous acidified sucrose was shown early to undergo specific acid catalyzed hydrolysis.⁸⁸ Mandal *et al*⁹⁰ found that the kinetic behavior of acid catalyzed sucrose hydrolysis in four non protic solvents was exactly similar to that in water and therefore assumed specific acid catalysis. And Lönnberg and Gylén⁸⁹ found the rate limiting step in hydrolysis of alkyl fructofuranosides to be formation of the fructosyl carbocation and not protonation of the glycosidic oxygen. It is uncertain whether or not these results may be applied to anhydrous melts of inulin/citric acid. Experiments that monitor and control each acidic species present during thermolysis might resolve the question of whether DFDA formation and decay are catalyzed specifically by hydrogen ion. Lacking these experiments, I am forced to presume specific acid catalysis and develop the mechanistic model accordingly. In that case, protonation of the glycosidic oxygen (first step in **Scheme**

11) occurs rapidly, and formation of the carbocation is the rate controlling step, assuming subsequent reaction of the carbocation is also fast. The overall kinetics will be pseudo 1st order or pseudo 2nd order, depending on whether the hydrogen ion concentration remains constant or changes during thermolysis.[‡]

- pH During Thermolysis - A series of pH measurements was carried out on thermolysis samples to establish whether or not a pseudo 1st order treatment was appropriate. **Table 13** lists thermolysis time, pH, and citric acid concentration for inulin/citric acid mixtures containing 1.0, 1.5, 2.0, and 2.9 wt% citric acid. Pure citric acid was tested also. Each

		t (hr) @ 160°C					Avg
		0	.5	2	5	9	
pH*	Citric acid	2.45 (2.54e ⁻²)	2.28 (2.94e ⁻²)	2.25 (3.34e ⁻²)	2.39 (2.80e ⁻²)	2.47 (3.04e ⁻²)	2.37 (2.54e ⁻²)
	Inulin/ 1.0%	3.68 (2.86e ⁻⁴)	3.69 (2.66e ⁻⁴)	3.67 (2.66e ⁻⁴)	-	3.66 (2.67e ⁻⁴)	3.68 (2.71e ⁻⁴)
	Inulin/ 1.5%	3.52 (4.09e ⁻⁴)	3.55 (4.67e ⁻⁴)	3.50 (3.76e ⁻⁴)	3.46 (3.85e ⁻⁴)	3.42 (4.47e ⁻⁴)	3.49 (4.17e ⁻⁴)
	Inulin/ 2.0%	3.44 (5.57e ⁻⁴)	3.39 (5.18e ⁻⁴)	3.35 (5.63e ⁻⁴)	-	3.37 (5.18e ⁻⁴)	3.39 (5.39e ⁻⁴)
	Inulin/ 2.9%	3.41 (8.02e ⁻⁴)	3.34 (8.05e ⁻⁴)	3.32 (8.28e ⁻⁴)	-	3.36 (7.73e ⁻⁴)	3.36 (8.02e ⁻⁴)

* molar concentration of citric acid is shown in () beneath each pH value.

Table 13 - pH of citric acid and inulin/citric acid mixtures after thermolysis at 160°C.

[‡] If citric acid were the only acidic species present and its concentration were constant throughout the reaction period, then the system could obey general acid catalysis and still be pseudo 1st order. It is not known how low the concentrations of acidic by-products must be to satisfy this condition.

sample (~10mg) was subjected to the same thermolysis treatment as used throughout this study. The residues were dissolved in distilled H₂O (2.0 mL) and the pH recorded. Variations in pH between samples was due in part to variations in acid concentration; in general, lower concentrations gave higher pH readings, and vice versa.

The color of the glassy citric acid residue changed during heating from light yellow after 30 minutes through yellow/orange to orange/brown after 9 hours, indicating some degradation. However, the pH of pure citric acid was relatively unaffected by heating at 160°C for 9 hours. The pH of the inulin/citric acid mixtures was also relatively constant throughout the reaction time. This constant pH during thermolysis supports the hypothesis that DFDA decay is pseudo 1st order.

- **Effect of Citric Acid Concentration on Wt% Conversion** - A number of experiments were conducted on mixtures of inulin with 1.0, 2.0, and 2.9% citric acid. A plot of mean wt% conversion of total DFDA for these systems in the first hour of thermolysis is presented in **Figure 44**. Trends in the data for 1.0, 1.5, and 2.0% citric acid can be interpreted in terms of competing formation and decay rates for DFDA, each dependent on [H⁺]. The discussion of the 2.9% data is deferred until later.

At citric acid concentration of 1.0%, DFDA decay rate is slow and the data describe a smooth curve that gradually approaches a maximum (at ~40-50 min). When citric acid is increased to 1.5% the formation rate increases, as evidenced by more rapid conversion in the early stages. The higher maximum conversion for 1.5% citric acid may be due to a higher proportion of the starting material going toward DFDA formation, while in the 1.0% system

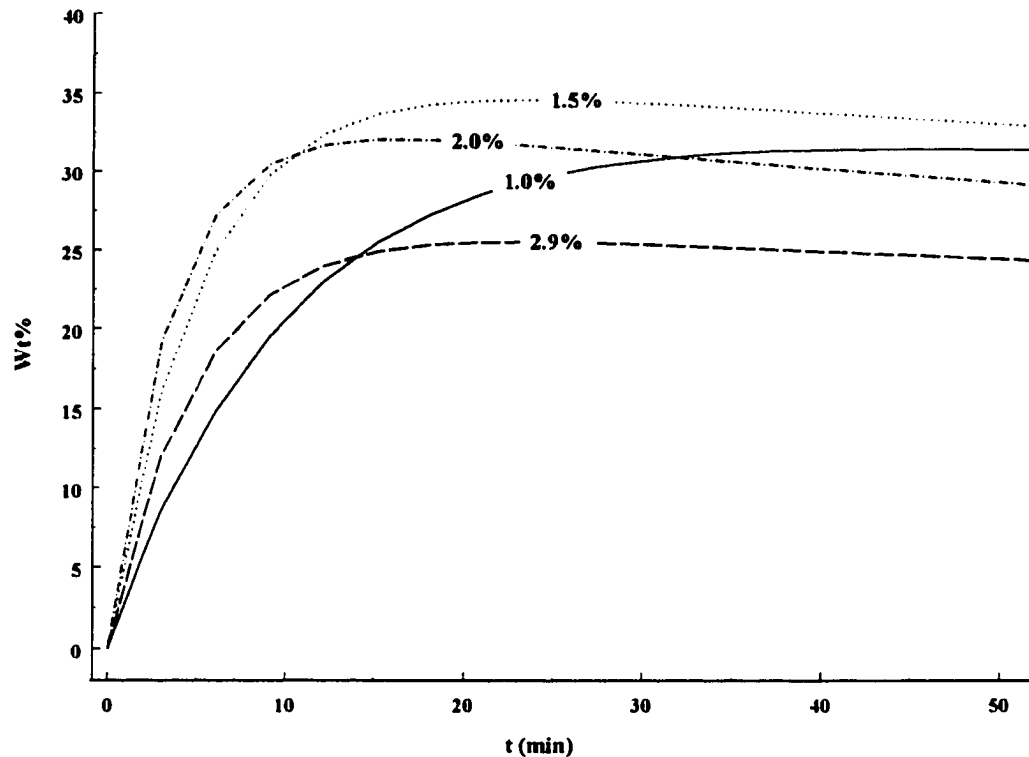


Figure 44 - Mean wt% conversion (0-60 min) to total DFDA from inulin with citric acid concentrations of 1.0, 1.5, 2.0, and 2.9 wt%.

less starting material goes into DFDA formation and more into reactions that result in non-DFDA products. The decay rate also increases for the 1.5% system, causing the maximum conversion to occur earlier (~25-30 min). The slope of the curve after 30 minutes is negative, indicating that decay has become the dominant process.

The formation rate at 2.0% citric acid is only slightly greater than at 1.5%, which might indicate that the "nominal" acid concentration has been reached. The lower maximum conversion and slightly steeper decay indicate that degradation is competing more efficiently than in the 1.0 and 1.5% systems.

If the data are plotted out to five hours (**Figure 45**) the above trends for 1.0, 1.5, and 2.0% continue. The decay curves for these three descend toward equilibrium at relative rates in accord with citric acid concentration - *i.e.* fastest descent for highest acid concentration.

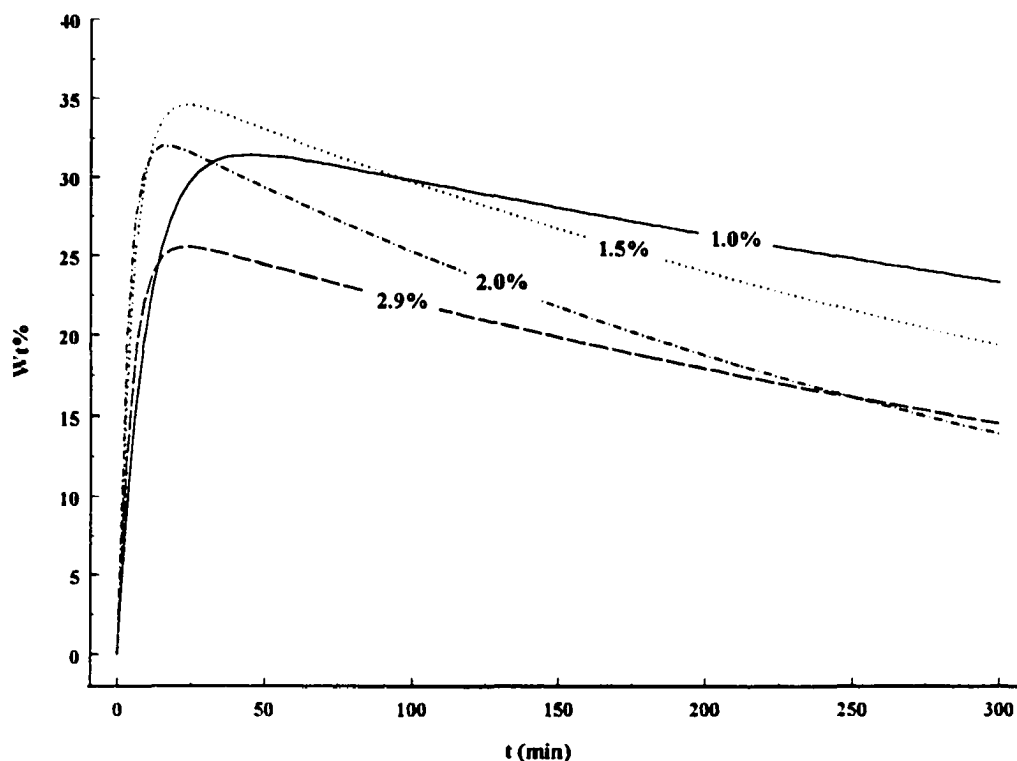


Figure 45 - Mean wt% conversion (0-300 min) of inulin to total DFDA from inulin with citric acid concentrations of 1.0, 1.5, 2.0, and 2.9 wt%.

Table 14 shows the abundance of the difuranoses (*ff*) relative to pyranose-containing DFDA (*fp/pp*) at 40 and 210 minutes for all four systems. The ratios (*italics* in the table) were calculated as the sum of the mean wt% conversion for DFDA 1, 5, 8, 10, and 12 divided by the same sum for DFDA 2, 4, 6, 7, 9, 11, 13, and 14. The fact that the ratio is greater in all cases at 40 minutes than at 210 minutes reflects the rapid formation and greater

overall abundance of the difuranoses.

	[Citric acid]			
	1.0%	1.5%	2.0%	2.9%
40 min.	6.6	5.5	5.3	7.9
210 min.	4.8	4.0	3.7	6.4
% decrease	27	27	30	19

Table 14 - Average ratio and % decrease of difuranoses to pyranose-containing DFDA's at 40 and 210 minutes.

The ratio decreases gradually as citric acid increases for the 1.0, 1.5, and 2.0% systems. This is true at both 40 and 210 minutes and reflects the ease of difuranose decay relative to the pyranoses. The *ff:fp/pp* ratio decreases by the same amount (~30%) after 210 minutes reaction time, indicating a consistent decline of difuranoses in all three systems.

The 2.9% system contains anomalies. The DFDA formation rate, instead of increasing slightly as in the 2.0% system (**Figure 44**), was markedly slow. In all of these systems some balance exists between acid catalyzed formation of DFDA's from inulin oligomers and degradation of the D-fructose moieties of those oligomers to non-specific products. Lower citric acid concentrations presumably catalyze anhydride formation (and scission of glycosidic bonds, etc.) to a greater extent than degradation of fructofuranose and fructopyranose rings. Evidently, at 2.9% the balance tips toward ring degradation and fructose residues are removed from the pool of material that might otherwise go toward DFDA formation. Thus, a paucity of starting material, rather than increased decay rate, could be responsible for low yield in the early stages. This does not, however, explain the slow decay rate. There is no apparent

reason why increased ring degradation would not affect the starting material and the DFDA products in a similar manner. Therefore, no reasonable explanation is offered for the decay behavior of the 2.9% system.

The relative abundance of difuranoses (**Table 14**) was higher in the 2.9% system than in the other three systems, and the change in this abundance from 40 to 210 minutes was less than in the other systems. It is possible that ring degradation has caused the formerly more stable pyranose-containing DFDA's to decay faster. In other words, decay is less selective at higher acid concentration and the difference in the rate of decay for the two groups is smaller. This would explain both the higher *ff:fp/pp* ratio and the fact that the ratio changes less.

Thermolysis at Higher Temperature - A series of thermolysis experiments were conducted at elevated temperatures. Bond scission reactions of the type described in this work have high activation energies and are relatively more sensitive to temperature changes than other reaction types. Both the Arrhenius equation and Transition State Theory⁸⁶ predict a strong temperature dependence for reactions with high activation energies. Also, since thermolysis occurred in viscous melts, there was some concern that diffusion control might be operating. According to a traditional rearrangement of the Stokes-Einstein equation,⁹⁰ the rate constant of a diffusion controlled reaction is insensitive to temperature changes relative to changes in viscosity.

Thermolysis data for inulin/1.5% citric acid at 170 and 180°C are compared in **Figure 46** to data for the same mixture at 160°C. As the graph shows, the formation and decay of DFDA's from inulin are quite sensitive to temperature. As the temperature increases from 160

to 170 to 180°, the time at which maximum wt% conversion occurs decreases from 25 to 15 to 5 minutes. The decay rate displays a similarly large temperature dependence. This result highlights the importance of activation energy and the absence of diffusion control in the current thermolysis systems.

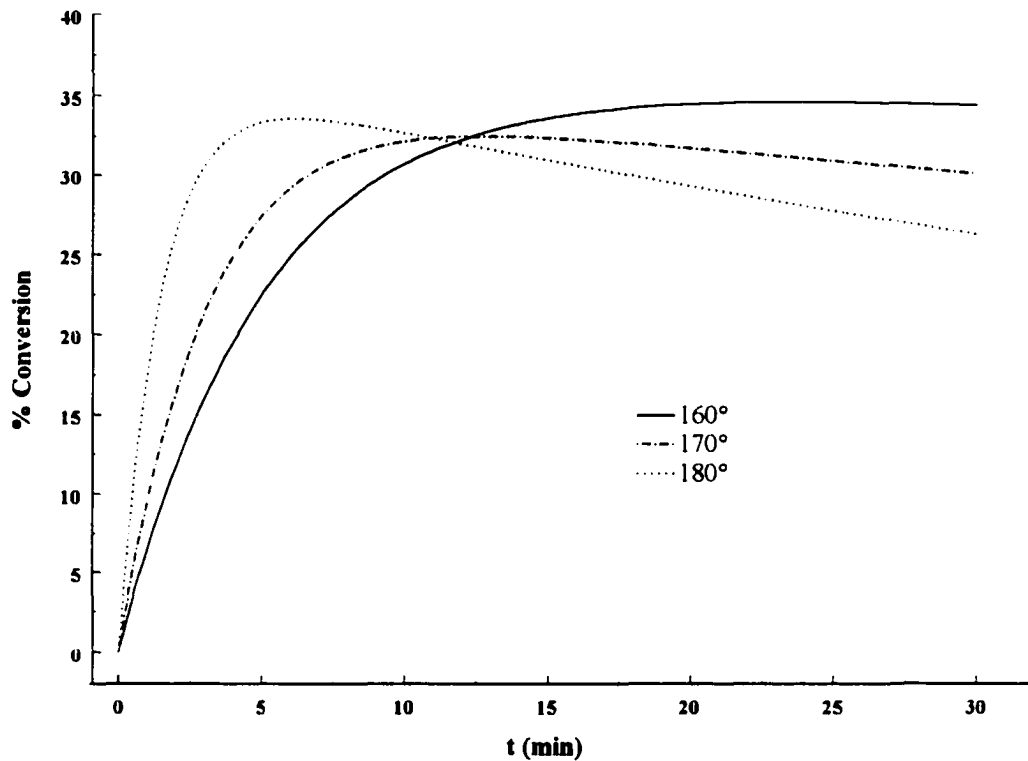


Figure 46 - Inulin/1.5% thermolysis at 160, 170, and 180°C.

Reaction Mechanisms

The previous sections have provided a foundation for numerical simulations. The following concepts are those upon which the kinetic model will be constructed.

1. The fructosyl cation holds a central role in DFDA growth and decay. DFDAs, glycosylated DFDAs, and oligomers of inulin are ketals and will react *via* fructosyl cations under acidic conditions (page 106). They will also react according to *specific* acid catalysis and obey pseudo 1st order kinetics. Two experimental results, in addition to aforementioned literature references, reinforce this view: 1) graphical treatments of the degradation data for difuranoses are most successful when applied to a 1st order rate equation (page 100), and 2) pH remains constant throughout the reaction (page 109). However, the 1st order graphical treatment was not entirely satisfying and a portion of DFDA decay is likely to occur *via* 2nd order processes. This is not unreasonable given the abundance of fructose-containing compounds in the reaction mixture which may form fructosyl cationic species.

2. Five of the six difuranoses can form directly from inulin oligomers of $dp > 2$ (**Scheme 8**, page 81). Assuming protonation is rapid and there is no buildup of fructosyl cation, the formation of the cation will be the rate controlling step and a simple, one-step mechanism ($A \rightarrow B$) can be written for the formation of these five.

3. Four more DFDAs can form from inulin oligomers whose fructofuranosyl cationic form has isomerized *via* the 2,6-anhydrofructose intermediate to the fructopyranosyl form (**Scheme 8**, page 81). The effects of the anhydro intermediate on the validity of applying pseudo 1st order kinetics to DFDA formation are not known. Recall (page 80) that these four DFDAs were not present at very early reaction times. The simplest approach is to exclude

the intermediate from the model. If numerical simulation is unable to duplicate the data for these four DFDA, the anhydro species may need to be incorporated into the mechanism.

4. The remaining five DFDA differ from the foregoing in that they do not contain β -D-fructofuranose rings and cannot form directly from inulin oligomers. Their mechanism of formation must be determined from a combination of experimental evidence and common sense. In accordance with the ketal mechanism already put forth, isomerization provides a route to these five. A protonated anhydride linkage may open to a glycosylated cation, then re-close to form a different (or the same) DFDA. The 2,6-anhydrofructose intermediate may play a role. Also, fragmentation of inulin in the acidic melt yields fructose and sucrose, both candidates for source material for DFDA.

5. The pyranose-containing DFDA do not appear to degrade significantly. Degradation of these DFDA will play a minor role and inaccuracies in their decay rate constants should not overtly influence the model.

6. The difuranoses α -D-Fruf-1,2':2,3'- β -D-Fruf (1), β -D-Fruf-1,2':2,3'- β -D-Fruf (5), α -D-Fruf-1,2':2,1'- α -D-Fruf (8), α -D-Fruf-1,2':2,1'- β -D-Fruf (10), and β -D-Fruf-1,2':2,1'- β -D-Fruf (12) constitute >80% of the DFDA at 30 minutes in the inulin/1.5% citric acid/160°C system. Each is a possible "trickle" source for other DFDA. One of the anhydride linkages may be protonated and the linkage opened to form a glycosylated fructosyl cation. A variety of subsequent closures of the linkage involving the cation and an OH group of the glycosyl moiety are possible, each resulting in formation of a different difuranose. The 2,6-anhydrofructose intermediate may accompany this process and lead to one of the furanose/pyranose DFDA.

7. The isomerization steps above might begin with a furanose/pyranose, in which case dipyranses could form. The only two dipyranses identified in these systems are α -D-Frup-1,2':2,1'- β -D-Frup (**6**) and β -D-Frup-1,2':2,1'- β -D-Frup (**14**). The abundance of the former is not known for certain, although the combined maximum wt% conversion for **6** and **7** is less than 1%. DFDA **14**, the latter, is the least abundant of the known DFDA products, never reaching more than ~0.1%.

8. D-fructose forms early and constitutes a source for DFDA, especially those that cannot form from inulin.

Assembling a Mechanism - The kinetic mechanism for inulin/citric acid thermolysis will certainly contain many reactions. Nine DFDA can form from inulin in pseudo 1st order processes. The other five must come from somewhere else, including isomerizations and likely 2nd order reactions between two fructose moieties. Fructose could conceivably give rise to all 14 DFDA. Each difuranose can isomerize to 13 other DFDA. There are six difuranoses, which makes nearly 70 reaction pathways from isomerizations alone. Decay reactions other than loss to isomerization include reaction with cationic and OH-containing species, and non-specific degradation. ESMS analysis of thermolysis samples (page 47) and of several commercial chicory products⁹¹ showed that dehydrations of DFDA also occur during thermolysis. A kinetic mechanism that includes each of these pathways would surpass 100 reactions.

Exact determinations of the rate constants for all of these reactions were not possible. Instead, the conversion data were used to provide rough estimates of the formation and decay

rate for each DFDA. The numerical simulations that follow have taken these estimates into account. There is an inherent danger in attempting numerical simulations on systems for which too few variables have been determined empirically. The investigator that assigns values for rate constants at will, without regard for experimental evidence or chemical appropriateness, invites the construction of a "house of cards". Out of necessity, many of the rate constants reported here are estimated. The system under investigation is complex and is not easily broken down in the laboratory into its component parts. It is impossible to proceed without making assumptions where experimental evidence is lacking.

Use of LSODE on a Single DFDA - The "mechanics" of performing numerical simulations for this study are straightforward. The user creates an ASCII text file that contains information about the mechanism, including reactants and products for each reaction in the mechanism, the rate constant for each reaction, the initial concentrations of each reactant and product, start and stop times, and the number of data points to generate.[‡] Convergence criteria in the form of tolerances for absolute and relative error are adjustable. The error tolerance values suggested by the simulation program were used throughout this study.

Once the input data file is written, LSODE is invoked. The program integrates the differential equations represented by the mechanism being modeled and writes the solution to a text file. This output file, containing time/concentration data pairs for each reactant and product, is imported into Axum and plotted against actual wt% conversions and the fit of the predicted concentrations to the data checked visually. In this way many simulations can be

[‡] The numerical simulator includes a utility that prompts the user for information and writes it to an ASCII file formatted for direct import into the simulation program.

performed on the same mechanism until an acceptable fit is obtained. The difficulty, therefore, is not in performing the simulations, but in deciphering the true details of the mechanism. Very subtle changes to a rate constant may have profound effects on the quality of the fit, while gross changes to another rate constant within the same mechanism may have little or no observable effect.

DFDA **10** (α -D-Fruf-1,2':2,1'- β -D-Fruf) was used for the first simulation attempts for two reasons. First, **10** is the most abundant DFDA. Wt% conversion values include absolute errors that are associated with such tasks as the measurement of the starting material and integration of GC peaks. These errors will have the least relative effect on the most abundant product, making the conversion data for that product the most reliable. Second, **10** is a difuranose and so isomerizes to other DFDA's. This adds an extra level of complexity, but it also forces the concept of isomerization to be integral to the model from the start.

The following three mechanisms were tested against the data with varying degrees of success.[‡] The rate constant for the overall disappearance of inulin in these mechanisms is 0.20 min⁻¹. This is the value produced by the nonlinear least squares method for α -D-Fruf-1,2':2,1'- β -D-Fruf (**10**) (Table 12, page 96), which is the most abundant DFDA product and, as such, exerts the most influence on the overall mechanism.

- Simple 1st Order Growth and Decay - In the first trial (**mechanism 1**), DFDA **10** forms directly from inulin (i) and decays to non-specific products (np). This is the same 1st order parallel-consecutive mechanism used earlier for nonlinear least squares curve fitting and was not expected to duplicate the data. Inulin forms other DFDA's as well. These are

[‡] These and all subsequent simulations were performed on thermolysis data from inulin/1.5% citric acid at 160°C.

i → 10

i → sp

10 → np

mechanism 1

designated as specific products (sp), which represent a "gene pool" from which additional DFDA's may be added to the mechanism. Inulin disappears by more than one reaction pathway. For each mechanism, the rate constant for the disappearance of inulin is the sum of the rate constants for all 1st order reactions in which inulin is the reactant. The value of this constant is 0.20 min⁻¹.

The concentrations predicted by **mechanism 1** are plotted against the actual data in **Figure 47**. The two plots in the figure differ only in the x-axis range. As in the nonlinear least squares treatment, the mechanism does not duplicate the curvature in the decay data very well, although the formation rate and extent of decay at 40 hours are approximately correct.

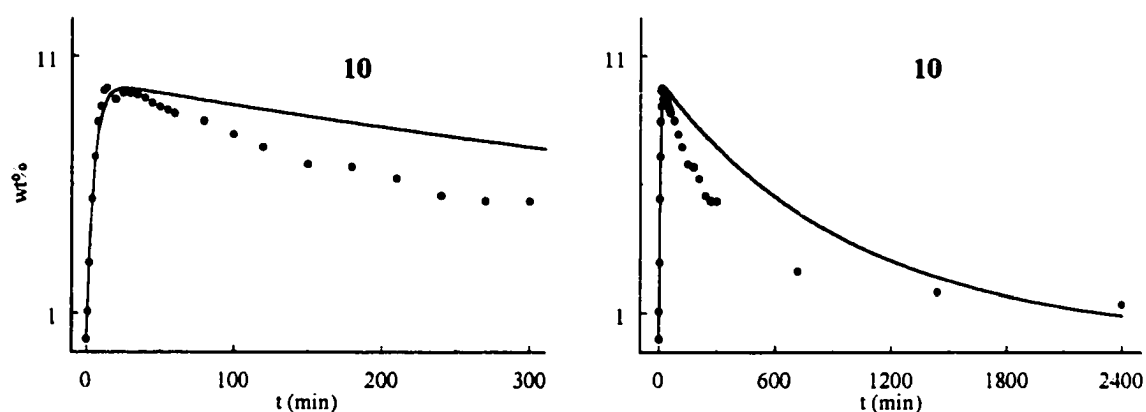
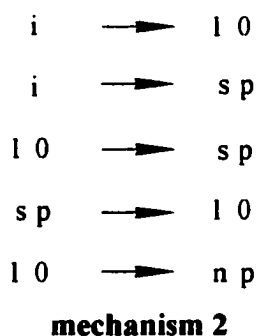


Figure 47 - Comparison of **mechanism 1** simulated curve to wt% conversion data for DFDA 10. (Inulin/1.5% citric acid/160°C)

- Inclusion of Isomerization - The second mechanism in these preliminary trials (**mechanism 2**) includes isomerization of **10** to other DFDA. Isomerization is generalized in the following way: the contribution to the decay of a DFDA (**10** in this case) by



isomerization is represented as DFDA \rightarrow sp, and isomerization of other DFDA to the one under scrutiny is represented by the reverse reaction sp \rightarrow DFDA. This generalization reduces the nearly 70 possible isomerization pathways to a more manageable number.

The addition of a secondary source of **10** through isomerization improved the fit considerably (**Figure 48**). The curve predicted by the mechanism now more closely duplicates both the region around the maximum and the curvature of the decay data out to 12 hours or more. This mechanism could not quite simulate the extent of decay at 40 hours.

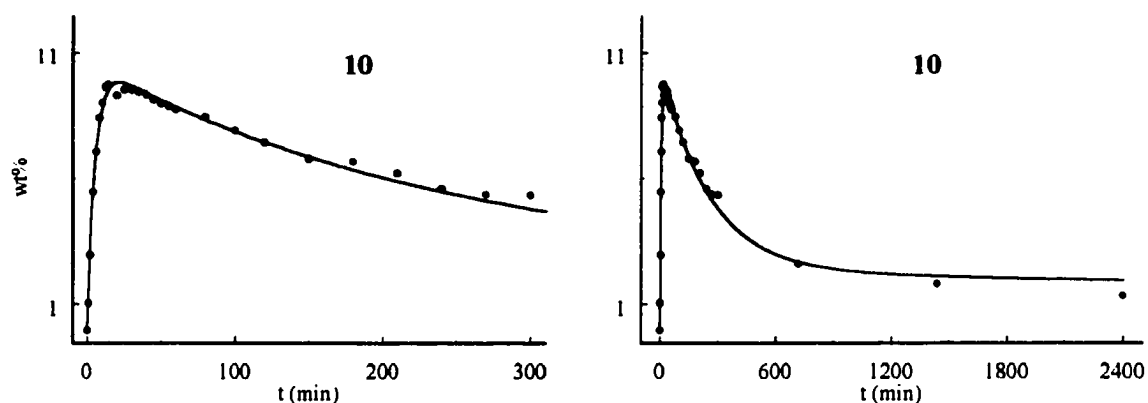
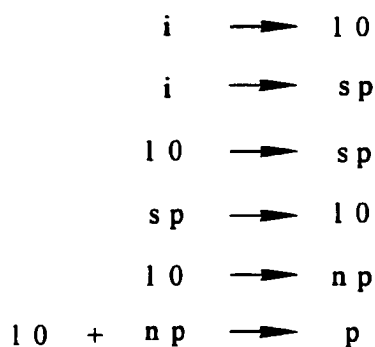


Figure 48 - Comparison of **mechanism 2** simulated curve to wt% conversion data for DFDA 10. (Inulin/1.5% citric acid/160°C)

- A 2nd Order Decay Pathway - When thermolysis samples were dissolved in H₂O and chromatographed by SEC (**Figure 11**, page 41) one peak contained predominantly trimers. ESMS of this fraction (**Figure 14**, page 45) revealed a large peak corresponding to glycosylated DFDA. Also, mild hydrolysis of this same trimer fraction in a previous inulin/citric acid thermolysis study⁶¹ revealed a disproportionately greater abundance of difuranoses over pyranose-containing DFDA. It is reasonable then to assume that some fraction of the disappearance of the difuranoses involves 2nd order reactions with fructosyl (or



mechanism 3

glucosyl) carbocations. Therefore, a third form of the mechanism for **10** (**mechanism 3**) was written that includes a 2nd order decay pathway. In this pathway np reacts with **10** to form products p. The products p do not differ in nature from the products np. They are both nonspecific products but are labeled differently. This avoids the implication that 2nd order decay is product catalyzed.

As shown in **Figure 49** the 2nd order decay pathway has a small but noticeable influence on the extent of decay at very long times. The curve fit for the first 12 hours is indistinguishable from the previous trial.

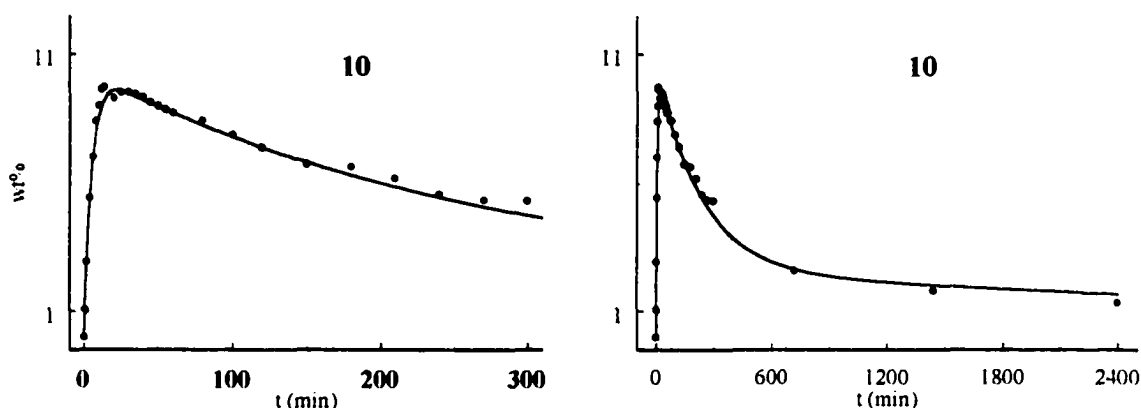


Figure 49 - Comparison of **mechanism 3** simulated curve to wt% conversion data for DFDA **10**. (Inulin/1.5% citric acid/160°C)

Extension of Numerical Simulation to Four Difuranoses - Numerical simulations of identical form to **mechanism 3** were carried out on conversion data for the four remaining difuranoses that can arise directly from inulin - α -D-Fruf-1,2':2,3'- β -D-Fruf (**1**), α -D-Fruf-1,2':2,6'- β -D-Fruf (**3**), β -D-Fruf-1,2':2,3'- β -D-Fruf (**5**), and β -D-Fruf-1,2':2,1'- β -D-Fruf (**12**). The plots for these four DFDA's are grouped together in **Figure 50**. Once again a pair of graphs that

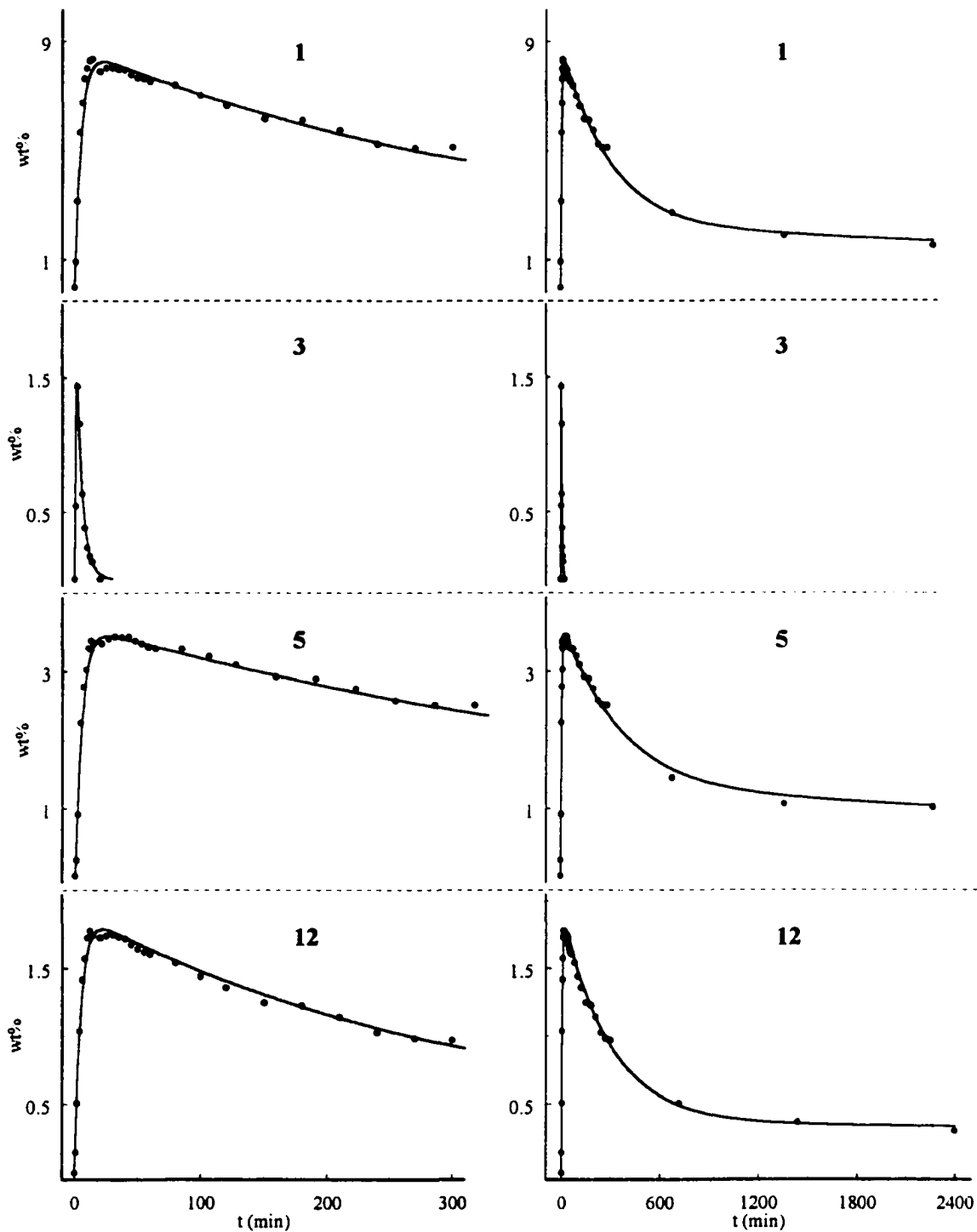


Figure 50 - Simulated curves for DFDA 1, 3, 5, 10, and 12.

differ only in x-axis scale is shown for each DFDA. It should be borne in mind that these simulations were performed separately using the same mechanism for each.

This mechanism accounts very well for the formation and decay of five difuranoses. Two discrepancies appear that may be attributed to the quality of the data rather than to the accuracy of the mechanism. The data near the maximum (10-20 min) for **1**, **5**, **10**, and **12** are discontinuous. This problem has been addressed (page 73) and the most obvious outliers were discarded from the data set. Some scatter remains, however, and is reflected in the mean wt% conversion plots. The second discrepancy is more subtle. The simulated curves consistently underestimate wt% conversion at 5 hours (300 min). This may indicate that the data for 12 hours and beyond are not accurate. One can imagine, looking at **Figures 49** and **50**, a decay with slightly less curvature that passes above the 12 hour data points but that still connects with the 40 hour data. This discrepancy is more evident in simulations on less abundant DFDA's.

Table 15 lists the simulated rate constants for DFDA's **1**, **3**, **5**, **10**, and **12**. The estimates from nonlinear least squares (**Table 12**, page 96) are shown in parentheses.[‡] The 1st order parallel-consecutive reaction scheme is the dominant process for these five DFDA's. Isomerization and 2nd order decay are critical to the success of the mechanism but their rates are slow in comparison. The 1st order rate constants from the simulation are similar to those predicted by nonlinear least squares.

A less obvious trend exists. The rate of 1st order decay to non-specific products

[‡] The units of pseudo 1st order rate constants are min⁻¹. The units for the pseudo 2nd order rate constants in this study can only be defined if wt% data are converted to moles per unit volume. This is not feasible. The reactions did not take place in a fixed volume of solvent and the exact nature of the non-specific products involved in 2nd order decay is not known.

	DFDA				
	1	3	5	10	12
i → DFDA	.0183 (.026)	.042 (.015)	.0077 (.0092)	.0215 (.0247)	.004 (.005)
i → sp	.1817	.158	.1923	.1785	.196
DFDA → sp	.0008	.6	.0015	.001	.00085
sp → DFDA	.0001	0	.0002	.00015	1.3e ⁻⁵
DFDA → np	.0024 (.0020)	1.5 (.40)	.0045 (.0015)	.003 (.003)	.0025 (.0026)
DFDA + np → p	.0001	0	.001	.00015	5.0e ⁻⁵

Table 15 - Simulated rate constants for DFDA 1, 3, 5, 10, and 12.

(DFDA → np) is three times the rate of decay to specific products (DFDA → sp) for four of the five difuranoses in this group. (α -D-Fruf-1,2':2,6'- β -D-Fruf (3) forms and decays at much higher rates and cannot be considered in the same class as the other four.) This result is approximately reflected in the degradation data for 10 (**Figure 28**, page 67). In those experiments the concentration of other DFDA's increased by ~10% in 5 hours. In the same period 80% of 10 had disappeared, suggesting that decay to non-specific products (np) was faster than decay to other DFDA's (sp). No effort was made to maintain this ratio during the simulations. However, experimentation with the ratio during simulations, including complete and partial reversal, did not produce better curves.

It must be remembered that the rate constant values in **Table 15** are the result of assigning a specific rate to disappearance of inulin (0.20 min⁻¹). As explained, this value was not determined by experimentation but rather by inference. All other rate constants depend

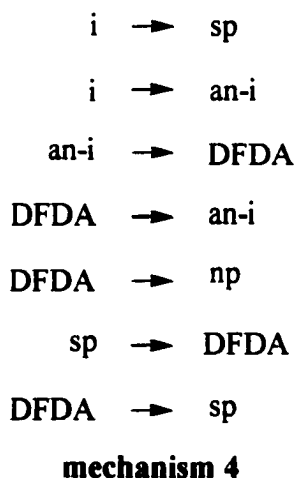
in some way on this one and must be adjusted if a different disappearance rate for inulin is used. In any case, it is an average, since inulin oligomers span a wide molecular weight range. The higher the molecular weight of the oligomer, the slower its disappearance rate, assuming chain length does not significantly influence the rate of cleavage of glycosidic bonds in these systems. This means that inulin is disappearing at many rates, depending on chain length, and that it is not completely gone until all oligomers are gone.

DFDAs from Inulin via the Anhydro Intermediate - The next group of DFDAs to be modeled were those that can form indirectly from inulin *via* the 2,6-anhydro intermediate - β -D-Fruf-2,1':3,2'- α -D-Frup (2), β -D-Fruf-2,1':3,2'- β -D-Frup (4), β -D-Fruf-1,2':2,1'- α -D-Frup (7), and β -D-Fruf-1,2':2,1'- β -D-Frup (13). The combined data for α -D-Frup-1,2':2,1'- β -D-Frup (6) and β -D-Fruf-1,2':2,1'- α -D-Frup (7) are included in this group under the assumption that at any time during thermolysis 7 is the major contributor to wt% conversion for the two. The justification for this lies in the fact that β -D-Frup-1,2':2,1'- β -D-Frup (14), the only other dipyranoose present, does not reach greater than ~0.1% relative abundance at any time.

As stated it was not clear what part the anhydro species would play and the simplest approach would be to exclude it. But numerical simulations of 2, 4, 7, and 13 using **mechanism 3** could not provide a suitable fit. The simulation process involves working on sections of the curve one at a time. Once one section - *e.g.* initial rate - matches the data fairly well, the rate constants controlling another section - *e.g.* middle decay from 1-5 hours - are adjusted incrementally until that section begins to match the data. Other aspects - overall extent of decay, abruptness of change from predominantly formation to predominantly decay,

maximum conversion, depth of curvature, etc. - begin to enter the picture. The investigator works back and forth among sections. If, after many of these manual iterations the curve still fails to resemble the data, the mechanism must be modified.

At no point was **mechanism 3** able to match the more gentle change from formation to decay near the maximum that DFDA's 2, 4, 7, and 13 exhibit without sacrificing the remainder of the fit. Inspection of the wt% conversion plots for these DFDA's (**Figure 38**, page 95) reveals a slower initial formation rate than for the difuranoses from the previous group (1, 3, 5, 10, and 12). The anhydro species could account for slower formation and is the obvious candidate for an additional rate controlling step between inulin and this group. Including the anhydro species gives **mechanism 4**, which retains most of the features of the previous mechanism. The oligomeric 2,6-anhydro-D-fructose intermediate is designated an-i



(anhydro-inulin). All other designations are the same. Many different values for the rate constant for 2nd order decay in this mechanism did not improve the fit over that obtained when this value was set to zero. This may be a reflection of the results obtained in ref⁶¹ in which

glycosylation of DFDA's favored the difuranoses over the pyranose-containing DFDA's. The primary OH groups of a DFDA are less sterically hindered than the secondary OH groups and will react more easily with fructosyl carbocations. Incorporation of pyranose into DFDA's reduces the number of primary hydroxyls and thus the probability of glycosylation. Therefore, the 2nd order glycosylation process will be less important for **2**, **4**, **7**, and **13**, and may be excluded from this mechanism with little adverse effect.

The simulated curves for **mechanism 4** are presented in **Figure 51**. The early data for β -D-Fruf-2,1':3,2'- α -D-Frup (**2**) are unreliable. This simulation was the last of the four to be performed for that reason. Its rate constants were developed by inserting and adjusting the values for β -D-Fruf-2,1':3,2'- β -D-Frup (**4**), rather than beginning from "scratch" as in other simulations.

There is a subtle indication of an induction period (lag time) in these data; formation does not commence immediately from time zero. The introduction of the anhydro intermediate (an-i) into the mechanism provided some compensation for this feature. Without the anhydro intermediate the mechanism could not duplicate the slower initial formation rate without grossly overestimating maximum wt% conversion. The curvature in and around maximum conversion also improved with the inclusion of the anhydro species. It was possible to more closely match the transition from growth to decay, which is less abrupt than in the difuranoses. However, **mechanism 4** still cannot quite duplicate the formation rate in the early stages of the reaction.

The fit after ~1 hour, when degradation has become the dominant process, out to ~5 hours is very good. But looking at **Figure 51**, the eye perceives that the 12 hour data points

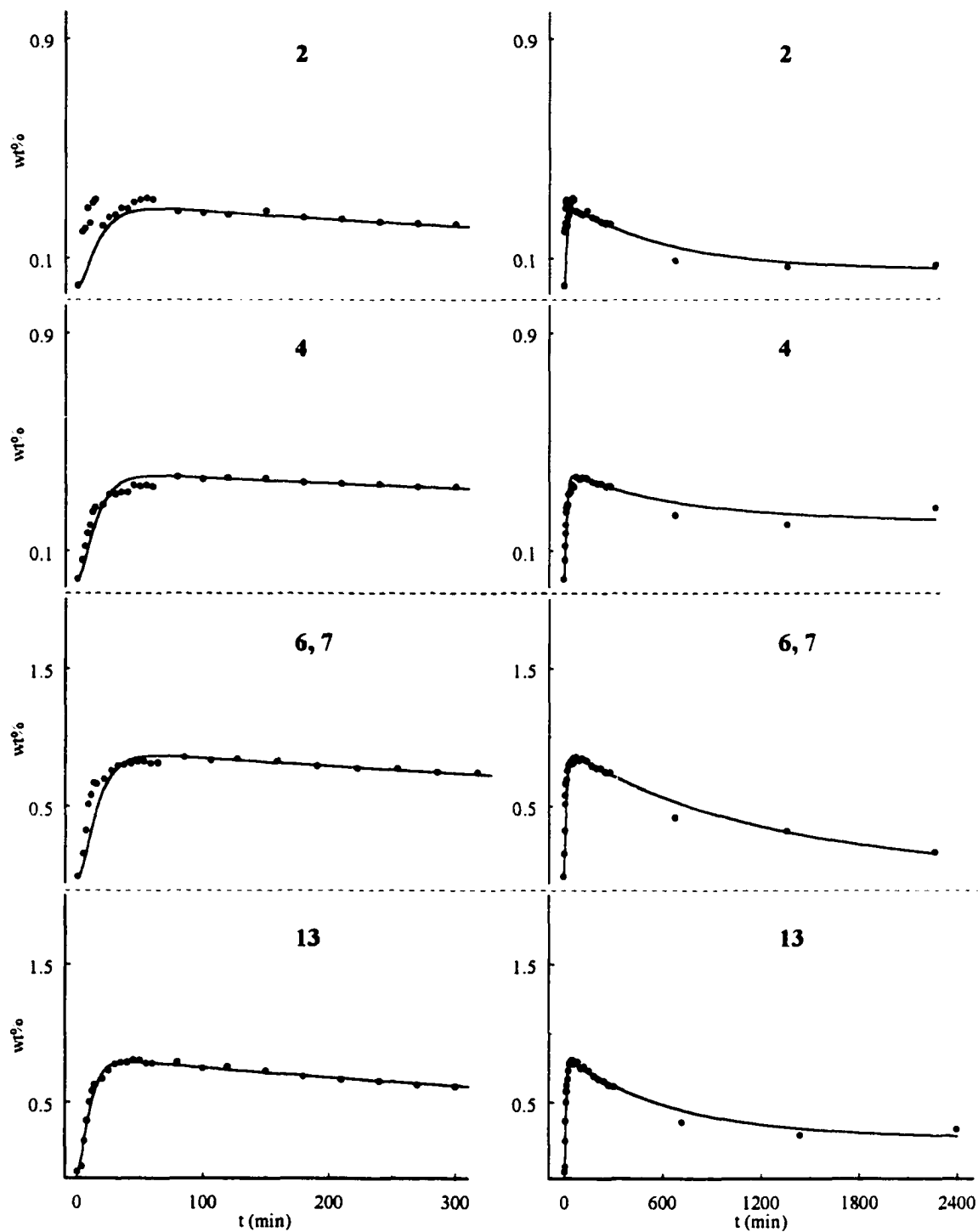


Figure 51 - Simulated curves for DFDA 2, 4, 7, and 13.

all lie below the arc that describes a smooth continuation of the earlier data. "Deepening" the decay curvature to match the 12 hour data sacrifices the earlier fit considerably. It would be appropriate to redetermine wt% conversion at 12 hours and longer before assuming that the 30 or more experiments that comprise the 1-5 hour data are inaccurate.

The simulated rate constants for DFDA 2, 4, (6)7, and 13 are listed in Table 16. The nonlinear least squares estimates for growth and decay are not listed because the inclusion of the anhydro species as a stable intermediate in equilibrium with each DFDA precludes a direct comparison between the two methods.

	DFDA			
	2	4	(6)7	13
i → sp	.19	.19	.19	.188
i → an	.01	.01	.01	.012
an-i → DFDA	.0043	.006	.017	.022
DFDA → an-i	.045	.06	.07	.13
DFDA → np	.015	.0172	.004	.004
sp → DFDA	1.5e ⁻⁵	5.5e ⁻⁵	1.0e ⁻⁶	3.0e ⁻⁵
DFDA → sp	.01	.005	2.0e ⁻⁵	.007

Table 16 - Simulated rate constants for DFDA 2, 4, 7, and 13.

The dependence on isomerization as a source for these DFDA (sp → DFDA) is small; in all cases the rate constant for the reverse reaction (DFDA → sp) is the larger. The opposite was true for the difuranoses (Table 15), where the isomerization equilibrium favored DFDA formation. This reflects the relative stability of D-fructopyranose over D-fructofuranose. For a one-step isomerization to occur, the bond between oxygen and an anomeric carbon opens

to form a glycosylated fructosyl carbocation and the oxygen just released re-attacks the cation from the opposite side to form a new DFDA. It is assumed the anhydride linkage will break in such a way as to form the most stable cationic intermediate. This means the fructofuranosyl cation will predominate over the fructopyranosyl. Thus the source material for **2**, **4**, **(6)7**, and **13** is limited to those DFDA's that already contain a pyranose and the major components in the mixture - the difuranoses - are excluded for the most part.

Indirect Formation of DFDA's - Five DFDA's form during inulin/citric acid thermolysis that cannot arise directly from inulin. One of these - α -D-Frup-1,2':2,1'- β -D-Frup (**6**) - was modeled in the previous section because its conversion data could not be separated from that of β -D-Fruf-1,2':2,1'- α -D-Frup (**7**). The other dipyranoose - β -D-Frup-1,2':2,1'- β -D-Frup (**14**) - is never present in more than trace quantities. Early (0-20 min) wt% conversion for **14** is zero in the data set, not necessarily because it had not formed, but because its abundance was low enough to approach the minimum detection level of the analytical method. Simulations on **14** are of decidedly lower quality, partially because of missing data and low overall abundance. The remaining three DFDA's in this group are α -D-Fruf-1,2':2,1'- α -D-Fruf (**8**), α -D-Fruf-1,2':2,1'- β -D-Frup (**9**), and α -D-Fruf-1,2':2,1'- α -D-Frup (**11**). This group of five DFDA's presents the most difficulty in terms of a sensible chemical mechanism that can reproduce the data.

- **A Unique Mechanism for DFDA 8** - The initial rate of formation for DFDA **8** is nearly as rapid as for the other five difuranoses, yet both residues are α anomers. **8** cannot form

directly from inulin oligomers by intramolecular attack, since inulin contains only β anomers, and must arise rapidly from some other source that is present very early in the reaction. DFDA 10 forms early and could give rise to **8** via a one-step isomerization. Efforts to employ this isomerization in simulations failed to duplicate the rapid formation and decay rates that **8** exhibits.

HPAE-PED chromatograms of inulin suggest some fructose is present at time zero (**Figure 52**), and that fructose concentration increases for the first 15 minutes of thermolysis (**Figure 36**, page 87). But trial simulations using a 2nd order mechanism of the type 2

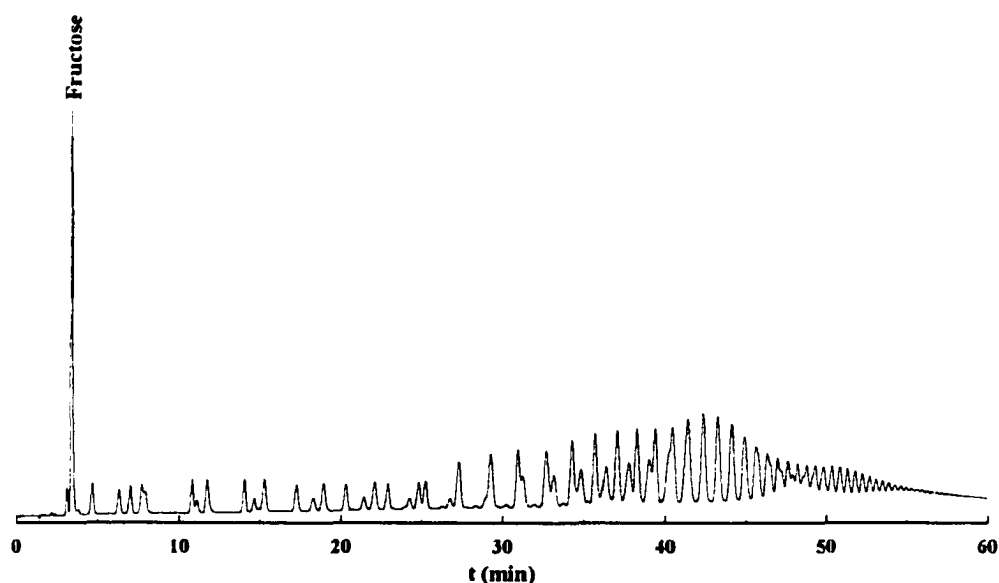
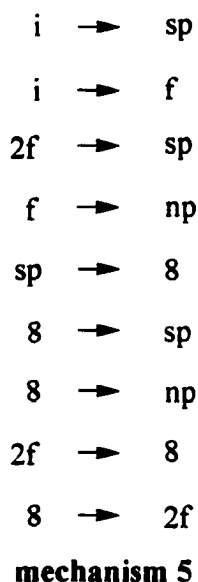


Figure 52 - HPAE-PED chromatogram showing D-fructose content of inulin/1.5% citric acid.

Fructose \rightarrow DFDA also failed to match the data. This type of mechanism, in combination with the same decay pathways used in previous mechanisms, yields a conversion plot with a more gentle transition from growth to decay. The initial formation rate is too slow and the

change from positive to negative slope at the maximum is not abrupt enough.

Formation by both 1st order isomerization and 2nd order bimolecular reaction of fructose[‡] are incorporated into **mechanism 5**. The initial concentration of fructose $[f]_0$ was



estimated as 5%. A portion of inulin in this mechanism goes toward production of fructose, which may go on to form **8** and other DFDAs (sp), or degrade to non-specific products (np). The large 1st order decay rate constants that were necessary to duplicate the steep decline from maximum conversion completely overshadowed the minimal contribution from the 2nd order pathway $8 + np \rightarrow p$. This path was therefore excluded from the mechanism.

The simulation of wt% conversion data for DFDA **8** according to **mechanism 5** is presented in **Figure 53**. The curve matches the data well for the first 5 hours. There is an almost imperceptible induction period followed by rapid growth and decay. The simulation

[‡] One D-fructose must have undergone protonation and loss of H₂O to form the fructosyl carbocation, which then reacts quickly with a molecule of D-fructose.

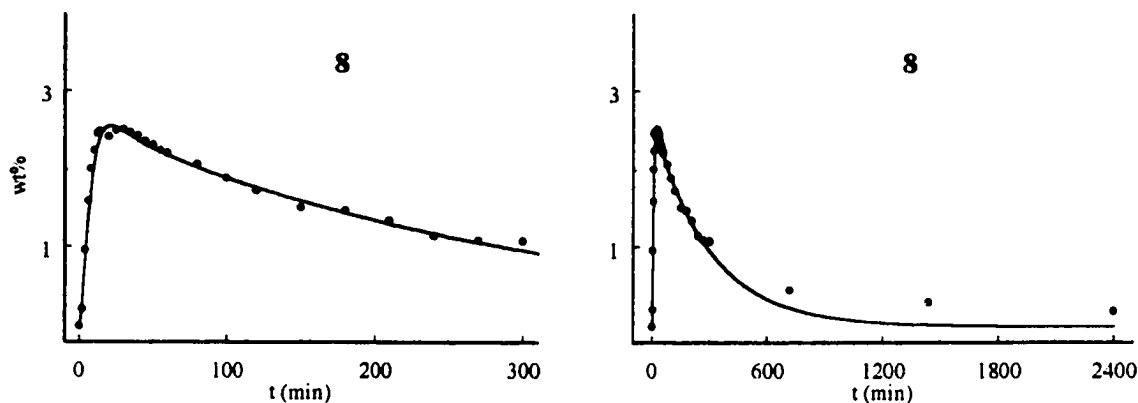


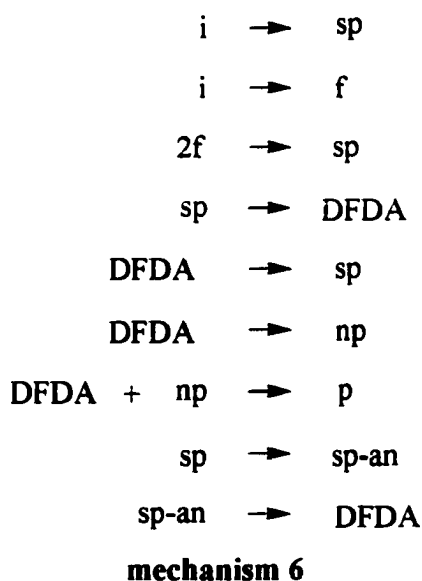
Figure 53 - Simulation of DFDA **8** according to **mechanism 5**.

out to 5 hours is as good or better than those for the other difuranoses. But as mentioned, large decay constants were necessary to obtain this early fit. This resulted in almost complete disappearance of this DFDA after ~25 hours, even though the data specify a more gradual decay to a small but definite concentration at 40 hours.

- **An Additional Anhydro Species** - Without introducing a further mechanistic pathway, the possible formation routes through isomerization to α -D-Fruf-1,2':2,1'- β -D-Frup (**9**) are limited. Only α -D-Fruf-1,2':2,1'- α -D-Frup (**11**) and β -D-Fruf-1,2':2,1'- β -D-Frup (**13**) can open to a carbocation and re-close to form **9**. An underlying theme to the most successful mechanisms so far is the availability of more than one source material for DFDA formation. Without that, in every case the mechanism failed in some way to give satisfactory results. Simulations of **9** using a mechanism that was limited to one source material were no exception.

It is reasonable to expect the cationic form of DFDA's to undergo the same

isomerization *via* 2,6-anhydro-D-fructose that has been postulated for inulin. With this two-step pathway included in the mechanism, any 1,2-linked α -D-fructofuranose or β -D-fructopyranose can isomerize to **9**. This increases the source material for **9** to include most notably α -D-Fruf-1,2':2,1'- α -D-Fruf (**8**) and α -D-Fruf-1,2':2,1'- β -D-Fruf (**10**), both of which form early to relatively high abundance. It also provides what appears to be the crucial second source material, providing a great deal more flexibility in balancing formation and decay in such a way as to obtain the curve shape stipulated by the data. In **mechanism 6** DFDA (sp) form anhydro species (an-sp) that can go on to form the DFDA under scrutiny. This mechanism was applied to **9**, **11**, and **14** with more success than previous attempts to model these DFDA, but with less overall success than for those DFDA that form from inulin.



The simulated curves for **9**, **11**, and **14** are presented in **Figure 54**. The initial formation rate for **9** is too rapid to be modeled accurately by this mechanism. Increasing $1''$

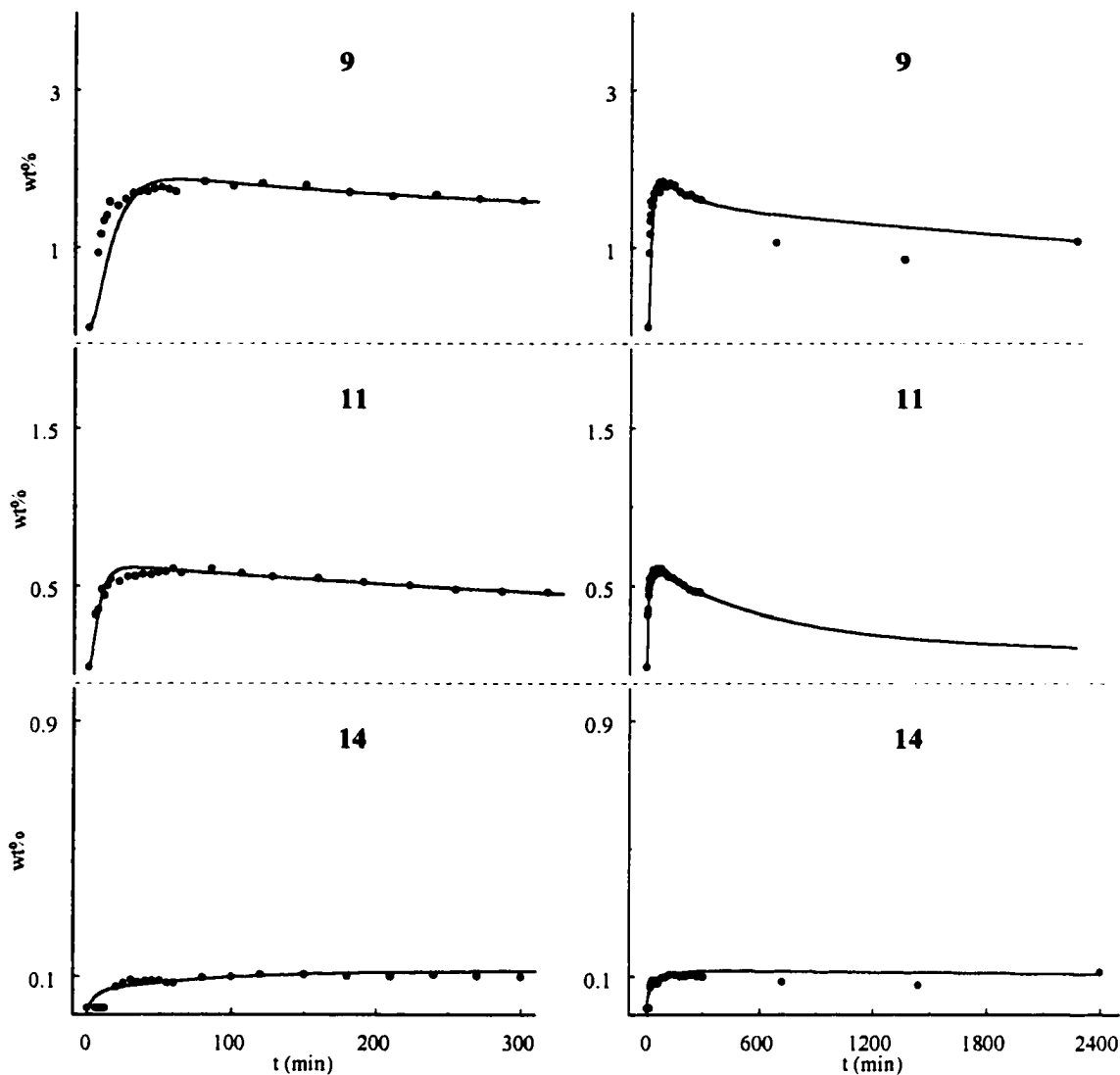


Figure 54 - Simulated curves for DFDA 9, 11, and 14.

order formation rate to match the data in the 0-20 minute region causes the simulated curve to rise well above the actual maximum. It was not possible to correct for this by increasing decay rates without completely sacrificing the fit in the 1-5 hour range and overestimating the extent of decay. The earlier observations concerning the validity of the 12 hour data are reinforced by the low 12 and 24 hour conversion data for 9.

The simulation of **11** matches the 0-5 hour data well except in the region near maximum conversion. The later data for this DFDA were lost during a file transfer; the simulated curve is extended to 40 hours simply to demonstrate its shape.

The rate constants for **8**, **9**, **11**, and **14** are given in **Table 17**. The major common feature among these four is that they do not form from inulin, yet three distinct structural

	DFDA			
	8	9	11	14
i → sp	.18	.2	.2	.2
i → f	.02	-	-	-
2f → sp	5.0e ⁻⁵	5.0e ⁻⁵	5.0e ⁻⁵	5.0e ⁻⁵
f → np	.0004	.00042	8.1e ⁻⁵	.0003
sp → DFDA	.011	.00165	.0037	.0007
DFDA → sp	.26	.07	.5	1.11
DFDA → np	.12	.007	.05	.04
DFDA + np → p	-	.00015	.0001	.0001
sp → sp-an	-	.004	.0009	.0009
sp-an → DFDA	-	.0012	.0003	.01
2f → DFDA	.001	-	-	-
DFDA → 2f	.0001	-	-	-

Table 17 - Simulated rate constants for DFDAs **8**, **9**, **11**, and **14**.

types are represented: difuranose, furanose/pyranose, and dipyranoose. The conversion data for **8** closely resemble the other difuranoses. The success of the simulations for those difuranoses (**Figures 49** and **50**) reinforces the belief that they form directly from inulin, while

the structure of **8** guarantees that it does not. 1st order decay constants for **8** are two orders of magnitude greater than those for four of the other five difuranoses.

9 and **11** are structurally similar, differing only in the anomeric configuration of the pyranose residue. The formation rate constants for these two DFDA are similar and the higher 1st order decay constants for **11** reflect its lower abundance. Along the same line of reasoning, **14** is the least abundant DFDA during thermolysis and its large 1st order decay constants are exceeded only by α -D-Fruf-1,2':2,6'- β -D-Fruf (**3**), which disappears completely after ~20 minutes.

Modeling of Combined Reaction Mechanisms - Each of the above partial mechanisms was written to address the formation and decay of one of four DFDA groups - (i) difuranoses directly from inulin that contain β -D-fructose, (ii) furanose/pyranoses from inulin *via* the anhydro-inulin intermediate, (iii) the difuranose **8** which contains only α -D-fructose, and (iv) pyranose-containing DFDA from sources other than inulin. The wt% conversion data for each DFDA within each group were modeled in the previous sections one DFDA at a time. The difuranoses of group (i) were the easiest to model. As modeling proceeded to each successive group, the mechanisms required to approximate the data became more and more complex and the results of simulations were less and less satisfactory. This general progression of increasing difficulty resurfaced during the following attempts to combine the partial mechanisms into a whole.

- Five Difuranoses from Inulin - The reactions of **mechanism 3** were written into a single mechanism incorporating DFDA's **1, 3, 5, 10, and 12**. Rate constants were copied directly into the combined mechanism without modification. A single numerical simulation using these constants gave rise to the curves in **Figure 55**. Only one plot encompassing the entire 40 hour reaction period is presented for each compound.

The quality of the fit from 0-5 hours in all five cases was virtually unaffected. The extent of decay at 40 hours for **1** and **12** is somewhat overestimated and the curvature of the decay region for **5** is decreased somewhat. Both of these "symptoms" were amenable to improvement with minor adjustments in the decay constants. The fit to **3** is unchanged and the fit to **10** is marginally better than in the individual treatment. This result speaks to the relative solidity of **mechanism 3** in terms of its ability to reproduce the data. It does not guarantee completeness. For example, formation from fructose ($2f \rightarrow \text{DFDA}$) was left out of the mechanism even though there is no evidence to suggest that fructose gives rise to the difuranose **8** more readily than to the other difuranoses. It was merely the case that formation directly from inulin was capable of reproducing the data without the inclusion of fructose.

Neither was degradation of DFDA's to fructose ($sp \rightarrow 2f$) included in this or in any of the mechanisms. It is not known what contribution this pathway would have on the overall mechanism. One way in which DFDA's could degrade to fructose is given in **Scheme 12**. The glycosylated fructosyl cation results from acid catalyzed opening of one dianhydride linkage. In order for the other linkage to open also, the cationic anomeric carbon must first react with H_2O and lose H^+ to form a fructose-fructose disaccharide. The remaining glycosidic oxygen

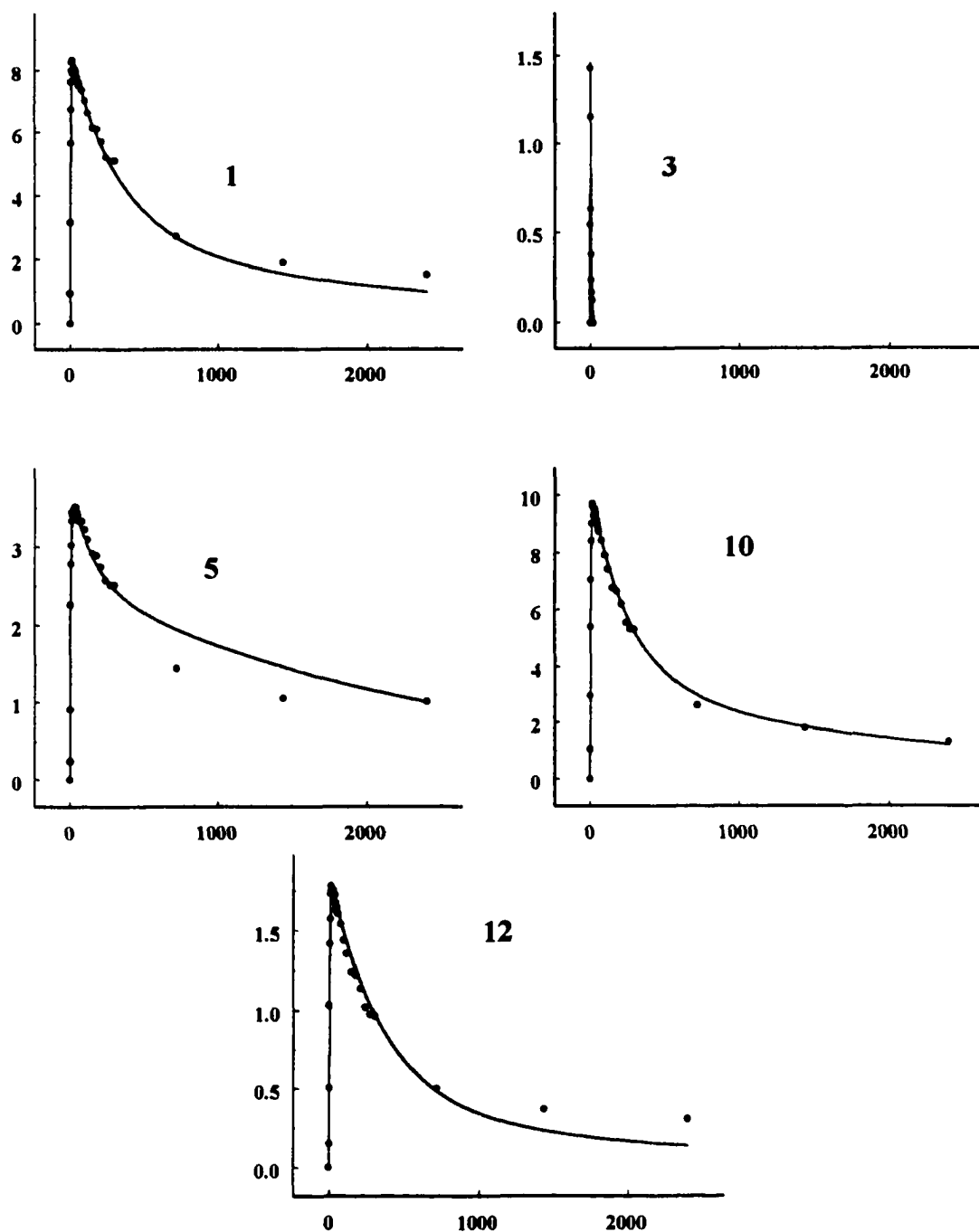
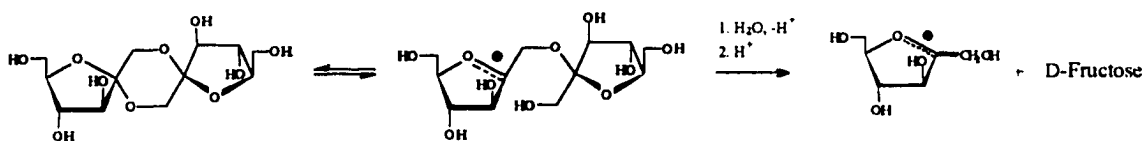


Figure 55 - Combined simulation of difuranoses that form directly from inulin.

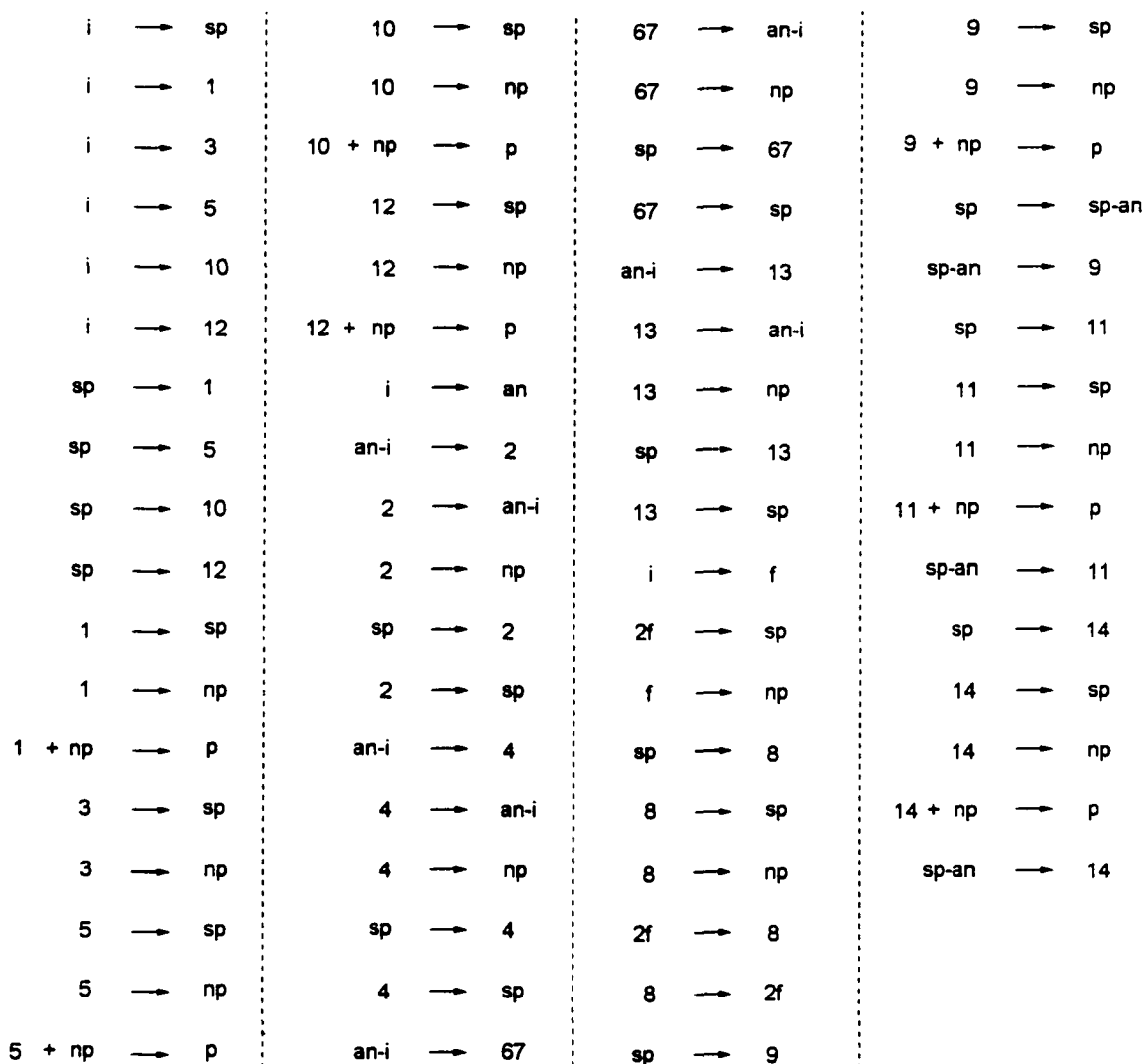
could then be protonated and the linkage break to form D-fructose and D-fructosyl. Inulin/citric acid samples in this study were anhydrous initially; any water that was available for this reaction must have formed during thermolysis.



Scheme 12

- A Mechanism for all 14 DFDA's - One overall mechanism was assembled that required 69 individual reactions to encompass all four mechanism types and all 14 DFDA's (**mechanism 7**). Once again the rate constants obtained from modeling individual DFDA's independently were copied directly into the mechanism and a single numerical simulation performed. **Figures 56 and 57** on the following pages depict the resulting curves for each of the 14 DFDA's. The quality of the fit is significantly reduced. Almost without exception the decay rate is too high and the simulated curves fall short of the data throughout the reaction period. It is not surprising that the combined mechanisms cannot model the system accurately without some adjustment. The number of interdependent reactions is multiplied many fold in going from one of the relatively simple partial mechanisms to this overall mechanism. It would be possible to further refine the rate constants to obtain curves that match the data as well as those presented earlier. Such a task, however, would push the emphasis of this study too far into the realm of speculation; too few empirical rate constants exist for this system already. It is more appropriate to return to the laboratory and endeavor to isolate reaction

pathways that belong to the partial mechanisms given earlier, the focus being to establish realistic rates for as many reactions as possible and to remain open to the possibility of changes and improvements to the existing set of reactions.



mechanism 7

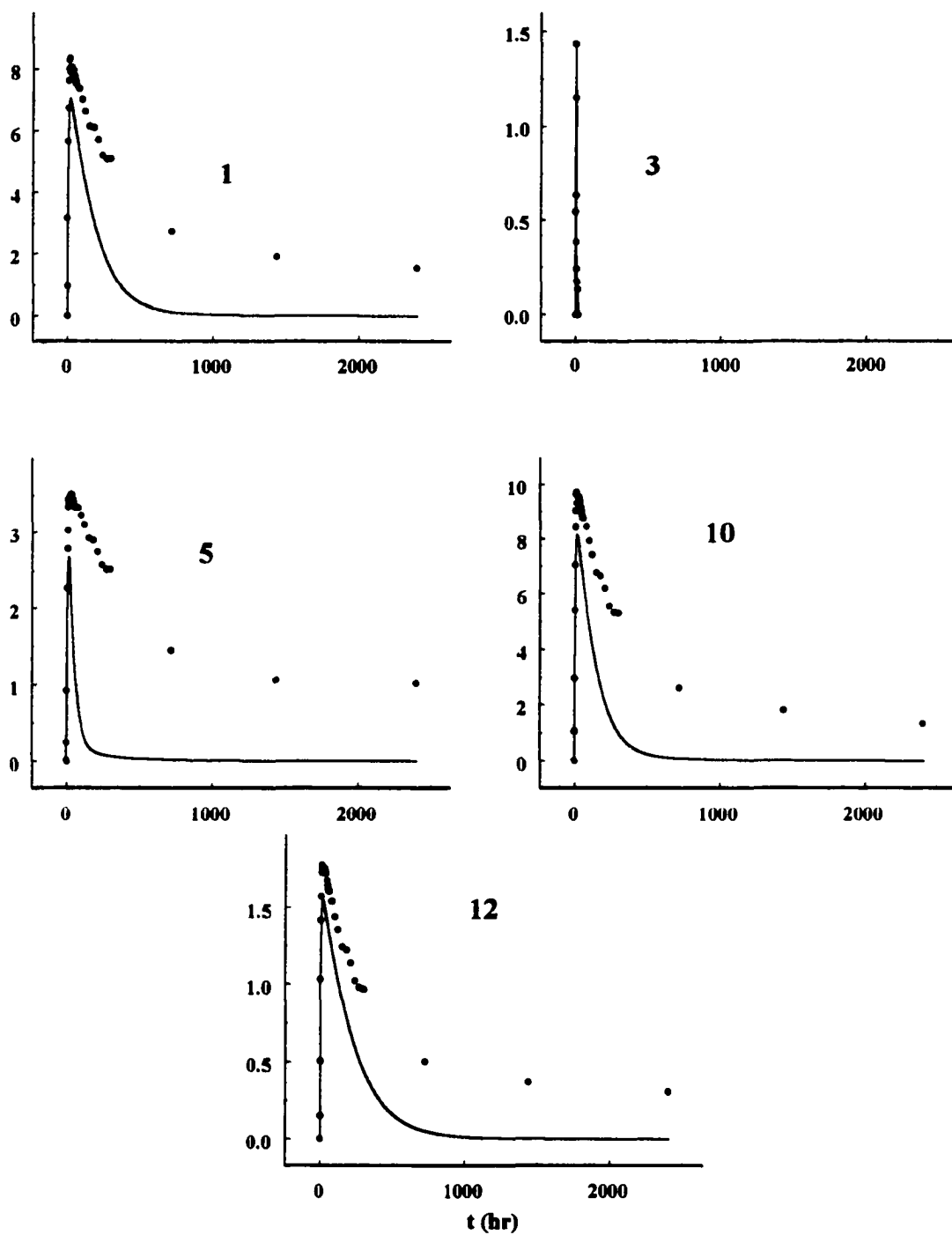


Figure 56 - Overall reaction mechanism applied to 1, 3, 5, 10, and 12.

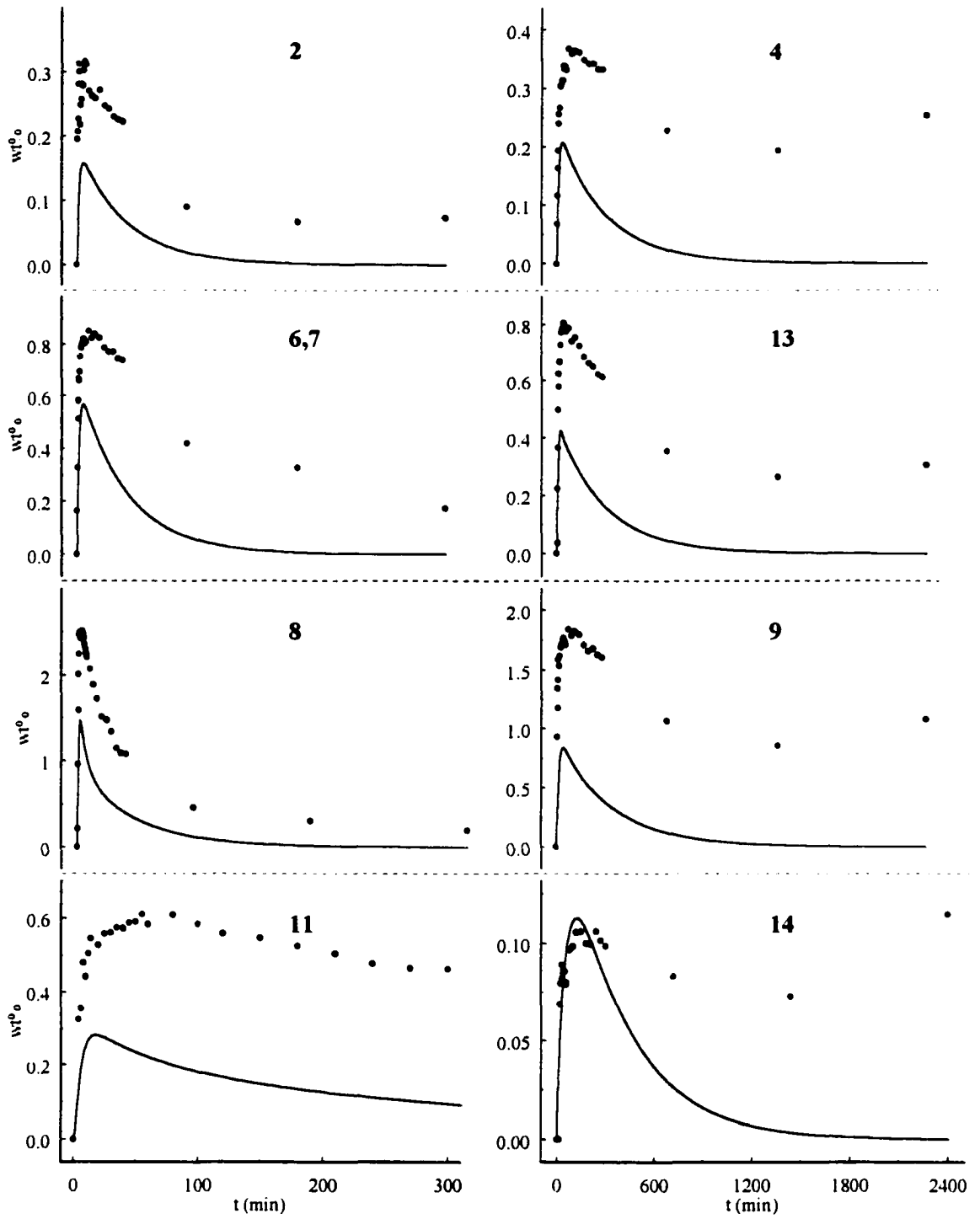


Figure 57 - Overall reaction mechanism applied to remaining 9 DFDA's.

CONCLUSION

The thermolysis of inulin in the presence of citric acid involves a complex set of chemical reactions and equilibria, most of which cannot be studied independently. It was the goal of this study to elucidate the nature of the kinetic factors that control these reactions and equilibria and to propose a suitable kinetic mechanism. The various pieces of evidence available to achieve that goal can be classified according to how many assumptions were required to justify their use. Empirical evidence of course forms the foundation. It was possible to determine experimentally the concentrations of all 14 DFDA's over the entire course of the reaction under varying reaction conditions.

The move from experimentation to interpretation required a number of assumptions. Perhaps the most serious of these is the extrapolation to thermal melts of compounds and processes known to occur in aqueous systems. In thermal melts the solvent is the reactant that is in highest abundance. Literature precedents for how to proceed in this situation are few.

In proposing a kinetic model I have endeavored to maintain a balance between empirical evidence, justifiable assumption, and the freedom that might be expected in any field where the researcher is essentially the first to attempt a specific problem. I believe the complex kinetic mechanism of this system, and the many rate constants that accompany it, are deserving of some measure of freedom. The result is a set of 1st and 2nd order reactions that succeed to some extent in explaining the data.

As it stands, the kinetic model provides a qualitative understanding of the processes occurring. One quantitative description of those processes, in the form of specific rate

constants, has been given. Even if it cannot be assumed to provide a complete quantitative description, the model fits together intellectually and makes reference to common-sense chemistry.

FURTHER WORK

The direction that this work takes in the future will be largely dictated by the inclinations of the next investigator. As it stands, this work provides insight into the reaction conditions that might be best suited for optimizing (or minimizing) DFDA production from inulin. But the thermolysis of inulin produces myriad components, only some of which have been identified and fewer of which have been quantified. Organic acids probably form pyrolytically from inulin and its primary degradation products. It is not clear to what extent acidic species other than citric acid contribute to the rates of DFDA growth and decay. Commercial preparations of chicory, for example, contain organic acids as well as proteins and free amino acids, and their affect on DFDA reaction rates is unknown.

From a kinetics perspective, the mechanisms proposed in this study are only capable of duplicating the data on an individual basis or in groups of structurally similar DFDA. The contribution to decay in the later stages from 2nd order processes has likely been under emphasized. Individual experiments involving one DFDA or class of DFDA and a specific compound that occurs during thermolysis - *e.g.* fructose, fructosylated DFDA, HMF, etc. - might remove some of this ambiguity.

Finally, the general public is increasingly aware of specific ingredients in foods and consumables. Witness the many nutritional and supplemental products containing non-digestible oligosaccharides. It is not known to what extent DFDA occur in these products nor what fraction of the beneficial properties associated with them can be attributed to DFDA. Many of these products are subjected to elevated temperatures during processing or preparation in the home and the presence of DFDA is likely.

EXPERIMENTAL

Instrumentation

Gas Chromatography - Thirteen DFDA's from the thermal treatment of inulin had been identified previously.^{59,61} This work is a continuation of those studies and employs similar techniques. The primary quantitative tool was capillary gas chromatography with flame ionization detection (GCFID). The instrument used was a Hewlett-Packard 5890 Series A gas chromatograph with on-column injector and cross-linked 5% phenyl-dimethyl siloxane column (HP Ultra-2, 25m x 0.33mm x 0.53 μ m). The temperature program was 55°C for 1 minute, 30°/min. to 170°C, 3°/min. to 320°C, and hold for 10 minutes. Total acquisition time was 65 minutes. In order to ensure the chromatographic peaks for this system were the same as those identified in the earlier studies, the column was installed in a Hewlett-Packard 5890 GC with HP 5971 mass spectral detector at 70eV (GCMS) and representative samples run under the same temperature program. Further evidence was provided by installing a 100% dimethyl siloxane (HP-1, 25m x .33mm x 0.53 μ m) column in the GCMS. On the former column α -D-Fru p -1,2':2,1'- β -D-Fru p (**6**) and β -D-Fru f -1,2':2,1'- α -D-Fru p (**7**) coelute. On the latter these two DFDA's are resolved but α -D-Fru f -1,2':2,1'- α -D-Fru p (**11**) and β -D-Fru f -1,2':2,1'- β -D-Fru f (**12**) coelute. All other elution orders are the same for both columns.

Liquid Chromatography - Four LC methods were employed. *Method (i)*: Preparative liquid chromatography was performed on aqueous samples (~1g/mL) using Waters Delta Pak C₁₈

cartridges (3 - 25 x 100mm, 15 μ 100Å, plus guard pak) eluted at 10.0 mL/min with H₂O.

Method (ii): Analytical LC (HPLC) was performed using Waters Resolve C₁₈ Radial Pak cartridge (8 x 100mm, 5 μ , plus guard pak) eluted at 1.0 mL/min with H₂O. Waters 515 HPLC pumps and a Waters 410 differential refractometer were used with these two systems.

Method (iii): Dionex High Performance Anion Exchange HPLC system with Pulsed Electrochemical Detection (HPAE-PED) was used to examine the inulin profile. Elution was by sodium hydroxide/sodium acetate gradient (NaOH/NaAc) at 1.0 mL/min. Eluents were made up by first dissolving weighed amounts of reagent grade NaAc·3H₂O in degassed, ultra pure water (>17 M Ω cm⁻¹), then adding measured volumes of reagent grade certified 50% NaOH solution. The column was a Dionex CarboPac PA1. The gradient profile and detector potentials are shown in **Table 18**. The method included 10 minute equilibration times at the beginning and end of each run. The reference electrode was Ag/AgCl and acquisition was *via* analog/digital interface to Dionex AI-450 Chromatography software. *Method (iv):* Size exclusion chromatography (SEC) was performed on a Pharmacia glass column (2.6 x 90cm

Elution Gradient			Detector Settings	
t (min)	%A*	%B**	t (s)	E (V)
0	95	5	0 - .50	+ .10
60	0	100	.51 - .60	+ .60
			.61 - .65	- .60
			.30 - .50	Integration Period

* 150 mM NaOH
** 150 mM NaOH/500 mM NaAc

Table 18 - Elution gradient and electrode potentials for Dionex LC system.

≈ 475 mL) packed with BioRad BioGel P2 ultra fine (<45μ) media eluted with H₂O at 0.5 mL/min. The refractive index detector (Waters 410) output was amplified and routed through a PICO AD-100 analog to digital interface to a DOS-based computer.[‡] Acquisition time was approximately 15 hours.

NMR Spectroscopy - ¹H and ¹³C spectra of individual DFDAs were recorded using a Bruker ADV DRX400 spectrometer at 400 and 100 MHz, respectively. Samples were dissolved in D₂O and referenced to internal *t*-butanol.

Electrospray Mass Spectroscopy - Electrospray mass spectra were acquired on a Fisons/Micromass VG Platform II instrument with the probe temperature set at 60°C. Aqueous carbohydrate samples (~4mg/mL) were spiked with a drop of 0.1M NaCl and analyzed in positive ion mode at a cone voltage of +180V⁹² with methanol as the mobile phase. They were then re-injected in negative ion mode with H₂O as mobile phase and cone voltage of +30V.⁹³ Nitrogen was employed as nebuliser (15 L/hr) and drying gas (250 L/hr). Data acquisition and processing were performed using Mass Lynx[®] 2.0 software.

Thermolysis of Inulin, Nystose, and Individual DFDAs

Preparation of starting material - To obtain 1.5% citric acid by weight, inulin (Sigma, from Dahlia tubers) and milled citric acid (Aldrich) were dissolved independently in ratios of 19.70g inulin in ~300 mL water and 0.30g citric acid in ~10 mL water. Inulin does not dissolve easily

[‡] Budget constraints and frugality compelled me to beg or borrow the necessary components and to assemble a 386-based computer from scratch in order to collect and store the data from this LC system.

so the inulin solution was heated to $\sim 50^{\circ}\text{C}$ and allowed to cool to room temperature. Once cool, the two solutions were combined, mixed thoroughly by stirring, and freeze dried immediately to yield an inulin/citric acid powder. The process was repeated with appropriate amounts to obtain citric acid concentrations of 1.0, 2.0, and 2.9% by weight.

Thermolysis - A bank of 9 screw-cap vials (5 mL capacity), each containing approximately 10mg (accurately weighed to $\pm 0.01\text{mg}$) inulin/citric acid powder, was lowered in heated silicon oil. At timed intervals, each vial was withdrawn and plunged immediately into ice water. One thermolysis experiment in this work is defined as the data obtained from a set of 9 thermolysis samples.

Derivatization - Immediately after completing a thermolysis experiment, all 9 samples were dissolved with sonication in 0.75mL pyridine. To each was then added 100 μL internal standard ($\sim 6 \pm 0.01\text{mg/mL}$ xylitol in pyridine) and 0.25 mL neat chlorotrimethylsilane (Tri-Sil[®], Pierce). The samples were quickly capped and held at 100°C for one hour, then allowed to cool to room temperature.

Sample cleanup - Pyridine[†] was blown off with dry nitrogen at room temperature and replaced with 2 mL *n*-hexane (R.P. Normapur AR) that had been glass distilled. The samples were sonicated for 10 minutes, centrifuged for 5 minutes at $1.5 \times 10^3\text{g}$, and decanted.^{**} The final

[†] Suspected carcinogen

^{**} Tri-Sil reacts with water from the atmosphere that enters the vials during work up, and with the
(continued...)

samples were stored below 0°C in clean vials while awaiting GC analysis.

Analysis - Samples were analyzed by GCFID. Response factors (RF) for four individual DFDAAs (α -D-Frup-1,2':2,1'- β -D-Frup (6), α -D-Fruf-1,2':2,1'- β -D-Frup (9), α -D-Fruf-1,2':2,1'- β -D-Fruf (10), and β -D-Fruf-1,2':2,1'- β -D-Frup (13)), at concentrations similar to those encountered in the experiments, were determined relative to the internal standard xylitol. The average RF (0.60) was applied to all DFDAAs.

Preparation of 1-Kestose and Nystose - 1-kestose (GF₂) [α -D-glcp-(1 \rightarrow 2)- β -D-fruf-(2 \rightarrow 1)- β -D-fruf-(2 \rightarrow 1)] and nystose (GF₃) [α -D-glcp-(1 \rightarrow 2)- β -D-fruf-(2 \rightarrow 1)- β -D-fruf-(2 \rightarrow 1)- β -D-fruf] were isolated in gram quantities from the commercial product Nutraflora[®] (Golden Technologies, Inc., Golden, CO) using *LC Method (i)*. 1-kestose and nystose are the only major components of this product detectable by standard GCFID and reversed phase LC methods, and are easily resolved. Their identities were confirmed by comparison of ¹³C spectra with published values.⁸³ They are hygroscopic and required storage under vacuum over phosphorus pentoxide (P₂O₅) at 40°C for 48 hours or more to remove water after freeze drying. Continued storage under vacuum over a desiccant was sufficient to keep the samples dry. Preparation of nystose with 1.5% citric acid was carried out in the same fashion as with inulin.

** (...continued)

small amount of water that forms from dehydration reactions during thermolysis, to form a fine white precipitate. This precipitate tends to freeze glass injection syringes and clog the fine tubing found in chromatography systems.

*Individual DFDA*s - The same techniques used to prepare inulin/citric acid starting material were applied to dried, amorphous DFDA_s isolated as described below.

Preparation of Individual DFDA_s

Inulin/citric acid - Two separate preparations were carried out. In the first, ~0.5g (accurately weighed) previously prepared inulin/1.5% citric acid was placed in a round bottom flask, immersed in silicon oil at 160°C, and continuously rotated for 20 minutes. The flask was open to the atmosphere. This procedure was repeated 20 times, the residue each time being dissolved in minimum water and stored below 0°C. The combined products of these thermolyses were fractionated by *LC Method (i)*. The resultant fractions were analyzed for DFDA content by GCFID of the per-*O*-methylsilyl derivatives.

In the second preparation, ~20g of inulin/1.5% citric acid was placed in two open containers and heated in an oven at 160°C for 15 minutes. The resultant caramel was dissolved in a minimum of H₂O and fractionated by *LC Method (i)*, followed by trimethylsilylation and GC analysis.

Fructose/HCl - 5g Crystalline D-(-)-fructose (BDH Chemicals Ltd, glucose free) was dissolved in reagent grade concentrated hydrochloric acid (20g) that had been pre-cooled to near 0°C. The reaction mixture was stored at -5°C for 72 hours. The resultant black liquid was then poured over 35g of ice, allowed to dissolve, and passed through a glass column (3.5 x 35cm ≈ 350mL) packed with IRA-400 ion exchange resin. It was necessary to regenerate the resin midway through and repeat the ion exchange to neutralize the sample completely.

The details of this treatment are as follows:

1. Prepare resin
 - a. Wash column with 1200 mL distilled H₂O at ~50 mL/min
 - b. Load with 500 mL 1.5M NaOH and let stand for 60 minutes
 - c. Wash with distilled H₂O until pH<9 (~1L at ~50 mL/min)
 - d. Load with 500 mL 1.5M NaCl and let stand for 60 minutes
 - e. Wash with ~1L distilled H₂O
2. Activate resin with 1.5M NaOH (~1L at high flow) and wash with distilled H₂O until pH<9
3. Load sample, followed by H₂O, and elute at ~20mL/min until sample volume ≈ 1L
4. Regenerate resin with ~500 mL 2.0M NaOH at high flow, wash with H₂O until pH<9
5. Reload entire sample from previous run, followed by 500+ mL H₂O.

After ion exchange, the sample was taken to dryness under vacuum, redissolved in 7.0 mL distilled H₂O, and the pH adjusted to neutral with dilute HCl or dilute NH₄OH. Repeated preparative LC fractionation of this sample gave six major fractions, three of which each contained a single DFDA (DHL I, α -D-Fru_p-1,2':2,1'- β -D-Fru_p, ~580mg; DHL II, α -D-Fru_f-1,2':2,1'- β -D-Fru_p, ~600mg; or DHL III, β -D-Fru_f-1,2':2,1'- β -D-Fru_p, ~75mg).

Miscellaneous Procedures

Mass Balance - Experiments to estimate losses incurred during thermolysis and sample workup were carried out using *LC Method (iv)*. ~100mg (accurately weighed) inulin/1.5% citric acid was thermolyzed at 160°C for 20 minutes, cooled, and dissolved in 1.0 mL H₂O. The entire sample was then loaded onto the P2 column and fractions collected. Each fraction was taken to dryness under vacuum and the residual weight determined to ±0.1mg.

Response Factors - ~9 mg (± 0.01 mg) of xylitol, α -D-Fru μ -1,2':2,1'- β -D-Fru μ (**6**), α -D-Fru μ -1,2':2,1'- β -D-Fru μ (**9**), α -D-Fru μ -1,2':2,1'- β -D-Fru μ (**10**), β -D-Fru μ -1,2':2,1'- β -D-Fru μ (**13**), D-fructose, D-glucose and sucrose were prepared individually using the derivatization and sample cleanup methods above. Aliquots of these stock solutions were then combined and diluted by pipette to provide a series of standards from which response factors were determined.

Mass, freeze drying, thermolysis temperature, melting point - Masses reported to ± 0.01 mg were recorded on a Mettler AT201 top loading electronic balance. Less demanding measurements (± 0.1 mg) were carried out on a Mettler AE200. Three freeze driers were employed depending on the quantity of material being prepared. For <g quantities, a bench top model (FTS Systems FlexiDry MP) was used. For larger amounts, floor standing units with heated shelves and higher capacity (Dynovac FD12 at the University of Waikato, VirTis Genesis 12 LL at the University of Montana) were employed. Freeze dried carbohydrate samples were held for 48 hours at $\sim 40^\circ\text{C}$ over P_2O_5 before use, and were stored in vacuum desiccators. Thermolyses were performed in Teflon[®]-lined, screw-capped glass vials (Supelco) immersed in silicon oil (United Chemical Technologies, polymethylphenylsiloxane) at 160 - 180°C . Temperature was maintained to within $\pm 0.2^\circ\text{C}$ with a thermostated recirculating pump (Braun Thermomix II). Melting points were determined on a Reichert-Jung Thermovar apparatus.

Data Analysis and Kinetic Modeling

Quantitation - GCFID integration results were obtained with HP ChemStation for each sample.[‡] These were then exported to ASCII text files, parsed using a QBasic program to remove all information but the actual data, and imported into Axum[®] (MathSoft, Inc. Ver. 5.0) for calculation of percent conversion and for graphical treatment.^{**}

Preliminary Curve-Fitting - Initial estimates for the rate of formation and disappearance of each DFDA were obtained in Axum using a nonlinear least squares routine.⁹⁴ This algorithm combines Taylor Series or the Gauss-Newton method with the gradient, or steepest descent, method.⁸⁷ The user provides a mathematical model (rate equation), specifies the value of initial reagent concentrations, and gives initial estimates for each variable in the model. The rate equation used in this part of the study was $[I]_n = \frac{k_n[inulin]_0}{k'_n - k} (e^{-kt} - e^{-k'_nt})$, where $[I]_n$ is the concentration at any time of the individual DFDA that is under scrutiny, $[inulin]_0$ is the initial inulin concentration, and k , k_n , and k'_n are the rate constants for disappearance of inulin, individual DFDA formation, and individual DFDA decay, respectively. The nonlinear LS program solves the equation iteratively until the solution converges to within prescribed boundaries, or criteria. The user may specify convergence criteria that compare the relative change in the estimates for successive iterations. Since nonlinear curve-fitting was used in this study as a rough estimate only of rate constants, and since the rate equation at this stage was

[‡] Automatic integration of partially resolved peaks is sometimes not reliable using the ChemStation software. Therefore, to ensure consistency, it was necessary to draw certain baselines and peak start and stop times manually for every chromatogram.

^{**} It was necessary to compose macros, scripts, and/or computer programs to perform these functions.

purely a first approximation, the default convergence tolerances provided by the program were deemed acceptable. Graphs comparing the actual data with predicted values were used to gauge the appropriateness of the model.

Kinetic Plots of DFDA Degradation - Data for the disappearance of DFDA were plotted using 1st and 2nd order rate equations. Standard treatments of the form $v = k[A]$, $v = k[A]^2$, and $v = k[A][B]$ were replaced with analogous equations incorporating a physical property that is directly proportional to reactant concentration. That property, in this case, was wt% DFDA as determined by peak area. Since in general, DFDA did not decay completely to products - measurable amounts still remained after 40 hours thermolysis - the final concentration was incorporated into the rate equations as "infinity" concentration. Rearrangements of the integrated rate equations were subjected to linear and nonlinear LS analysis. The justification for, and limitations of, these kinetic treatments can be found in Espenson.⁸⁶

Kinetic Modeling - Computer models of tentative kinetic mechanisms were developed using SIMSODE,⁹⁵ a numerical simulation program for chemical reaction systems with mass-action kinetics. The user must first create a data file using the companion program DATED,⁹⁶ which records reactant and product names, individual reactions in the mechanism, and rate constants. SIMSODE is the "control" program which invokes LSODE,⁹⁷ the Livermore Solver for Ordinary Differential Equations, to calculate a solution based on the mechanism and rate constants set forth in the DATED file. SIMSODE writes an ASCII file containing

concentration/time data for each species in the mechanism. These data were then imported into Axum and visualized graphically.

REFERENCES

1. Suzuki, M. & Chatterton, J. (eds.) *Science and Technology of Fructans* (CRC Press, London, 1993).
2. Roberfroid, M. B. & Delzenne, N. M. Dietary fructans. *Annual Review of Nutrition* **18**, 117-143 (1998).
3. Roberfroid, M. B. Health benefits of non-digestible oligosaccharides. *Advances in Experimental Medicine and Biology* **427**, 211-219 (1997).
4. Roberfroid, M. B. Functional effects of food components and the gastrointestinal system: Chicory fructooligosaccharides. *Nutrition Reviews* **54**, S38-S42 (1996).
5. Hidaka, H., Hirayama, M., Tokunaga, T. & Eida, T. The effects of undigestible fructooligosaccharides on intestinal microflora and various physiological functions on human health. *Advances in Experimental Medicine and Biology* **270**, 105-117 (1990).
6. Fishbein, L., Kaplan, M. & Gough, M. Fructooligosaccharides: A review. *Veterinary and Human Toxicology* **30**, 104-107 (1988).
7. Mitsuoka, T. & Kaneuchi, C. Ecology of the bifidobacteria. *American Journal of Clinical Nutrition* **30**, 1799-1810 (1977).
8. Reddy, B. S. & Rivenson, A. Inhibitory effect of *Bifidobacterium longum* on colon, mammary and liver carcinogenesis induced by 2-amino-3-methylimidazo(4,5-f)-quinoline, a food mutagen. *Cancer Research* **53**, 3914-3918 (1993).
9. Reddy, B. S., Hamid, R. & Rao, C. V. Effect of dietary oligofructose and inulin on colonic preneoplastic aberrant crypt foci inhibition. *Carcinogenesis* **18**, 1371-1374 (1997).
10. Reddy, B. S. Prevention of colon cancer by pre- and probiotics - Evidence from laboratory studies. *British Journal of Nutrition* **80**, S 219-S 223 (1998).
11. Hidaka, H., Eida, T., Takizawa, T., Tokunaga, T. & Tashiro, Y. Effects of fructooligosaccharides on intestinal flora and human health. *Bifidobacteria Microflora* **5**, 37-50 (1986).
12. Hidaka, H. & Hirayama, M. Useful characteristics and commercial applications of fructooligosaccharides. *Biochemical Society Transactions* **19**, 561-565 (1991).
13. Mitsuoka, T. *Intestinal Bacteria and Health* (Harcourt, Brace, and Jovanovich, Tokyo, Japan, 1978).
14. Ibrahim, S. A. & Bezkorovainy, A. Inhibition of *Escherichia coli* by bifidobacteria. *Food Protection* **56**, 713-715 (1993).
15. Gibson, G. R. & Wang, X. Regulatory effects of bifidobacteria on the growth of other colonic bacteria. *Journal of Applied Bacteriology* **77**, 412-420 (1994).
16. Orban, J. I., Patterson, J. A., Sutton, A. L. & Richards, G. N. Effect of sucrose thermal oligosaccharide caramel, dietary vitamin-mineral level, and brooding temperature on growth and intestinal bacterial populations of broiler chickens. *Poultry Science* **76**, 482-490 (1997).
17. Patterson, J. A., Orban, J. I., Sutton, A. L. & Richards, G. N. Selective enrichment of bifidobacteria in the intestinal tract of broilers by thermally produced kestoses and effect on broiler performance. *Poultry Science* **76**, 497-500 (1997).

18. Manley-Harris, M. & Richards, G. N. Thermolysis of sucrose for food products - a sucrose caramel designed to maximize fructose oligosaccharides for beneficial moderation of intestinal bacteria. *Zuckerindustrie* **119**, 924-928 (1994).
19. Gibson, G. R. & Roberfroid, M. B. Dietary modulation of the human colonic microbiota: Introducing the concept of prebiotics. *Journal of Nutrition* **125**, 1401-1412 (1995).
20. Yun, J. W. Fructooligosaccharides - Occurrence, preparation, and application. *Enzyme & Microbial Technology* **19**, 107-117 (1996).
21. Devrese, M. Prebiotics. *Ernahrungs-Umschau* **44**, 398 ff. (1997).
22. Walker, W. A. & Duffy, L. C. Diet and bacterial colonization: Role of probiotics and prebiotics. *Journal of Nutritional Biochemistry* **9**, 668-675 (1998).
23. Ziemer, C. J. & Gibson, G. R. An overview of probiotics, prebiotics and synbiotics in the functional food concept - Perspectives and future strategies. *International Dairy Journal* **8**, 473-479 (1998).
24. Roberfroid, M. B. Prebiotics and synbiotics - Concepts and nutritional properties. *British Journal of Nutrition* **80**, S 197-S 202 (1998).
25. Byrne, M. Fortified future for functional foods. *Food Engineering International October* (1997).
26. Forsberg, K. H., Hamalainen, L., Melaja, A. J. & Virtanen, J. J. pH adjustment in fructose crystallization for increased yield. US 3883365.
27. Rearick, D. E. & Olmstead, L. J. in *Procedures of the Sugar Processing Research Conference* 97-103 (1993).
28. Chu, Y., Shiau, L. D. & Berglund, K. A. Effects of impurities on crystal growth in fructose crystallization. *Journal of Crystal Growth* **97**, 689-696 (1989).
29. Defaye, J., Fernandez, J. M. G. & Gabelle, A. Difructofuranose dianhydrides. FR 2680788 A1 93035.
30. Kondo, T., Katsuragi, T. & Nishimura, A. Di-D-fructofuranose 1,2':2,3'-dianhydride sweeteners for food. JP 03180155 A2 910806.
31. Kondo, T. & Nishimura, A. Sweetening compositions containing di-D-fructofuranose 1,2':2,3'-dianhydride and menthol. JP 03067560 A2 910322.
32. Ueda, M., Ogishi, H. & Sashita, R. Manufacture of difructose dianhydride I with inulinase of *Arthrobacter*. JP 03247295 A2 911105.
33. Defaye, J. & Fernandez, J. M. G. The oligosaccharide components of caramel. *Zuckerindustrie* **120**, 700-704 (1995).
34. McNaught, A. D. Nomenclature of Carbohydrates. *Carbohydrate Research* **297**, 1-92 (1997).
35. Manley-Harris, M. & Richards, G. N. in *Advances in Carbohydrate Chemistry and Biochemistry* (ed. Horton, D.) 207-266 (Academic Press, San Diego, 1997).
36. Pictet, A. & Chavan, J. Sur une hétéro-lévulosane. *Helvetica Chimica Acta* **9**, 908-814 (1926).
37. Wolfrom, M. L. & Hilton, H. W. Bimolecular dianhydrides of L-sorbose. *Journal of the American Chemical Society* **74**, 5334-5336 (1952).
38. Lowry, T. M. *Journal of the Chemical Society* **127**, 1371 (1925).
39. Boggs, L. A. & Smith, F. The formation of difructofuranose 2,1':1,2'-dianhydride

- from polyfructosans and its structural significance. *Journal of the American Chemical Society* **78**, 1878-1880 (1955).
40. Lemieux, R. U. & Nagarajan, R. The configuration and conformation of "Di-D-Fructose Anhydride I". *Canadian Journal of Chemistry* **42**, 1270-1278 (1964).
 41. Jackman, L. M. & Sternhell, S. *Applications of Nuclear Magnetic Resonance Spectroscopy in Organic Chemistry* (Pergamon Press, Oxford, 1969).
 42. Binkley, R. W., Binkley, W. W. & Grey, A. A. Conformational analysis of di-D-fructose dianhydrides by P.M.R. spectroscopy. *Carbohydrate Research* **28**, 365-370 (1973).
 43. Binkley, R. W., Binkley, W. W. & Wickberg, B. Application of C.M.R. spectroscopy to the problem of the anomeric configuration of the di-D-fructose dianhydrides. *Carbohydrate Research* **36**, 196-200 (1974).
 44. Moody, W. & Richards, G. N. Thermolysis of sucrose in the presence of alcohols. A novel method for the synthesis of D-fructofuranosides. *Carbohydrate Research* **97**, 247-255 (1981).
 45. Moody, W. & Richards, G. N. Effect of traces of acids on reaction of sucrose in dimethyl sulfoxide. *Carbohydrate Research* **108**, 13-22 (1982).
 46. Moody, W. & Richards, G. N. Effects of substituents on the acid-catalyzed thermolysis of sucrose in dimethyl sulfoxide. *Carbohydrate Research* **111**, 23-29 (1982).
 47. Moody, W. & Richards, G. N. Formation and equilibration of D-fructosides and 2-thio-D-fructosides in acidified dimethyl sulfoxide: Synthetic and mechanistic aspects. *Carbohydrate Research* **124**, 201-213 (1983).
 48. Angyal, S. J. & Bethell, G. S. Conformational analysis in carbohydrate chemistry. III The ¹³C N.M.R. spectra of the hexuloses. *Australian Journal of Chemistry* **29**, 1249-1265 (1976).
 49. Heyraud, A., Rinaudo, M. & Taravel, F. R. Isolation and characterization of oligosaccharides containing D-fructose from juices of the jerusalem artichoke. Kinetic constants for acid hydrolysis. *Carbohydrate Research* **128**, 311-320 (1984).
 50. Mandal, U., Das, K. & Kundu, K. K. Kinetic solvent effects on acid-catalyzed hydrolysis of sucrose in aqueous mixtures of some protic, aprotic, and dipolar aprotic solvents. *Canadian Journal of Chemistry* **64**, 1638-1642 (1986).
 51. Defaye, J. & Gadelle, A. The behaviour of D-fructose and inulin towards anhydrous hydrogen fluoride. *Carbohydrate Research* **136**, 53-65 (1985).
 52. Defaye, J., Gadelle, A. & Pedersen, C. The behavior of L-sorbose towards anhydrous hydrogen fluoride. *Carbohydrate Research* **152**, 89-98 (1986).
 53. Defaye, J., Gadelle, A. & Pedersen, C. Acetal and ester protecting-groups in the hydrogen fluoride-catalysed synthesis of D-fructose and L-sorbose difuranose dianhydrides. *Carbohydrate Research* **174**, 323-329 (1988).
 54. Defaye, J. & Fernández, J. M. G. Selective protonic activation of isomeric glycosylfructoses with pyridinium poly(hydrogen fluoride) and synthesis of spirodioxanyl oligosaccharides. *Carbohydrate Research* **237**, 223-247 (1992).
 55. Defaye, J. & Fernandez, J. M. G. Protonic reactivity of sucrose in anhydrous hydrogen fluoride. *Carbohydrate Research* **251**, 17-31 (1994).

56. Defaye, J. & Fernández, J. M. G. Protonic and thermal activation of sucrose and the oligosaccharide composition of caramel. *Carbohydrate Research* **256**, C1-C4 (1994).
57. Fernández, J. M. G. & Defaye, J. Difuctose dianhydrides from sucrose and fructo-oligosaccharides and their use as building blocks for the preparation of amphiphiles, liquid crystals, and polymers. *Carbohydrate Research* **265**, 249-269 (1994).
58. Ponder, G. R. & Richards, G. N. Pyrolysis of inulin, glucose, and fructose. *Carbohydrate Research* **244**, 341-359 (1993).
59. Blize, A. E., Manley-Harris, M. & Richards, G. N. Di-D-fructose dianhydrides from the pyrolysis of inulin. *Carbohydrate Research* **265**, 31-39 (1994).
60. Ponder, G. R. & Richards, G. N. Polysaccharides from thermal polymerization of glucosides. *Carbohydrate Research* **208**, 93-104 (1990).
61. Manley-Harris, M. & Richards, G. N. Di-D-fructose dianhydrides and related oligomers from thermal treatments of inulin and sucrose. *Carbohydrate Research* **287**, 183-202 (1996).
62. Chu, Y. & Berglund, K. A. Kinetics of difuctose dianhydrides formation under fructose crystallization conditions. *Starch/Stärch* **42**, 112-117 (1990).
63. Chu, Y. The formation of difuctose dianhydrides and their impact on fructose crystallization. Ph.D. Thesis, Department of Agricultural Engineering, Michigan State University. (1988).
64. Hamada, K., Yoshihara, Y., Suzukamo, G. & Hiroaki, O. The dehydration of ketohexoses into 5-chloromethyl-2-furaldehyde. The isolation of diketohexose dianhydrides. *Journal of the Chemical Society of Japan* **57**, 307-308 (1984).
65. Hilton, H. W. in *Methods in Carbohydrate Chemistry* (eds. Whistler, R. L., Wolfrom, M. L. & BeMiller, J. N.) 199-203 (Academic Press, New York, 1963).
66. Field, R., University of Montana, Personal communication (1998).
67. Doherty, L. A comparison of detector responses: a GC/FID versus a GC with Electron Ionization Detector (EID). Hewlett Packard Application Note, HP G1800A, GCD 94-9. (1994).
68. Matsuyama, T., Tanaka, K. & Uchiyama, T. Isolation and identification of the *Aspergillus fumigatus* difuctose dianhydride. *Agricultural and Biological Chemistry* **55**, 1413-1414 (1991).
69. Gardiner, D. The pyrolysis of some hexoses and derived di-, tri-, and poly-saccharides. *Journal of the Chemical Society*, 1473-1476 (1966).
70. Antal, M., Jr., Mok, W. S. L. & Richards, G. N. Mechanism of formation of 5-(hydroxymethyl)-2-furaldehyde from D-fructose and sucrose. *Carbohydrate Research* **199**, 91-109 (1990).
71. Scheer, M. D. Thermal dehydration kinetics of disaccharides. *International Journal of Chemical Kinetics* **15**, 141-149 (1983).
72. Fisons Instruments, Biotech MS, Tudor Road, Altrincham, WA14 5RZ, United Kingdom.
73. Goretti, G., Liberti, A. & Di Pablo, C. Gas chromatographic investigation on caramel aroma. *Annali di Chimica* **70**, 277-284 (1980).
74. Jackson, R. F. & Goergen, S. M. A crystalline difuctose anhydride from hydrolyzed inulin. *Bureau of Standards Journal of Research* **3**, 27-38 (1929).

75. Schlubach, H. H. & Knoop, H. Carbohydrates of the Jerusalem artichoke. *Annalítica* **504**, 19-30 (1933).
76. Schlubach, H. H. & Behre, C. Synthesis of a difructose anhydride from fructose. *Annalítica* **508**, 16-24 (1933).
77. Praly, J.-P. & Lemieux, R. U. Influence of solvent on the magnitude of the anomeric effect. *Canadian Journal of Chemistry* **65**, 213-223 (1987).
78. Tvaroška, I. & Bleha, T. Anomeric and exo-anomeric effects in carbohydrate chemistry. *Advances in Carbohydrate Chemistry and Biochemistry* **47**, 45-123 (1989).
79. Cramer, C. J., Truhlar, D. G. & French, A. D. Exo-anomeric effects on energies and geometries of different conformations of glucose and related systems in the gas phase and aqueous solution. *Carbohydrate Research* **298**, 1-14 (1997).
80. Manley-Harris, M. & Richards, G. N., University of Montana, Personal communication (1997).
81. Slaughter, L. H. & Livingston, D. P. Separation of fructan isomers by high performance anion exchange chromatography. *Carbohydrate Research* **253**, 287-291 (1994).
82. Dionex Corporation, 1228 Titan Way, P.O. Box 3603, Sunnyvale, CA, USA 94088-3603.
83. Bock, K., Pedersen, C. & Pedersen, H. Carbon-13 nuclear magnetic resonance data for oligosaccharides. *Advances in Carbohydrate Chemistry and Biochemistry* **42**, 193-225 (1984).
84. Capon, B. Mechanism in carbohydrate chemistry. *Chemical Reviews* **69**, 407-498 (1969).
85. Rodiguin, N. M. & Rodiguina, E. N. *Consecutive chemical reactions. Mathematical analysis and development* (D. Van Nostrand Co, Inc., Princeton, 1964).
86. Espensen, J. H. *Chemical Kinetics and Reaction Mechanisms* (McGraw-Hill, Inc., New York, 1995).
87. Cuthbert, D., Wood, F. S. & Gorman, J. W. *Fitting Equations to Data. Computer Analysis of Multifactor Data for Scientists and Engineers* (Wiley-Interscience, New York, 1971).
88. Leininger, P. M. & Kilpatrick, M. The inversion of sucrose. *Journal of the Chemical Society* **60**, 2891-2899 (1938).
89. Lönnberg, H. & Gylén, O. The acid-catalyzed hydrolysis of anomeric alkyl fructofuranosides. *Journal of Carbohydrate Chemistry* **2**, 177-188 (1983).
90. Edward, J. T. Molecular volumes and the Stokes-Einstein equation. *Journal of Chemical Education* **47**, 261-270 (1970).
91. Manley-Harris, M., University of Montana, Personal communication (1999).
92. Astwood, K., Lee, B. & Manley-Harris, M. Oligosaccharides in New Zealand honeydew honey. *Journal of Agriculture and Food Chemistry* **46**, 4958-4962 (1998).
93. Evans, C., University of Waikato, Personal communication (1999).
94. Marquardt, D. W. An algorithm for least squares estimation of nonlinear parameters. *Journal of the Society for Industrial and Applied Mathematics* **2**, 431-441 (1963).
95. Gyorgyi, L. SIMSODE. Institute of Inorganic and Analytical Chemistry, Eotvos

- Lorand University, Budapest-112, P.O.Box 32, Hungary, (1990).
96. Ambro, J. & Gyorgyi, L. DATED. Institute of Isotopes of the Hungarian Academy of Sciences, Budapest, Hungary & Institute of Inorganic and Analytical Chemistry, L. Eotvos University, Budapest, Hungary, (1990).
 97. Hindmarsh, A. C. LSODE. Mathematics and Statistics Division, L-316, Lawrence Livermore National Laboratory, Livermore, CA 94550, (1981).